ABSTRACT

MCCALL, JAMES VAUGHN. Assessment of Finger Individuation and Development of Finger Individuation Training Platform for Children with Hemiplegic Cerebral Palsy. (Under the direction of Dr. Derek G. Kamper).

Cerebral palsy (CP) is a common motor disorder with a high incidence rate in the U.S. (~0.3% of the population). For the 800,000 people living with CP in the U.S., the disorder can severely impact the entirety of their lives. CP can affect a wide variety of motor functions, such as gait or speech, as well hand function. Poor motor control of the hand due to cerebral palsy contributes significantly to the inability of many people to live independently or work.

In Chapter 1, we performed a review of literature on hand function assessment of children with CP. This review was focused on children with hemiplegic cerebral palsy (hCP) as they represent a large portion of the CP population and are often very keen to explore hand rehabilitation. We identified finger individuation as an important aspect of hand function that has received little attention for the hCP population.

In Chapter 2, we characterized the finger force individuation and movement individuation of 10 typically developing children and four children with hCP and found the relationship of these measurements to a clinical assessment of unimanual hand function. We used a custom finger force assessment platform to measure force individuation, and camera-based motion capture to assess movement individuation. High-density (HD) electromyography electrode arrays, placed over the extrinsic and intrinsic hand muscles, measured the activation patterns of hand muscles during individuated movement.

In Chapter 3, we assessed the contribution of each brain hemisphere to the control of individuated finger forces using transcranial magnetic stimulation (TMS). TMS was used to characterize the neural basis of finger individuation deficits and the relative contribution of each hemisphere to individuated finger control.

Lastly, in Chapter 4, we developed elastomer-based soft actuators for a glove exoskeleton to assist finger extension. These actuators were tested empirically; finite element model simulations were also performed to estimate variables difficult to measure in experiments, such as flow rate in the channel. These actuators were integrated into an instrumented glove and virtual reality environment, designed to facilitate targeted finger individuation training.

This work characterized hCP finger individuation deficits, examined their neural basis, and developed new soft actuators for a finger individuation training platform. The data generated and development of the training system will allow for better assessment of functional deficits and allow clinicians to rehabilitate finger individuation capability in a targeted manner.

Assessment of Finger Individuation and Development of Finger Individuation Training Platform for Children with Hemiplegic Cerebral Palsy

by
James V. M^{c}Call

A dissertation submitted to the Graduate Faculty of
North Carolina State University
in partial fulfillment of the
requirements for the degree of
Doctor of Philosophy

Biomedical Engineering

Raleigh, North Carolina
2022

APPROVED BY:

_____	_____
Dr. Derek Kamper Committee Chair	Dr. Xiaogang Hu
_____	_____
Dr. Nitin Sharma	Dr. Joshua Alexander
_____	
Dr. Eran Dayan	

DEDICATION

To my wife, Anna, for your love and patience. Your support made this possible.

BIOGRAPHY

I received my Bachelor of Science in Biomedical Engineering from North Carolina State University in 2014 graduating Cum Laude. For several years after graduation, I worked as an engineer for Robling Medical. During my time there, I discovered a desire to grow further as an engineer, a passion for research, and an interest in working more directly with the medical challenges many face every day. I enrolled in graduate school in 2016 to pursue a Masters/PhD program in the Joint Department of Biomedical Engineering at North Carolina State University and University of North Carolina at Chapel Hill. In 2019, I completed a MS in Biomedical Engineering, the research for which was focused on lower limb exoskeleton control. For my PhD dissertation, I studied under Dr. Derek Kamper.

ACKNOWLEDGMENTS

Anna, you have been consistently supportive of my choices, from enrolling in graduate school, to taking on additional coursework. You not only made this possible, you have made this time so enjoyable, even at times when things were difficult.

Thank you to my family for love and support.

Thank you to my friends for being there when I needed advice or just needed to take a break from research for a minute or two. Special thanks to Mike D., Adam Y., and Adam H. for keeping me company when writing.

I was lucky to have some excellent lab mates in the Hand Rehabilitation Lab. Thank you to Mohammad Ghassemi, Miranda Ludovice, and James Ailsworth for the camaraderie over the years.

To the families who volunteered to participant in studies, thank you. I appreciate you sacrificing your time. This research was possible because of you and I greatly enjoyed getting to know you.

To my committee members, thank you for your help and guidance. Whether it was help in understanding a method of data collection or analysis, or advice on participant recruitment, your contributions have been invaluable.

Dr. Kamper, thank you for the years of support and guidance. I feel that while in your lab I have learned an immeasurable amount from you, and that this has been a defining time in my life. You have often challenged me, and I have become a better researcher and person for it.

TABLE OF CONTENTS

LIST OF TABLES

LIST OF FIGURES

CHAPTER 1: INTRODUCTION

Adapted from J. McCall et al., "Hand Function Development of Children with Hemiplegic Cerebral Palsy: A Scoping Review", J. Pediatr. Rehabil. Med. (Accepted August 2021)

1.1 Hemiplegic Cerebral Palsy and Hand Dexterity

Cerebral palsy (CP), arising from neurological damage incurred during the prenatal, perinatal, or early postnatal periods [1], is one of the most common movement disorders among children. CP occurs in approximately 3 out of every 1000 births [2]. The vast majority of individuals with CP live into adulthood, thereby resulting in roughly 800,000 Americans dealing with the effects of CP [3]. The variety of chronic impairments resulting from the initial brain injury may greatly affect economic opportunities and societal participation. The associated costs of care and lost economic opportunity due to CP were estimated to be as high as $17 billion annually in 2004 (adjusted to 2016 dollars) [4].

Hemiplegic CP (hCP), the second most common form of CP [5], affects sensorimotor function of the limbs predominantly on one side of the body, often to a greater extent in the upper extremities. Almost half of all children with hCP have greater impairment in their upper limb than in their lower limb [6]. Within the upper limb, the hand is most likely to be impaired [7]. Hand impairment can lead to substantial disability since the hand is the primary means of interacting with the world. As 96% of all children with CP live into adulthood, chronic hand dysfunction will impact employment, recreational, and social opportunities impairment for decades [8].One of the primary impairments in individuals with CP is diminished sensorimotor control, potentially impacting the function of both the upper and lower limbs. Deficits are

especially marked in the distal upper extremity; children with hemiparetic cerebral palsy (hCP) are most impaired in the upper limb, and especially the hand, in over 50% of cases [6].

1.2 Literature Review of Hand Function in Children with Hemiplegic Cerebral Palsy

We decided to perform a literature review to better understand the current state of knowledge regarding the hand impairments associated with hCP and how sensorimotor deficits manifest over time. Despite the importance of the distal upper limb to overall function, reviews focused on characterization and quantification of deficits in the hand of children with hCP have been relatively limited. While a prior review article did examine quantitative measures of upper limb impairments in hCP, the primary focus was on reach, with relatively few cited studies describing grasp in conjunction with reach [9]. Other review articles describing upper limb sensorimotor control in children with CP have been limited in scope, restricted to areas such as clinical assessments and their reliability [10–12], three-dimensional limb kinematics, or bimanual task performance [9,13]. Thus, the study of motor control of the hand itself has not been well characterized. Furthermore, because past reviews focused on reliability of the assessments, they typically did not provide the absolute values of measures that could inform assessment of performance in children with hCP.

Since past reviews have preferentially focused on the arm rather than the hand, and on assessment of evaluation measures rather than the values of these measures, a review of published articles was warranted to address these gaps in knowledge. We performed a scoping review to allow for a broad search of the literature that would identify and summarize original research focused on assessing hand function in children with hCP. Primarily, this review was intended to provide an overview of quantitative measures of hand function in children with hCP and to create a summary of the current state of research in this area. This was accomplished by:

summarizing the results of common quantitative measures and assessments of hand function in children and adolescents with hCP; examining the extent of methodological variation for different hand assessments for children; and identifying areas for further research. While both qualitative and quantitative assessments can provide important information about hand impairment, this scoping review was limited to quantitative measures, as they enable more direct comparisons between children that can give insights into the underlying causes and effective treatments of hand function in hCP.

1.2.1 Methods

This work presents a scoping review of quantitative measures assessing hand function and associated brain activity in children (18 years old or less) with hCP. Search and data inclusion protocols were written prior to the start of the search, and this review was written to comply with Joanna Biggs Institute scoping review protocol requirements. Table 1.1 summarizes the inclusion/exclusion criteria for this scoping review. A comprehensive search for original research journal articles of the following databases was conducted in May and June of 2018 and updated in October of 2019: PubMed, PEDro, Web of Science, CINAHL, and SpringerLink. Conference proceedings and review articles were excluded to avoid potential "double counting" of the same data set appearing in multiple publications. The searches were performed using the combined keywords "cerebral palsy" and "hemiplegia", "hemiparetic" or "unilateral" to capture the population and "hand" to focus the search. These required terms were combined with optional terms that described different measures and outcomes (e.g., ''strength', 'force', 'kinetics', 'EMG', 'activation', 'brain', 'imaging', 'skill', 'function', or 'motor'). Articles using all types of study designs were included but some articles were excluded based on criteria such as subject population and characteristics of the reported data. To focus on hand function in

children, articles had to have three or more participants aged 18 years or under for inclusion. Results were limited to articles available in the English language due to a lack of access to translation services. No restriction was placed on the date of publication. As upper limb surgery or botulinum toxin treatment would acutely alter the natural progression of sensorimotor control, data collected following these interventions were excluded. Pre-operative data were included.

After examining the relevant papers, common measures were selected for evaluation and data extraction. For clinical assessments that evaluated the same or similar components of hand function, the most common assessment was used. Articles that assessed children (18 years of age or under) with hCP with at least one of the following quantitative measures of hand function were included: pinch strength, finger forces, grip strength, range of motion (ROM), electromyograph (EMG), two-point discrimination (2PD), pegboard tests, Box and Block Test (BBT), Jebsen-Taylor Test of Hand Function (JTTHF) [14], Melbourne Assessment of Unilateral Upper Limb Function (MUUL) [15], and the Assisting Hand Assessment (AHA) [16]. While this list is not exhaustive (e.g., the SHUEE [17]), preliminary analysis had revealed that this set included popular means of evaluation while covering a range of sensorimotor characteristics.

Table 1.1: Inclusion/Exclusion Criteria Summary

Inclusion Criteria	Exclusion Criteria
Hemiplegic cerebral palsy	Not available in English language
Participant age of 18 years or less	Upper limb surgery or botulinum injection within six months prior to the study
Sample size of 3 or more	Conference proceeding or review article
Includes one or more of the identified hand function measures	

The searches of the five databases yielded 1536 articles. The title and abstract of each of these articles was reviewed to screen them for potential inclusion in the review and their search results and inclusion decision were entered in shared data record. In cases where a determination could not be made from the abstract alone, the entire text was examined. Articles that failed to contain data that fit into one of the chosen categories (quantitative neuromechanics, clinical assessments, and clinical functional evaluations) were excluded from further analysis

Once the list of selected articles was finalized, the identified quantitative measure(s), along with participant ages, neurological status, assessment results, and MACS, GMFCS or Zancolli scores, were extracted from each article. The mean values for each group for participant age and characteristics and assessment outcomes in each study were extracted or calculated from reported values for individuals. In some cases, articles reported averaged values for all participants or groups of participants. In some cases, data for individual participants was also obtained, and data for each individual was screened for exclusionary criteria (age, hCP status) and the included data values were averaged or charted separately. Mean assessment outcomes were charted against mean ages or MACS scale. Data sets were identified as being associated with: children with hCP or typically developing (TD) children; paretic hand, non-paretic hand,

dominant hand, or non-dominant hand. Where practical, the sources for specific data points were identified in the legend and distinguished by marker shape and/or color. Studies reporting data from both the paretic and non-paretic hands may be referenced twice in a figure legend. Trend lines were added to figures to provide a rough visual guide; the trend lines were created by computing a least-squares linear fit to the data.

1.2.2 Results

Of the 1536 unique articles identified through the searches, 327 articles met the inclusion criteria for full text review. A total of 131 of the 327 articles met the inclusionary/exclusionary criteria in terms of subject number and age and the type of data collected (**Figure 1.1**). The other 196 articles were primarily excluded due to a lack of quantitative data, the inclusion of multiple forms of CP, or comingling of data from subjects over 18 years of age.

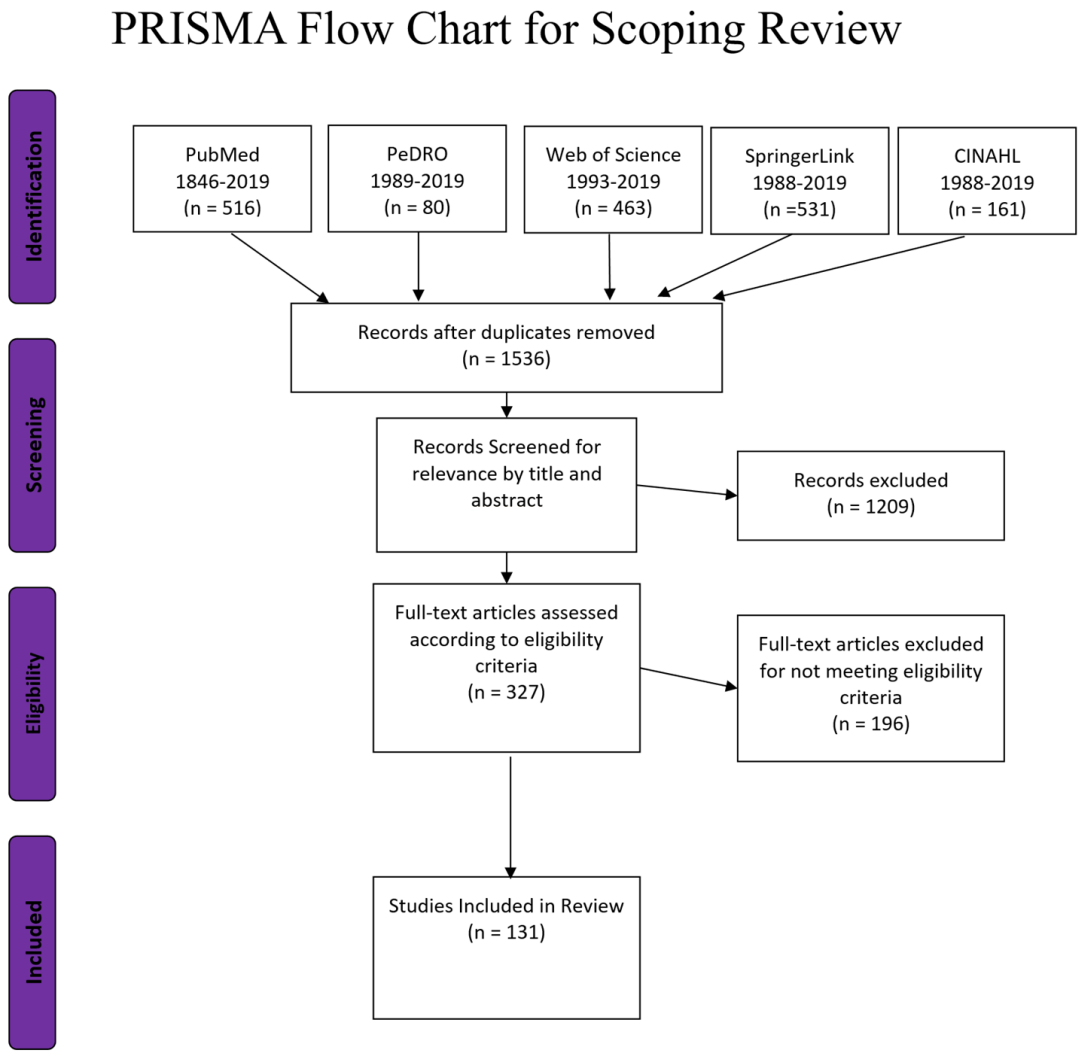

Figure 1.1: PRISMA diagram of article selection. A total of 327 articles were assessed; 131 articles met the desired criteria and were included in this review.

Of the 131 articles included in the review, 72 described neuromechanics, 34 evaluated clinical assessments, and 67 included data for functional evaluations. Most articles reported data covering more than one of the categories; in these cases, each qualifying set of data was reported separately in the appropriate section. Below, selected results from the literature review are presented.

1.2.2.1 Pinch

Of the 12 articles that measured pinch force, 8 articles included data for one or both hands of children with hCP; some also included pinch force data for both hands in TD children or normative data [18–25]. Data from these articles were aggregated (273 participants in total) to provide an overview of the development of lateral pinch strength with age in children with hCP.

Data for the TD non-dominant hand showed a mean lateral pinch strength of roughly 44 N at 6.5 years of age. Lateral pinch strength for the TD children increased up to 69 N by age 12 (**Figure 1.2)**. Lateral pinch strength was considerably lower even at a young age in the paretic hand in children with hCP, with a mean value of 19.0 N (44% of the TD value) at 8.2 years old. In contrast to the TD subjects, pinch strength showed no increase with age for the paretic hand in hCP subjects. Thus, hCP pinch strength was less than 29% of the TD value at age 12 (**Figure 1.2)**); impairment relative to TD children increased.

Across the studies, the dominant hand in TD children had a mean lateral pinch strength of 44 N at 6.5 years old and this value increased to 69 N by the age of 12.0 (**Figure 1.2)**). These pinch values were slightly less than the values reported for the TD non-dominant hand. Mean lateral pinch strength for the non-paretic hand in children with hCP was around 38.7 N, a value similar to the dominant hand in TD children, at 8.5 years old of age. Unlike the situation for the paretic hand, strength in the non-paretic hand increased with age, up to 50 N for 11-year-olds (**Figure 1.2)**). For the 6.5-year-olds with hCP, maximum lateral pinch was three times greater for the non-paretic hand in comparison with the paretic hand. This disparity was almost four-fold for 15-year-olds.

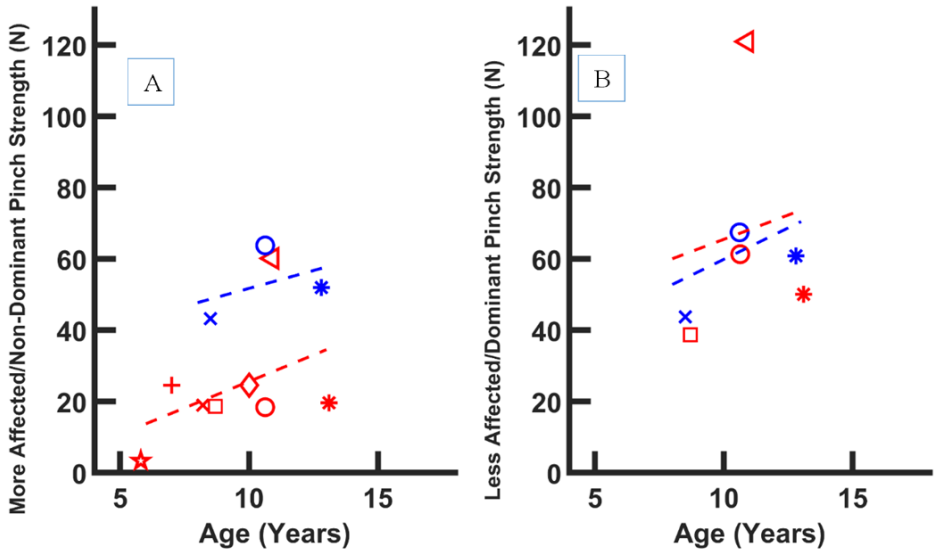

Figure 1.2: Maximum lateral pinch vs. age. A) The paretic hand in children with CP (red symbols, y = 2.97x - 4.086) and the non-dominant hand of TD children (blue symbols y = 2.00x + 31.69). Data aggregated from eight articles with a total of 257 participants with CP, 16 TD participants, and TD normative data. Trend lines represent a linear fit to the aggregated data. Reported paretic hand data appears to increase with age but was less than non-dominant hand strength at all ages. B) Maximum lateral pinch strength for the non-paretic hand of children with CP (red symbols y = 2.73x + 38.22) and the dominant hand for TD children (blue symbols y = 3.53x + 24.56). Values for non-paretic hand exhibit a more normative increase with age. Red symbols are associated with data from the paretic hand, blue symbols are associated with data from the non-paretic hand. Marker symbols indicate that each group of markers come from the same study. [18–25].

1.2.2.2 Finger Forces

Three articles were included in the review which examined finger flexion force or finger extension force. Participants ranged in age from 6.5 to 12.5 years old [26–28]. Finger flexion force was evaluated by having the index and middle fingers press together on a lever. The finger flexion force of the dominant and non-dominant hands of TD participants tended to be greater in older children, with similar values for both hands (dominant hand: 20N at 6.5 yrs and 40 N at 12.5 yrs; non-dominant hand: 18N at 6.5 yrs, 38 N at 12.5 yrs).

The finger flexion force values of participants with hCP were substantially reduced compared to the values for TD children, although older subjects with hCP were generally

stronger than younger children with CP (8 N at 6.5 yrs, 14 N at 10.9 yrs, 12 N at 12.5 yrs) [26,27]. The reported non-paretic finger flexion force of participants with hCP was relatively high for younger children but low for older children (non-paretic hand: 35N at 6.5 yrs and 25 N at 12.5 yrs). Only one of the articles located by the search reported measurements for extension force; the actual fingers used in the measurement, however, were not specified [28].

1.2.2.3 Range of Motion (ROM)

Studies investigated active range of motion (AROM) in both the wrist and digits of the hand. One article found a significant negative correlation between AROM of the wrist and the Ashworth score for the finger flexors [29]. Additionally, AROM was generally decreased in individuals who exhibited high variation of force (60% coefficient of variation or higher) when attempting to maintain an isometric force [29]. One article reported wrist ROM achieved during performance of several upper limb tasks [30]. Three articles, totaling 144 participants ranging in age from 4.6-7.8 years, reported AROM for the wrist together with either the Manual Ability Classification System (MACS) or Gross Motor Function Classification System (GMFCS) classification [31–33]. These articles reported that participants with higher overall function had greater wrist AROM. Participants classified as GMFCS I and either MACS I or II had a mean wrist AROM of 105°, while participants classified as MACS III had a mean wrist AROM of 22°. A fourth study reported maximum active wrist extension, together with Zancolli classification, for 20 children with hCP [29]. Those children classified as Zancolli I could achieve 27° of wrist extension beyond the neutral position, while those classified as Zancolli IIB could not extend the wrist beyond 42° of wrist flexion relative to the neutral position.

1.2.2.4 General Kinematics

Thirteen articles that analyzed hand or finger kinematics were identified [30,34–45]. Almost all these studies, however, examined displacement of the hand relative to the body or to an object rather than rotation of the joints of the digits. A few studies have tracked wrist joint angles during upper limb movements. Mutsaarts et al. measured the joint angles at the wrist, elbow, and shoulder during reaching and grasping. They reported differences in the velocity trajectories between children with hCP and typically developing children [44]. Mailleux et al. placed markers on the trunk, acromion, humerus, forearm, and hand and performed three-dimensional motion analysis on the upper limb during hand-to-head, hand-to-mouth, and reach-to-grasps tasks in children with hCP [43]. They found significant differences in the upper limb movement pathology among children with different impairment levels, as measured with MACS. Gaillard et al. 2019 created a method of using 3D kinematic assessment of bimanual performance in a game-like situation [30]. They were able to successfully use this system to detect differences in upper limb kinematics between typically developing children and those with hCP.

1.2.2.5 EMG

While use of EMG recordings was limited in the reviewed studies, three articles did measure wrist EMG signals during various hand tasks. One article found that muscle activation and coactivation in the wrist flexors and extensors were increased in the paretic hand when compared to the non-paretic hand during grip [46]. Another article described a correlation between grip and pinch and the integral of the EMG signal envelopes (IEMG) of the paretic wrist muscles (flexor carpi radialis and extensor carpi radialis) [47]. During grip, the children with hCP had significantly lower wrist IEMG values than TD children. No differences were detected in the arm IEMG (biceps and triceps). During pinch, the arm and wrist IEMG activations were

not significantly different between the CP and TD children [20]. Some studies discussed EMG but their results did not directly relate to hand function [48].

1.2.2.6 Magnetic Resonance Imaging (MRI)

Due to the disparity in methods used for acquiring and analyzing MR data, it was difficult to draw comparisons across the 49 studies reviewed which reported MRI and hand function data for children with hCP. Seven articles reported MRI data which was not easily comparable to other studies and did not include any of the other functional or clinical measurements sought for in this review [49–55]. Data from nine representative articles are presented: one reported asymmetry indices (AI) obtained from diffusion tensor imaging (DTI) data, four reported laterality index (LI) scores obtained from fMRI data, and four reported relationships between AI or LI scores and hand function measurement scores [56–64]. Five of these studies examined the relationship of AI or LI to MACS or GMFCS [56–60]. The AI values were calculated using the cross-sectional area of the corticospinal tracts at the level of the middle of the cerebellar peduncles [56]. Higher GMFCS levels (indicating a lower level of functioning) were associated with lower AI values. TD children had an average AI value of 0.99, while children with hCP GMFCS I had an average AI value of 0.54 and children with hCP GMFCS II had an average AI value of 0.45. Greater symmetry between the corticospinal tracts (indicated by an AI score closer to 1) has been associated with better scores on tests of digital dexterity, manual dexterity, stereognosis, and the ABILIHAND-Kids score [61]. The LI values were calculated using fMRI data recorded during cyclical squeezing of a sponge ball or extending and flexing the fingers at a rate of 2 Hz [57–60]. An LI = 1 indicates contralateral activation, LI = 0 indicates bilateral activation, and LI = -1 indicates ipsilateral activation [58]. The studies reported that higher LI

scores (closer to 1, thereby indicating activation of the contralateral hemisphere) were associated with less impairment, as measured with MACS (**Figure 1.3**).

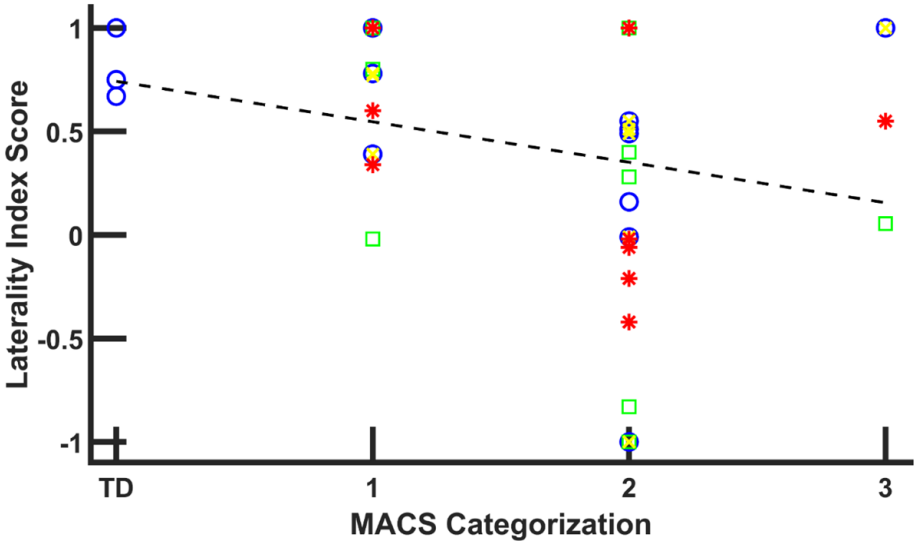

Figure 1.3: Laterality index (LI) values for children with hCP and TD children. [57–60] LI = 1 indicates activation entirely of the motor cortex contralateral to the hand; LI = 0 indicates bilateral activation; and LI = -1 indicates ipsilateral activation.[58] Greater contralateral activation was associated with less impairment. Trend lines indicate linear fit to LI data (y=-0.196+0.742). Marker symbols indicate that each group of markers come from the same study.

Several studies also reported associations between MRI measurements and performance on tests of hand function and sensory capability. One study found that improved AHA and MUUL scores were associated with more symmetrical cortical spinal tracts as measured by DTI [62]. One study found that LI values closer to 0 during bimanual tasks, indicative of better symmetry, tended to be associated with better performance on MUUL and AHA [63]. One study found that better two-point discrimination performance was associated with higher LI values for the primary and secondary somatosensory cortexes [64].

1.2.2.7 Purdue Pegboard Test

Ten articles described outcomes for subjects performing the Purdue Pegboard Test (PPT), an assessment requiring a participant to place as many pegs as possible (up to 50) in holes within 30 seconds [39,44,65–72]. The aggregated data from these studies came from 175 participants with hCP who ranged in age from 8 to 18 years.

Aggregated data show a trend for increasing PPT score as age increases from 8 to 19 years old for participants with hCP. TD participants scored higher on the PPT with their non-dominant hand than their hCP counterparts did with their paretic hand. Values for the non-paretic hand in children with hCP were quite similar to those of the dominant hand in TD children for the ages studied.

1.2.2.8 Jebsen Taylor Test of Hand Function (JTTHF)

Scores for the JTTHF, requiring the participant to perform a set of 7 tasks with one hand, were evaluated from 32 of the articles reviewed. From the mean data reported for different age groups for the 32 studies, it can be seen that across a range of ages (6 – 15 years old), children with hCP required substantially more time to complete the JTTHF with their paretic hand (**Figure 1.4)** [22,57,59,60,73–100]. In contrast, times for the non-paretic hand were quite similar to those of TD children. Seven studies provided individual data, including that from older children. These data suggest that JTTHF performance with the paretic hand may improve with age (**Figure 1.4**) [57,59,92,93,101–103]. The combined data from these seven studies shows that children younger than 10 years old had an average paretic hand JTTHF time of 449 seconds, while those older than 10 had an average JTTHF time of 242 seconds, still well above the time achieved with the non-paretic hand average (48.4 seconds) or by TD children with the dominant hand (38.4 seconds).

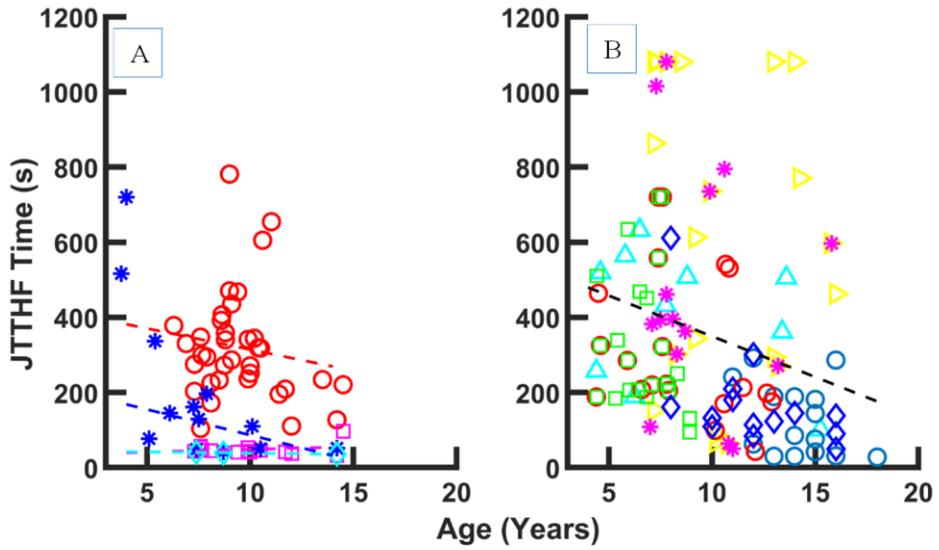

Figure 1.4: **A) Average JTTHF times reported across 32 studies.** [22,57,59,60,73–100]. Times for children with CP demarcated with shades of red (paretic hand: red symbols and linear fit, y = -11.25x + 426.6; non-paretic hand: magenta symbols and linear fit, y = -1.43x + 34.04). Times for TD children demarcated with shades of blue (dominant hand: cyan symbols and linear fit, y = -0.664x + 45.08.; non-dominant hand: blue symbols and linear fit, y = -13.63x + 222.85.) B) Individual JTTHF times vs. age for the paretic hand of children with CP from seven studies. [57,59,92,93,101–103] Regression: y = -21.66x + 566. Marker color and symbols indicate that each group of markers come from the same study.

1.2.3 Conclusions

In general, paretic hand function of children with hCP was worse than for the non-paretic hand or the dominant or non-dominant hands of TD children. For example, for both pinch and grip, substantial force deficits were evident in the paretic hand relative to the non-paretic hand or the hands of the TD children [19,20,91,104–106]. While absolute strength improved with age, relative deficits in comparison with typically developing peers stayed the same or even worsened with age. For older children with hCP, grip and pinch strength in the paretic hand was typically reduced by more than 50% in comparison with values for TD children. Strength of the non-paretic hand, however, was similar to that of the hands of TD children. Measures of hand dexterity, such as the JTTHF, showed greater relative improvement in performance with the

paretic hand, although completion time in older children with hCP was on average 6 times greater than for their TD peers.

1.2.3.1 Functional Performance

The use of standardized instruments, such as the JTTHF, facilitated aggregating data in order to examine performance across a large cohort and range of ages. General trends showed that older children with hCP typically performed better on the tasks with their paretic hand than younger children with hCP, although scores continued to lag those of the non-paretic hand or of typically developing children. In contrast to the strength measurements, the deficits of the paretic hand relative to scores of the TD hands tend to decrease with age. Part of the reduction may be attributable to a ceiling effect for time to perform a task (e.g., JTTHF) or number of objects that can be moved (e.g., PPT). Additionally, or alternatively, older children may have better learned how to best exploit existing capabilities of the paretic limb to perform tasks.

The clinical instruments included in this review place different relative requirements on hand and arm control and their coordination. The Purdue Pegboard Test, for example, may require considerable arm and trunk control to position the hand away from the body to complete the task. Other measures may better capture fine manual dexterity. Several the tasks of the Jebsen-Taylor Test of Hand Function focus on precise finger movements with limited arm movement. For the articles included in this review, the JTTHF was the instrument used most often. It has the added advantage that normalized data for the JTTHF have been produced for age ranges 5-19 years old in TD children [107,108].

Despite the profound functional role of the hand, sensorimotor characteristics of the hand have been studied to a lesser extent than those for the rest of the arm in children with hCP. The specific impairment mechanisms of the hand remain incompletely understood, thereby limiting

the capacity to target therapy for the individual. Data were especially limited for kinematics and kinetics of individual fingers and the thumb and both voluntary and reflexive muscle activation patterns. These data are needed to better mitigate possibly life-long disabilities.

1.3 Identification of Individuation as Understudied Area

Finger flexion forces for children were lower than their TD peers. Presumably force deficits are even greater for wrist and finger extension, but relatively few studies have examined finger extensor strength, despite prevalent deficits in hCP [28]. Only a few articles employed load cells to quantify fingertip forces [26–28]. Potential issues such as involuntary finger force coupling or differences in relative weakness across fingers require further investigation to direct rehabilitation efforts.

Most of the reviewed kinematic analyses focused on active or passive range of motion of the wrist or on reach-to-grasp tasks. Use of technology, such as 3D motion tracking, was limited to gross movement and was not used to examine movement of the fingers. Greater range of motion was associated with higher motor function and 3D kinematic analyses were successfully used to discriminate between children with different MACS levels.

The AROM of the paretic wrist could be quite limited, and greater wrist AROM was associated with higher function [31–33], as determined by the MACS or Zancolli scales. However, examination of finger and thumb movement was quite limited. The use of available measurement sensors and technologies could facilitate fully three-dimensional kinematic analyses of digit motion. Simultaneous tracking of individual digits, for example, would allow evaluation of finger individuation and fine motor control.

The results from the literature review highlighted that fine motor control of the hand has not been well described in children with hCP. Studies quantifying kinematics or kinetics have tended to focus on the entire upper limb or gross control of all fingers together.

Finger individuation, the ability to independently produce movement or force with each digit, is especially likely to be affected for children with hCP. Children with CP often exhibit diminished ability to independently generate finger forces or finger movement, thereby adversely impacting task performance. As individuation capability is responsible for 61% of total hand function [109], loss of individuation can profoundly impact overall function, especially as modern tools require an ever increasing degree of manual dexterity to operate. Individuation capability is well characterized for post-stroke adults [110–112], and some attention to this aspect of hand function has been given to adults with CP [113,114]. Yet, surprisingly few studies have addressed finger individuation in children with hCP. Because finger individuation and finger strength can improve independently [111], it is necessary to measure and rehabilitate finger individuation specifically.

1.4 Dissertation Outline

The goal of this project was thus to further the characterization and the understanding of the mechanisms leading to individuation deficits in children with hCP. The ability to independently control each digit in terms of movement and force production was assessed in children with CP and TD children. Neural control was evaluated with high density EMG electrode arrays and transcranial magnetic stimulation. As the ultimate goal of this research was to improve fine motor control, research was also undertaken to facilitate hand rehabilitation in children with hCP. Namely, a novel pneumatic actuator for a soft hand exoskeleton was developed and evaluated.

1.4.1 Chapter 2: Characterization of Individuation Capability

The individuation capability of typically developing children and children with hCP was evaluated. Participants performed individuated finger presses, individuated finger flexions, and completed a clinical evaluation of unimanual hand function (Jebsen-Taylor Test of Hand Function) [112,115]. Results between TD children and children with hCP were compared, and results between the paretic and non-paretic hands of the children with hCP were compared. This characterization of individuation capability sought to determine the extent of individuation deficits and the relationships between force individuation, finger movement individuation, and clinical assessments.

1.4.2 Chapter 3: TMS

An experiment was designed to the determine the contributions of the ipsilateral and contralateral hemispheres of the brain in children with hCP and TD children to control of individuated finger force production. TMS was used to evoke finger force during a resting state and during production of motor imagery of paretic/non-dominant finger force flexion [116]. TMS was also used inhibit motor areas during voluntary force production to estimate the relative contribution of those areas to individuation [117] .

1.4.3 Chapter 4: Actuators and AVK

A finger individuation training platform, based on the Actuated Virtual Keyboard system [112], was refined and made portable. The system is intended be used by populations with impaired hand function which might benefit from the system promoting targeted, and repetitive practice of individuated movements. The pneumatic finger extension actuators for this system were redesigned for fabrication out of elastomeric material. The new soft actuators were designed according to requirements for easy fabrication, high extension torque and low passive bending resistance. Various actuators designs were created. These were tested using finite

element model simulations to compare passive bending resistance, extension torque, and air flow characteristics. Based on the simulation results, several actuator designs were fabricated, and the performance of the actuator designs were characterized. Based on the optimal design of the pneumatic channel, a prototype finger extension exoskeleton was created using the elastomer actuators incorporated within an athletic glove.

1.4.4 Chapter 5: Conclusions

In the last chapter, the results and implications of the experiments and training platform development are discussed. Future testing of the target population and testing and use of the training platform are also discussed.

CHAPTER 2: Kinetic and Kinematic Assessment of Finger Individuation Capability of Children with Hemiplegic Cerebral Palsy

Adapted from: J. McCall et al., "A Platform for Rehabilitation of Finger Individuation in Children with Hemiplegic Cerebral Palsy", *in 2019 16th ICORR*

2.1 Introduction

With an incidence of three of every thousand lives births, cerebral palsy (CP) is the most common movement disorder in children. Currently, 800,000 people in the U.S. alone are living with CP [3,118], a condition resulting from a non-progressive brain insult. The majority of children with CP commonly experience impaired hand function [6,7], which can adversely impact quality of life and participation in society. As most children with CP live into adulthood [8], the impairments will affect functional capabilities for decades. Traditional therapies are typically unable to fully restore hand function; key aspects of manual dexterity, such as finger individuation, are often not adequately targeted for rehabilitation.

Almost half of all children with hemiplegic cerebral palsy (hCP), the second most common form of CP, experience greatest impairment in the upper limb [6], particularly in the hand [7]. Our literature review (Chapter 1) confirmed that fine motor function of the hand is compromised in the paretic hand of children with hCP, but that the way these deficits present is not well characterized. One aspect of fine motor function, finger individuation, is can be used to predict the majority of variance in hand function [109]. While finger individuation has been characterized in neurotypical adults and post-stroke adults [110,115,119,120], similar studies for children with hCP are lacking. Deficits and impairment mechanisms may differ greatly between adult stroke survivors and children with hCP, due to the injury occurring to a developing neural system in the latter group.

Thus, further study of fine motor control in children with hCP is warranted. Evaluation of finger individuation capability would facilitate identification of individuals who might benefit from targeted training of finger individuation. Control of both individuated fingertip motion and force production are important for function. As neurological control of these two aspects of finger function may differ [121], evaluation of both aspects of individuation is needed to characterize sensorimotor control of the hand. Additionally, force and motion control may require distinct training paradigms to spur improvement in individuals with neurological impairment [99].

For this study, we examined both individuated force and movement production across all five digits in both hands of children with hCP and in typically developing (TD) children. Muscle activation patterns were assessed with high-density electromyographic (HDEMG) electrode arrays. We hypothesized that children with hCP would have poorer ability to create force and movement individuation in their paretic hand than in their non-paretic hand or than TD children would demonstrate with either hand. We further hypothesized that TD children would have no significant difference in individuation capability between their dominant and non-dominant hands, as force individuation is roughly equivalent between hands in adults [115], and finger individuation may approach maturity in performance around 10 years of age [122].

2.2 Methods

2.2.1 Participants

Children with hCP and TD children participated in the study. All participants were required to be 8-14 years old and to be free of orthopedic issues affecting use of the hand or arm. Children with hCP needed to have a Manual Ability Classification System (MACS)[123] score of I, II, or III to qualify . Participants provided informed written assent, and their parents provide

informed, written consent to participate in the protocol. The protocol was reviewed and approved by the Institutional Review Board of the University of North Carolina at Chapel Hill.

2.2.2 Experimental Protocol

Fine motor control was evaluated in both hands of each participant using three different assessments: Jebsen-Taylor Test of Hand Function (JTTHF), finger force individuation, and finger movement individuation. Each participant first performed all seven timed sub-tests of the JTTHF [14]. with the non-dominant or paretic hand. They then completed these tests with the dominant or non-paretic, hand.

During evaluation of force individuation, participants sat in a chair with their shoulder abducted (~45°) and the forearm pronated and supported using foam blocks. Each hand was tested separately. During assessment each digit tip rested on a separate six degree-of-freedom (DOF) load cell (Nano-17 or Mini40, ATI Industrial Automation, Cary, NC) (**Figure 2.1**). The position and orientation of each load cell were adjusted to fit each hand using mounting hardware such as adjustable ball-and-socket joints (RAM MOUNT, Seattle, WA), and magnetic bases. The hardware was positioned such that the wrist was in a neutral position and the digits were fully extended (**Figure 2.1**).

Figure 2.1: Participant's fingers resting on five 6-DOF load cells. The forearm is supported, and the wrist is in a neutral position. Digits were fully extended during testing.

HDEMG electrode arrays were placed on the forearm and hand to capture finger muscle activation patterns. Specifically, two 64-electrode EMG arrays, in a 5 x 13 configuration, were placed on the dorsal and ventral sides of the forearm, over the long finger extensors, such as extensor digitorum communis (EDC), and the long finger flexors, such as flexor digitorum superficialis (FDS), respectively. A 32-electrode HD EMG array, (4 x 8 configuration), was placed on the dorsal side of the hand to target the intrinsic muscles (**Figure 2.2)**. The EMG signals were sampled at 2048 Hz and bandpass filtered (10-900 Hz) by an EMG-USB2+ device (OT Bioelettronica, Italy). Sampled EMG signals were subsequently normalized by the peak values recorded during testing or maximum voluntary contraction trials.

Figure 2.2: HD EMG arrays on forearm and hand. Arrays were placed over the extrinsic finger extensor, extrinsic finger flexor, and intrinsic muscles. Flexor array placement is not visible in the figure.

At the start of the session, the subject was asked to produce maximum voluntary force (MVF) with each digit separately. Visual feedback was provided on a computer screen to encourage MVF production. During subsequent trials, the subject was instructed to create 25% of these MVF values with the specified digits while keeping all digits in contact with the load cells. Subjects were told to relax the digits not participating in the specified force generation. Visual feedback of the desired and actual force levels was provided for the instructed digit. Two different tasks were tested. In one, the participant was instructed to create force with a single digit. In the other task, participants created force with adjacent pairs of digits (e.g., thumb – index). Thus each hand had a total of 9 test conditions, and each condition was performed three times in succession during a given trial.

To evaluate finger movement individuation, passive, reflective markers were placed on the joints and tip of each digit in the hand, as well as on the back of the hand. Marker positions were continuously captured with a 12-camera motion capture system (120 Hz, VICON, Oxford, UK). Participants were seated, with the forearm pronated and supported, and the elbow flexed to 90°. Participants were instructed to start with their fingers maximally extended and then to

sequentially flex each finger individually while maintaining extension of the non-instructed finger. Each finger flexion was repeated three times.

2.2.3 Data Analysis

Finger Force Individuation:

To analyze force individuation, for each trial, a 250-ms window corresponding to minimal force variation during the isometric digit press was first identified. This window was used for subsequent analysis. The average force produced in the normal direction was determined for each digit. Force individuation of the digit(s) was calculated as a ratio of instructed digit force(s) to the total force across all of the digits (**Eqn. 2.1**) [122]. The higher the FI metric, the better the individual was able to independently create force with the instructed digit. For two-finger presses, the force of both instructed fingers was combined to compute $F_{instructed}$.

$$FI_j = F_{instructed}/[\sum_{j=1}^{n}[\left[\left(\sum_{i=1}^{n}(F_{ij})\right)\right]/(n)] \quad (2.1)$$

To calculate the relative spread of force production across the digits, another metric, FI_DEV, was computed. This metric weighted force produced by uninstructed digits by their normalized distance from the instructed digit (**Eqn. 2**).

$$FI\_DEV_j = \left[\left(\sum_{i=1}^{n}(F_{ij} * abs(Finger_{instructed} - Finger_{ij})\right)\right] \quad (2.2)$$

Finger Force EMG:

EMG signals were resampled at 2000 Hz to match the sampling rate of the force data. Electrical noise and motion artifacts were removed from EMG data using an algorithm described in the literature [30]. Common average reference spatial filtering was employed across all channels of each electrode array at each time point of the recording to minimize common noise.

A 20-Hz high-pass filter was then applied, the data were rectified, and a 250-ms moving average filter was applied. The resulting signal for each channel was normalized according to its peak value recorded during the experiment. 2D activation maps were generated for each electrode array for the time window used to calculate force individuation. For each activation map, the centroid of activation was calculated (**Eqn. 2.3 & 2.4**):

$$C_x = \sum_{i=1}^{n}[\sum_{j=1}^{n}[AMP_{ij} * x_i]] \setminus \sum_{i=1}^{n}\sum_{j=1}^{n}[AMP_{ij}] \quad (2.3)$$

$$C_y = \sum_{i=1}^{n}[\sum_{j=1}^{n}[AMP_{ij} * y_i]] \setminus \sum_{i=1}^{n}\sum_{j=1}^{n}[AMP_{ij}] \quad (2.4)$$

The sum of squared differences (SSD) between activation maps resulting from different tasks and for the same type of tasks were calculated (**Eqn. 2.5**).

$$SSD = \sum_{i=1}^{n}[\sum_{j=1}^{n}[A_{AMP_{ij}} - B_{AMP_{ij}}]^2 \setminus \sum_{i=1}^{n}\sum_{j=1}^{n}[A_{AMP_{ij}} + B_{AMP_{ij}}]^2 \quad (2.5)$$

Finger Movement Individuation:

Marker position data from the VICON were filtered using a 2nd-order Butterworth low-pass filter with a 10-Hz cutoff. These data were used to calculate the flexion/extension angles of the metacarpophalangeal (MCP) and proximal interphalangeal (PIP) or interphalangeal (IP) of each digit during each movement. From the joint angles, a movement individuation index (MI), was then computed. For MI, the joint angles were identified at the time when the angular displacement of the MCP and PIP (IP for the thumb) joints of the instructed finger first summed to 90^0. The summed MCP and PIP (or IP) displacement of the uninstructed digits normalized to 90° were used to compute the individuation of the instructed finger using **Eqn. 2.6** [124]. The distribution of unintended finger flexion was weighted according to the difference in position between each finger and the instructed finger to create the metric MI_DEV (**Eqn. 2.7**).

$$MI_j = \emptyset_{instructed}/[\sum_{j=1}^{n}[\left[\left(100\% * \sum_{i=1}^{n}(\emptyset_{ij})\right)\right]/(n)] \quad (2.6)$$

$$MI\_DEV_j = \left[\left(\sum_{i=1}^{n}(\emptyset_{ij} * abs(Finger_{instructed} - Finger_{ij})/(\sum_{i=1}^{n}(\emptyset_{ij}))\right)\right] \quad (2.7)$$

2.2.4 Statistical Analysis

Means and standard deviations were calculated for the primary outcome measures: JTTHF score (the difference in total task completion time between the dominant/non-paretic and non-dominant/paretic hands [14]), finger force individuation for single finger presses, and finger movement individuation. A one-way Multivariate Analysis of Variance (MANOVA) was performed with the independent factor Hand (paretic, non-paretic, non-dominant, and dominant and the primary outcome measures as the dependent variables. If Hand significantly affected the multivariate analysis, then post-hoc univariate ANOVA was performed for each outcome measure. Pairwise testing of Hand was performed for ANOVAs exhibiting a significant effect using the Tukey Honest Significant Difference. Additionally, Pearson correlation coefficients were calculated between the primary outcome measures.

2.3 Results

A total of 10 TD children (5 male/ 5 female) and 4 children with hCP (2 male/ 2 female) participated in the study. The TD and children with hCP were well matched in terms of age (Table 2.1).

Table 2.1: Study Participant Data

TD Participants	**Sex**	**Age** (years)	**MACS** (I-V)
TD01	M	14	N/A
TD02	M	11	N/A
TD03	F	12	N/A
TD04	F	11	N/A
TD05	M	10	N/A
TD06	M	10	N/A
TD07	F	13	N/A
TD08	F	10	N/A
TD09	M	13	N/A
TD10	F	14	N/A
Mean ± SD	**5 M/5 F**	**11.8 ± 1.6**	N/A

hCP Participants	**Sex**	**Age** (years)	**MACS** (I-V)
CP01	F	10	3
CP02	M	10	1
CP03	F	13	3
CP04	M	12	1
Mean ± SD	**2 M/2 F**	**11.25 ± 1.5**	**2 ± 1.15**

Results of the one-way MANOVA revealed that Hand had a significant effect on the primary outcomes measures of JTTHF score, force individuation index value, and the movement individuation index and explained a significant portion of the variance ($p < 0.001$, 0.480). Subsequent ANOVAs were performed for each dependent variable.

2.3.1 Finger Force Individuation

The univariate ANOVA showed that Hand significantly affected the force individuation index, FI, averaged across all 5 digits ($p < 0.001$, $\eta p^2 = 0.639$) (**Figure 2.3**). The TD participants had a larger FI compared to the children with hCP (paretic: 0.338, non-paretic: 0.519, non-dominant: 0.599, dominant: 0.657). Post-hoc Tukey tests revealed that the score for the paretic hand was significantly smaller (poorer individuation) than the values for both the non-dominant

and dominant hands in the TD children (p-value < 0.001). The non-paretic hand also had a lower FI than the dominant hand (p = 0.035). Scores for the dominant and non-dominant hands and for the paretic and non-paretic hands were not significantly different (p = 0.717 and p = 0.093, respectively).

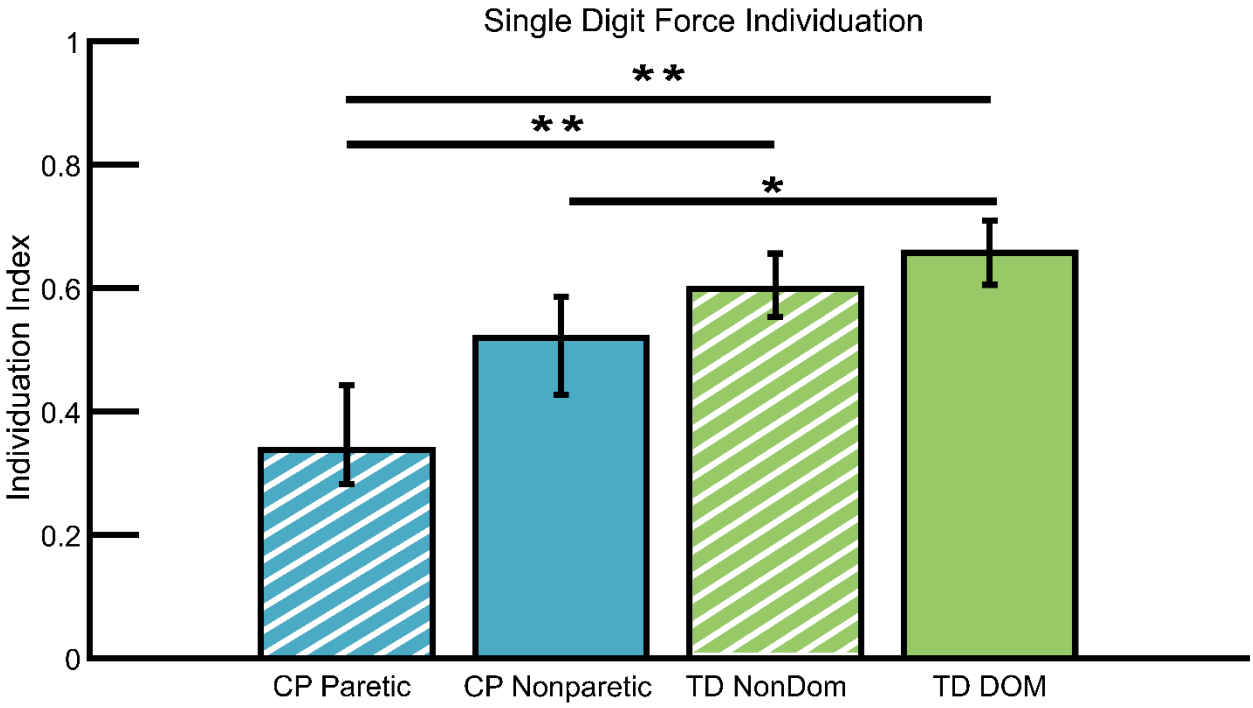

Figure 2.3: Single finger force individuation for each hand. (Non-paretic - Paretic: Dashed Blue, TD Non-dominant - Paretic: Blue, TD Dominant – TD Non-dominant: Dashed Green, and TD Dominant Non-paretic- Non-paretic: Green). Error bars represent 95% Confidence Interval. Horizontal significance lines indicate that two groups are significantly different. * p < 0.05, ** p < 0.01.

We examined individuation across individual digits as well. Across hands, individuation tended to be greatest for the thumb and index finger and least for the ring and pinky fingers (**Figure 2.5).** For the children with hCP, deficits between the paretic and non-paretic hands were greatest for the index, middle, and pinky fingers. The raw force data shows how the spread in force production was much wider across digits for the children with hCP, especially for the paretic hand (**Figure 2.4**).

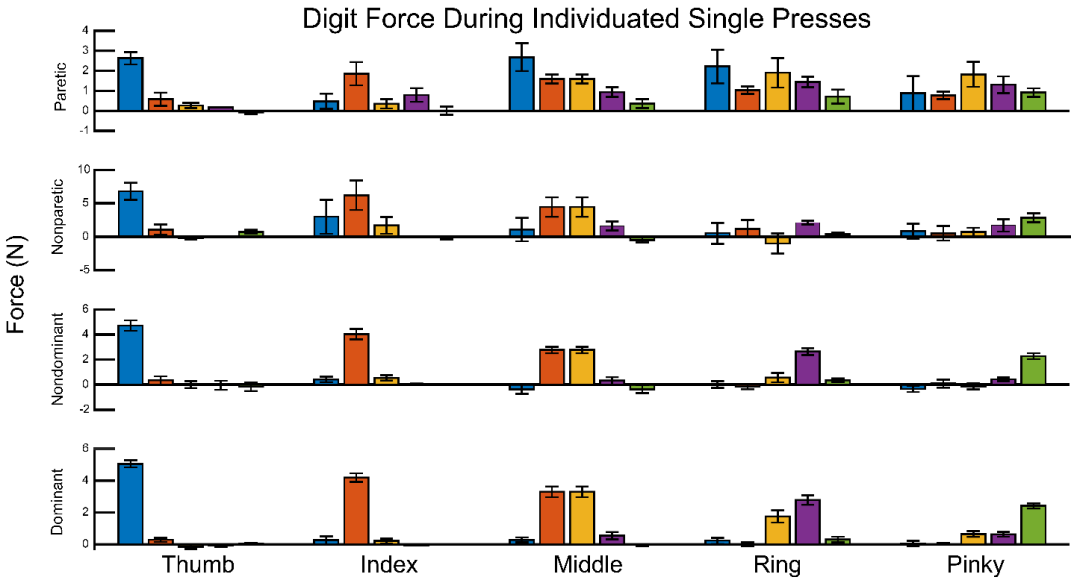

Figure 2.4: Flexion force for each finger during each type of single finger press. A) Paretic CP, B) Non-paretic CP, C) Non-dominant TD, D) Dominant TD. (Thumb: Blue, Index: Orange, Middle: Yellow, Ring: Purple, Pinky: Green). Error bars represent standard error.

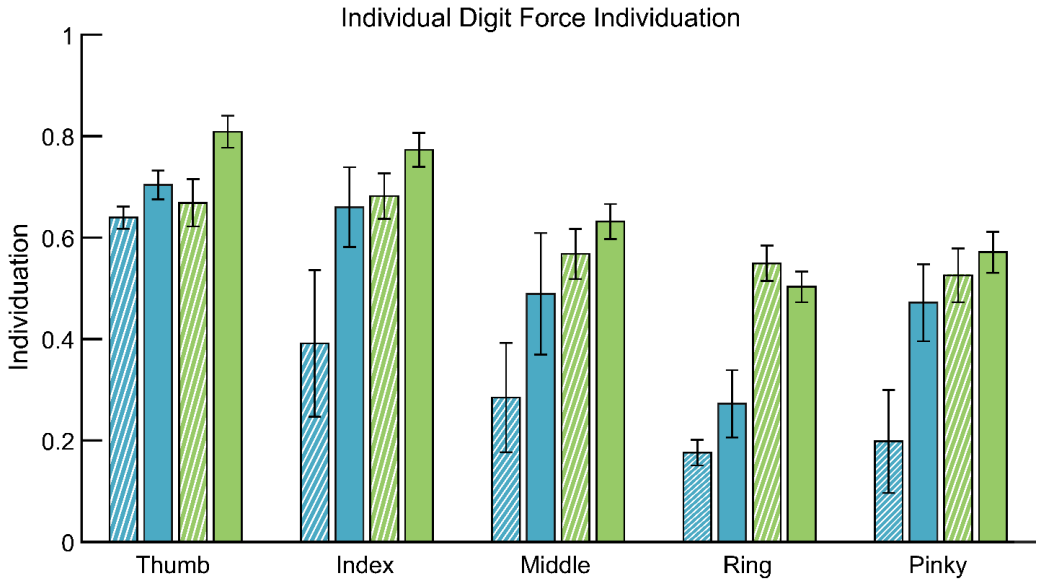

Figure 2.5: Single finger force individuation for each type of press for each hand. (Paretic: Dashed Blue, Non-paretic: Blue, Non-dominant: Dashed Green, and Dominant: Green). Error bars represent standard error.

Examination of force individuation deviation, $FI\_DEV_{SingleFinger}$, confirmed that the TD participants had better force localization during attempted force individuation compared to the children with hCP (paretic: 8.71, non-paretic: 9.45, non-dominant: 4.89, dominant: 3.18 individuation deviation). For the TD children, force created in uninstructed digits tended to be concentrated in adjacent digits, with relatively little to no force generated by non-adjacent fingers. For children with hCP, the distribution of unintended forces relative to the location of the instructed finger, was higher for the paretic and non-paretic hands than for the hand of the TD children (**Figure 2.6**). The thumb had the least deviation, and deviation increased with proximity to the pinky for the paretic and non-paretic hands (**Figure 2.7**).

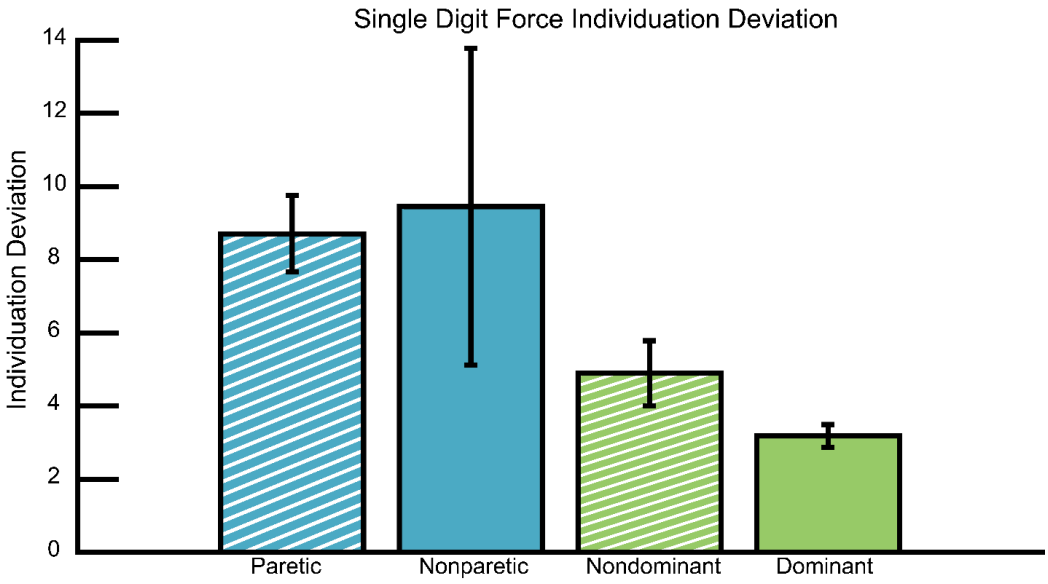

Figure 2.6: Uninstructed finger force weighted by deviation from the instructed position. (Force*Position Difference). Average value is displayed for each hand (Paretic: Dashed Blue, Non-paretic: Blue, Non-dominant: Dashed Green, and Dominant: Green). Error bars represent standard error.

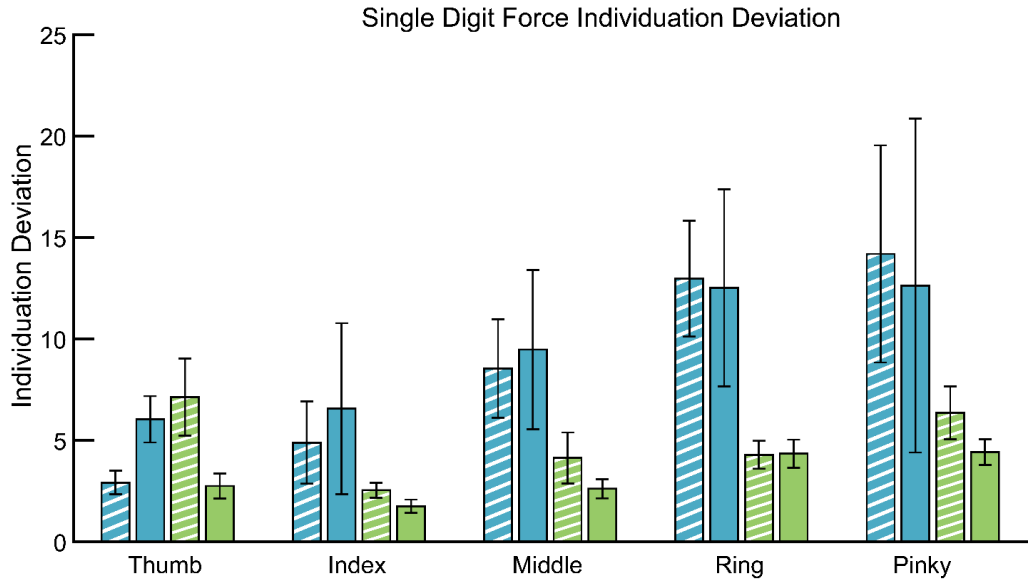

Figure 2.7: Finger Force Individuation Deviation for each type of press. (Force*Position Difference). Data is displayed for each hand (Paretic: Dashed Blue, Non-paretic: Blue, Non-dominant: Dashed Green, and Dominant: Green). Error bars represent standard error.

Each participant also performed two finger presses for each adjacent finger pair (Thumb-Index, Index-Middle, Middle-Ring, Ring-Pinky. TD children tended to exhibit a higher level of

force individuation for the two finger press than the children with hCP (FI values - paretic: 0.470, non-paretic: 0.629, non-dominant: 0.795, dominant: 0.779) (**Figure 2.8, Figure 2.9**). On average, two finger presses were more highly individuated than single finger presses (compare Figures 3 and 8)**.** However, the non-paretic hand only performed slightly better while the dominant and non-dominant hands of TD children performed much better on two finger presses. Additionally, two finger presses saw finger forces which were more frequently higher than the 25% MVC instructed force (**Figure 2.4, Figure 2.10)**. Participants were instructed to match 25% MVC for each instructed digit simultaneously. Presenting separate visual feedback for two fingers may have been cognitively demanding for the participants.

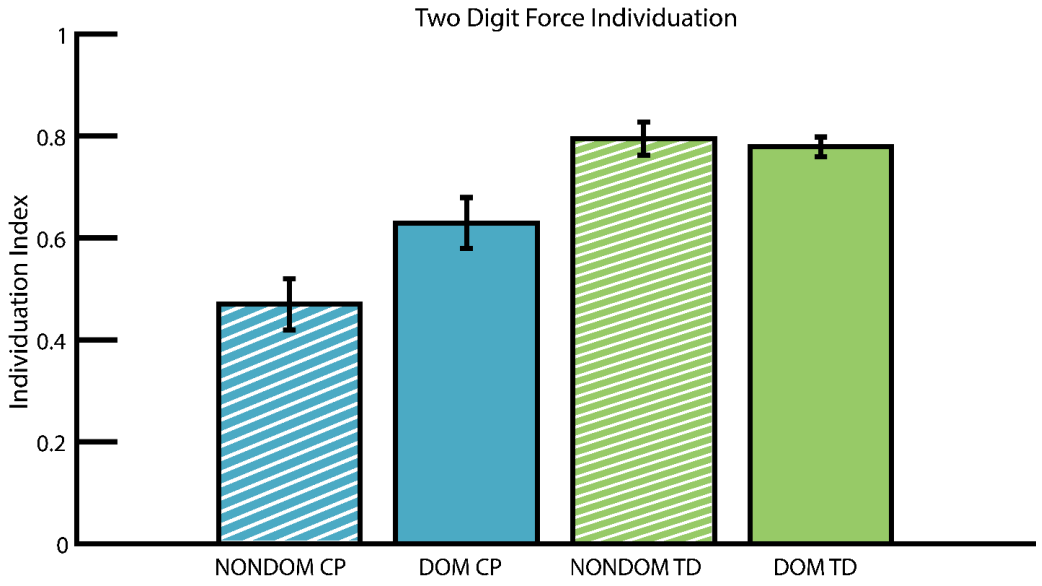

Figure 2.8: Average two finger force individuation for each hand. (Paretic: Dashed Blue, Non-paretic: Blue, Non-dominant: Dashed Green, and Dominant: Green). Error bars represent standard error.

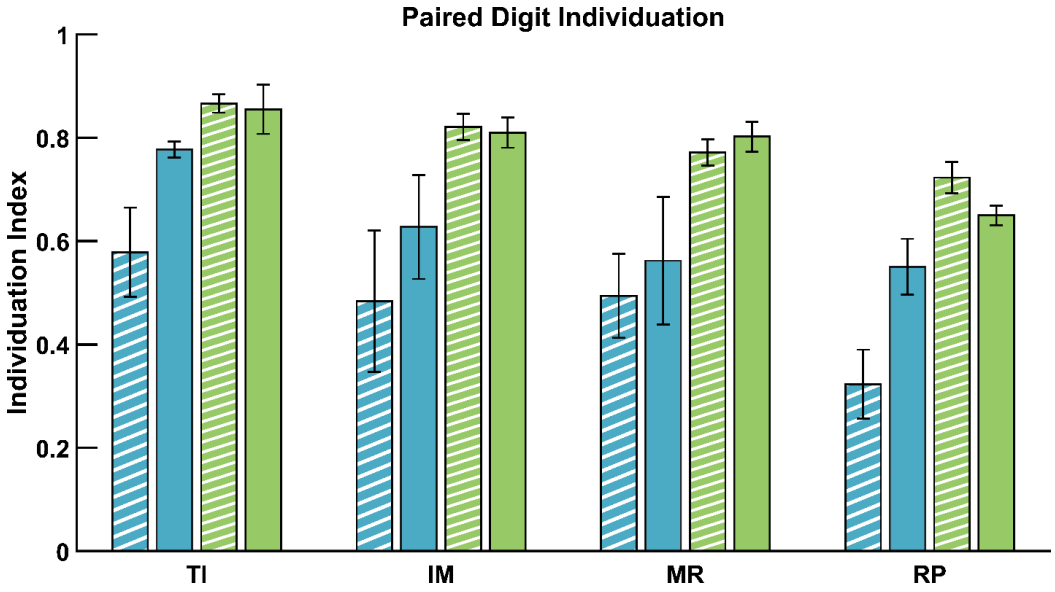

Figure 2.9: Two finger force individuation for each type of press for each hand. (Paretic: Dashed Blue, Non-paretic: Blue, Non-dominant: Dashed Green, and Dominant: Green). Error bars represent standard error.

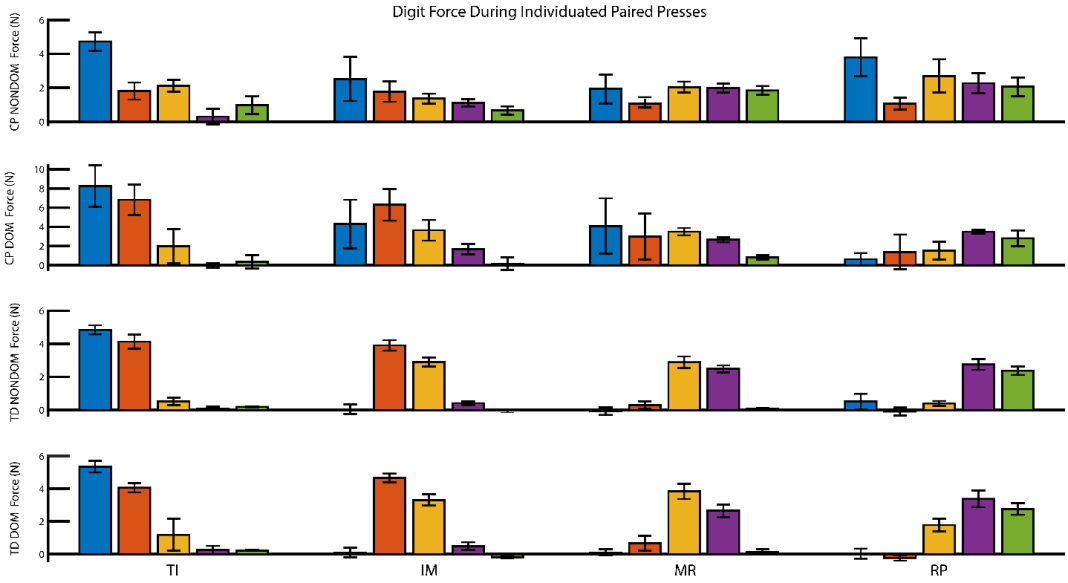

Figure 2.10: Flexion force for each finger during each type of two finger press. A) Paretic CP, B) Non-paretic CP, C) Non-dominant TD, D) Dominant TD. (Thumb: Blue, Index: Orange, Middle: Yellow, Ring: Purple, Pinky: Green). Error bars represent standard error.

Deviation of uninstructed finger force from the instructed finger position ($FI\_DEV_{TwoFinger}$) was higher for the non-paretic and paretic hand (9.42, 9.57 N*position) than for the non-dominant and dominant hands (2.79, 3.23 N*position) of the TD children (**Figure 2.11, Figure 2.12**). Children with hCP tended to have uninstructed finger forces more evenly distributed across adjacent and non-adjacent fingers, while TD children's uninstructed finger forces were generally located in fingers adjacent to the instructed fingers.

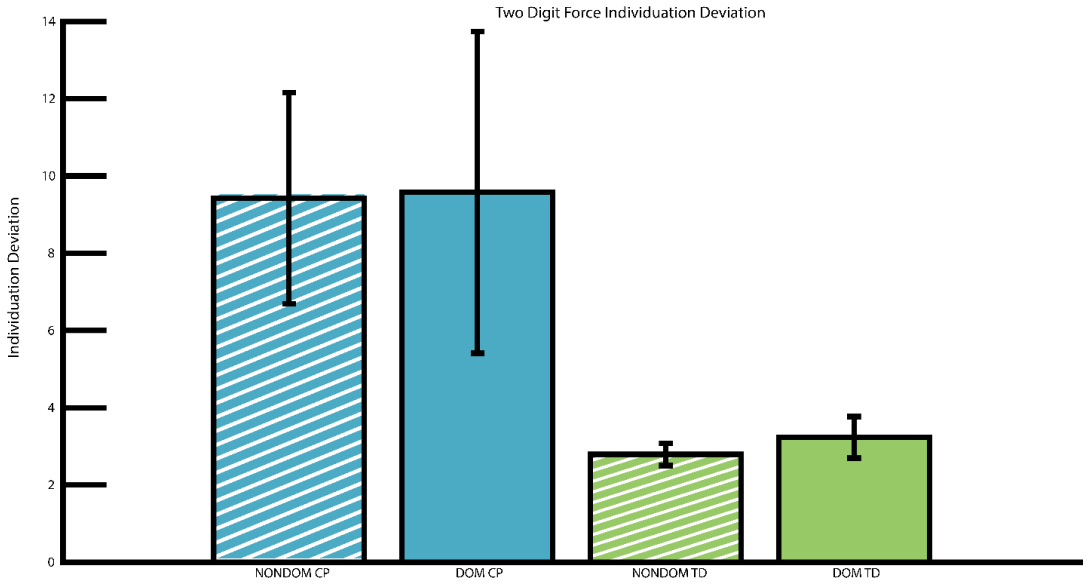

Figure 2.11: Two finger press individuation deviation. (Force*Position Difference). Average value is displayed for each hand (Paretic: Dashed Blue, Non-paretic: Blue, Non-dominant: Dashed Green, and Dominant: Green). Error bars represent standard error.

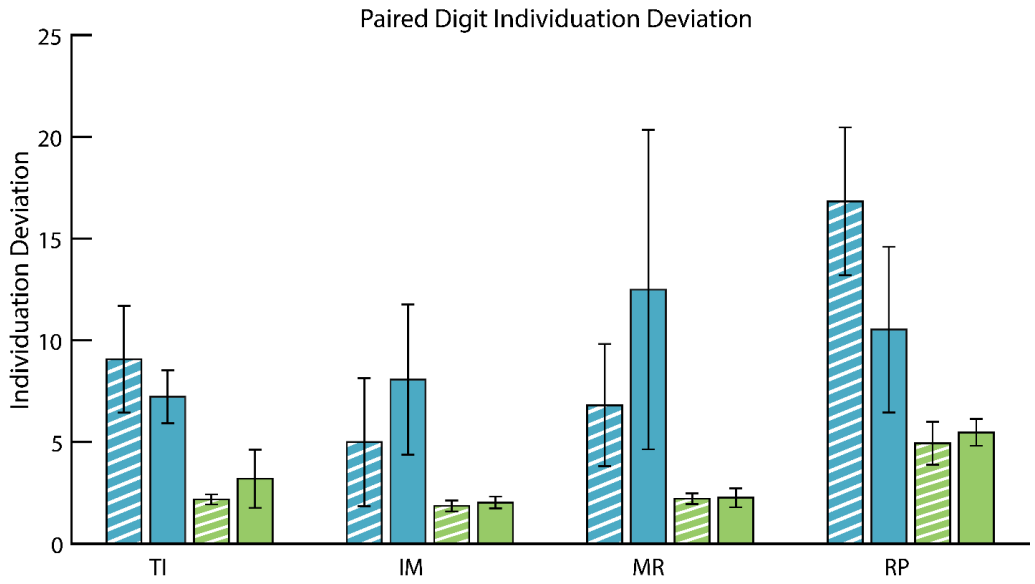

Figure 2.12: Two finger press individuation deviation for each press type. (Force*Position Difference). Data is displayed for each hand (Paretic: Dashed Blue, Non-paretic: Blue, Non-dominant: Dashed Green, and Dominant: Green). Error bars represent standard error.

EMG

Analyses were performed on the EMG data captured during force individuation tasks. These evaluations were focused on the data for the single-finger tasks for the index and middle fingers as the relevant activations were likely to be captured by the EMG electrode arrays and likely to be distinct from each other. The flexor and intrinsic separation of centroids of activation for the two presses were diminished in the paretic hand (paretic flexor: 5.5 mm (95% CI: 0.04-11.1mm), paretic intrinsic: 2.7 mm (95% CI: 0-10.4 mm)) compared to the non-paretic hand (non-paretic flexor: 10.4 mm (95% CI: 5.9-17.0 mm), non-paretic intrinsic: 13.3 mm (95% CI: 7.3-19.8 mm)) and the hands of TD children (non-dominant flexor: 9.7 mm (95% CI: 6.9-14.3 mm), non-dominant intrinsic: 10.0 mm (95% CI: 6.5-14.8 mm), dominant flexor: 8.5 mm (95% CI: 5.3-12.6 mm), dominant intrinsic: 8.0 mm (95% CI: 5.1-13.5 mm))(**Figure 2.13**).

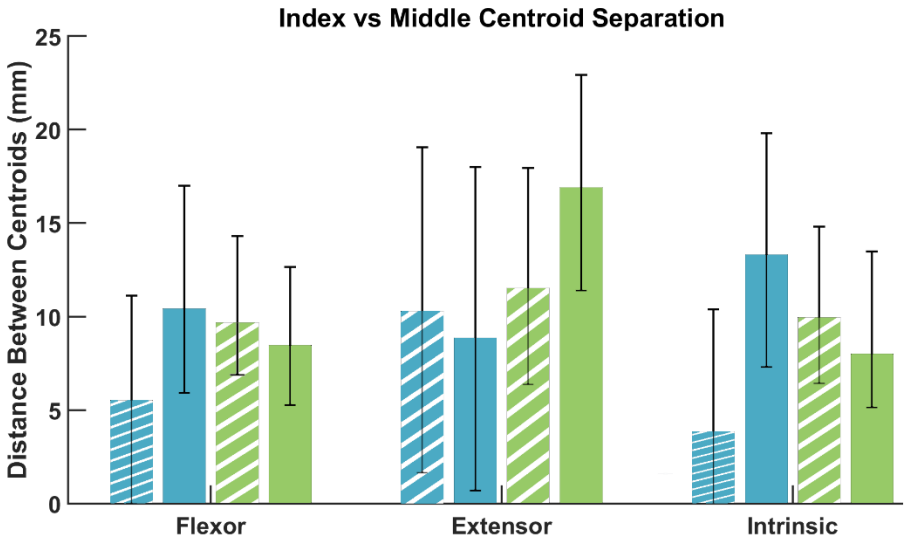

Figure 2.13: Separation of Centroids of Activation during Individuated Finger Presses. Data is displayed for each HDEMG array for each hand (Paretic: Dashed Blue, Non-paretic: Blue, Non-dominant: Dashed Green, and Dominant: Green). Error bars represent 95% Confidence Interval.

The SSD of activation maps for flexors, extensors, and intrinsic electrode arrays were calculated. For each participant the SSDs of activation maps between index vs middle, index vs ring, and middle vs ring were averaged for each hand (**Figure 2.14**). The average flexor, extensor and intrinsic activation map SSDs were lower for the paretic hand of children hCP than for the non-paretic, or for the dominant or non-dominant hand of TD children. The non-paretic hand of children had the highest average activation map for all three muscle groups, even compared to the dominant and non-dominant hands of TD children.

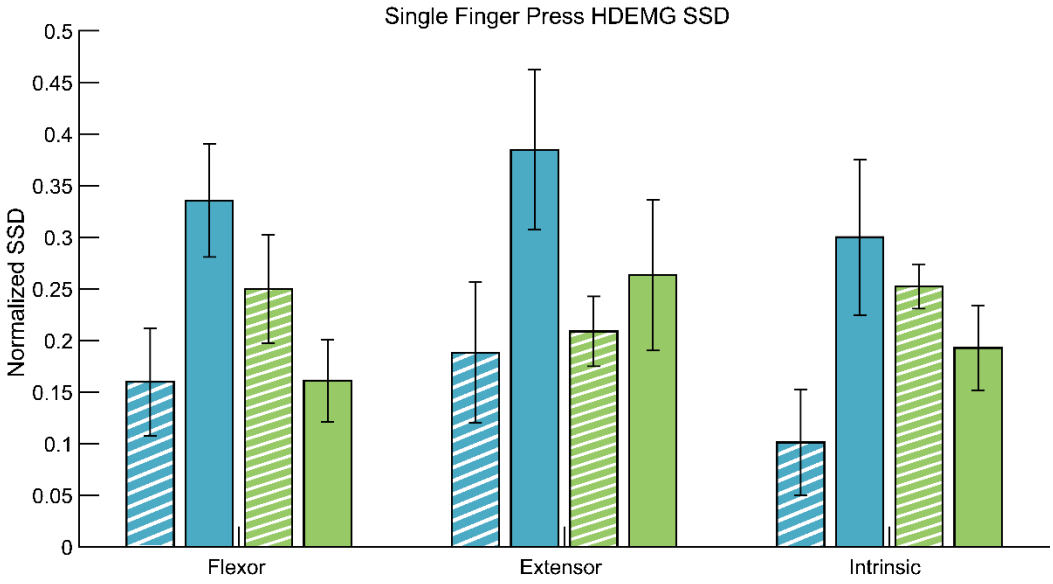

Figure 2.14: Averaged SSD of EMG activation maps. Average of Index vs Middle, Index vs Ring, and Middle vs Ring, for each hand (Paretic: Dashed Blue, Non-paretic: Blue, Non-dominant: Dashed Green, and Dominant: Green). Error bars represent standard error.

This high level of activation map modulation may be partially explained by the high level of activation map variation for the non-paretic hand even within the same type of press (**Figure 2.15**). This can be further explained by the inconsistent recruitment of unintended finger forces.

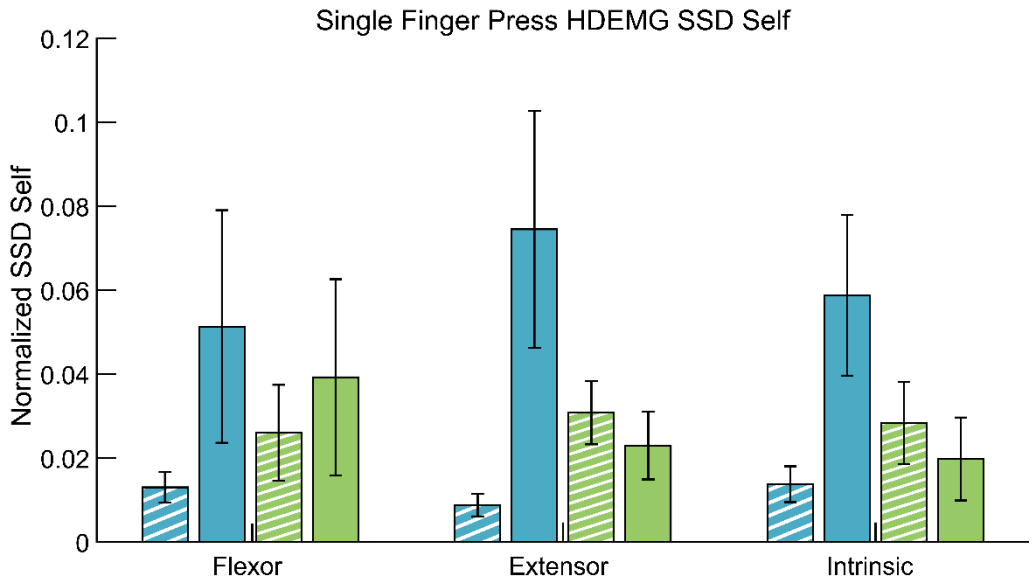

Figure 2.15: Averaged SSD of EMG activation maps within finger press types: Values averaged for Index, Middle, and Ring finger presses. Each hand is represented for each HDEMG array (Paretic: Dashed Blue, Non-paretic: Blue, Non-dominant: Dashed Green, and Dominant: Green). Error bars represent standard error.

Pearson correlation coefficients were calculated between intended force and each EMG channel. The channels with the three highest correlations were identified for each kind of press for each subject. In **Figure 2.16** a heat map indicates the fraction of the presses for which the channel has one of the three highest correlation values. The TD EMG channels with the highest correlation with instructed force tend to be clustered close together. The CP EMG channels with the highest correlation are spread more widely across the electrode array.

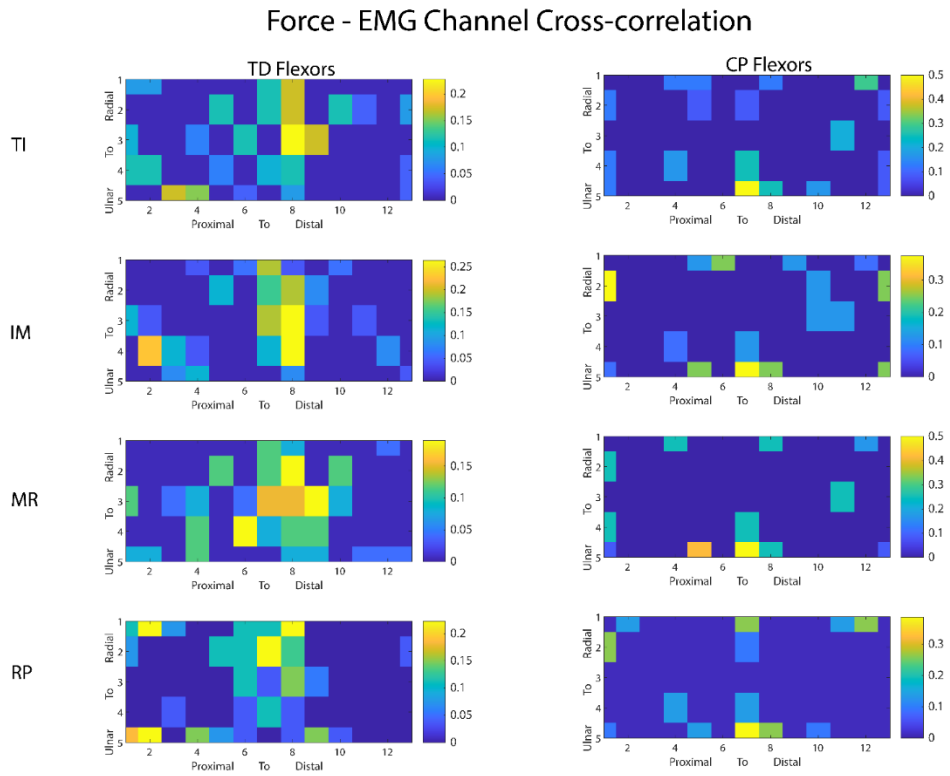

Figure 2.16: Cross correlation between EMG signal and instructed force. Flexor activation maps for different two finger presses (each row of plots) for TD participants (left column) and hCP participants (right column). The heat maps indicate the frequency with which each array is associated with being one of the three highest correlating channels with instructed finger force.

Visual representation of the change in the activation map and the location of the centroid are shown in Figure 2.17. More distinct changes between types of presses in centroid location and activation patterns are apparent in the TD maps than the CP maps.

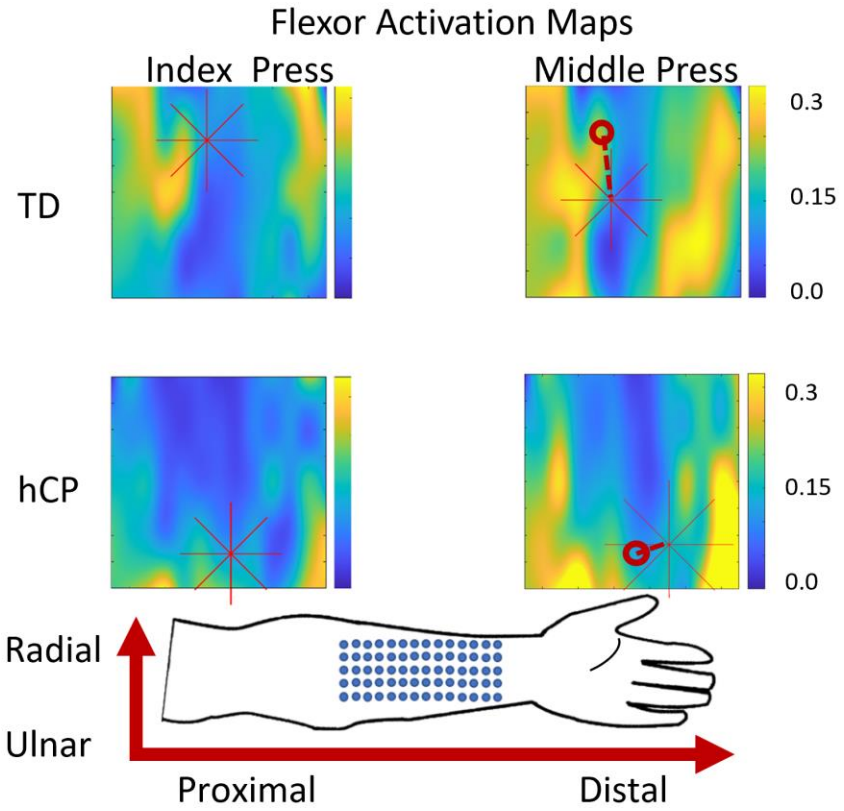

Figure 2.17: Representative TD (top row) and CP (bottom row) flexor activation maps. The maps shown are for index (left column) and middle finger (right column) finger presses. The centroid of activation for each map is indicated with a red marker, the difference in position between index and middle finger press is indicated with a red circle and dashed line. The image of a forearm indicates the ulnar/radial and proximal/distal directions for the 2D activation maps.

2.3.2 Movement Individuation

ANOVA results showed that the Hand factor also significantly affected the movement individuation metric, MI ($p < 0.001$, $\eta p^2 = 0.577$). Tukey pairwise comparisons revealed that MI for the paretic hand was significantly smaller than that of the dominant, non-dominant, and non-paretic hands ($p < 0.001$, $p < 0.001$, and $p = 0.021$, respectively) (**Figure 2.18**). No other significant differences were observed across hands. Aside from the paretic hand, MI tended to be greatest for the thumb and decreased modestly according to finger distance from the thumb (**Figure 2.19**). Overall, the MI values were much smaller than for the FI values. Interestingly, for the paretic hand, the MI values was greatest for the middle finger. In general, digit individuation was similar across fingers, slightly worsening moving from thumb to pinky (**Figure 2.20**).

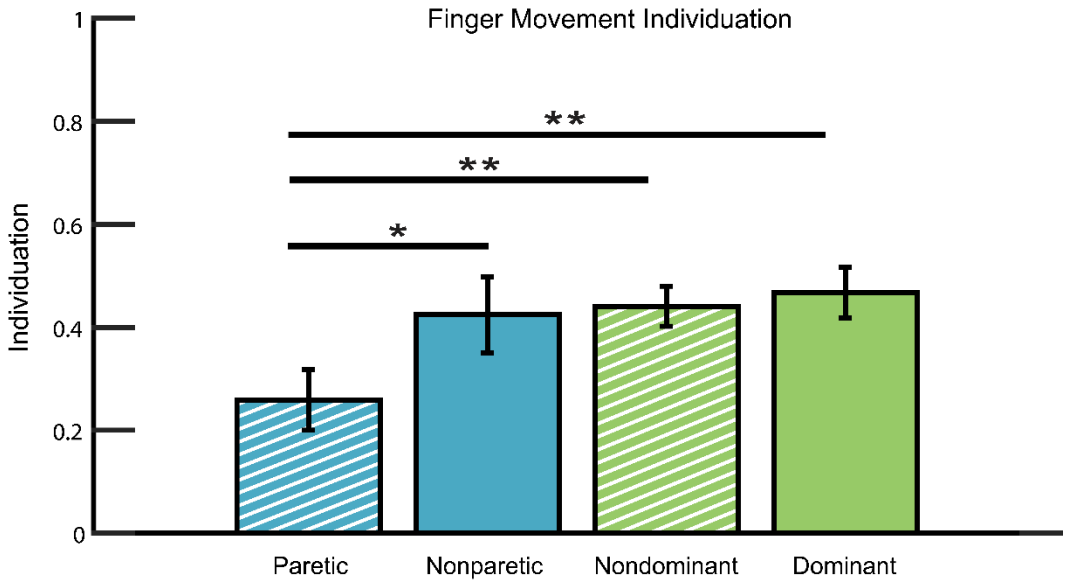

Figure 2.18: Movement individuation for each hand. (Paretic: Dashed Blue, Non-paretic: Blue, Non-dominant: Dashed Green, and Dominant: Green). Error bars represent 95% Confidence Interval. * $p < 0.05$, * $p < 0.01$

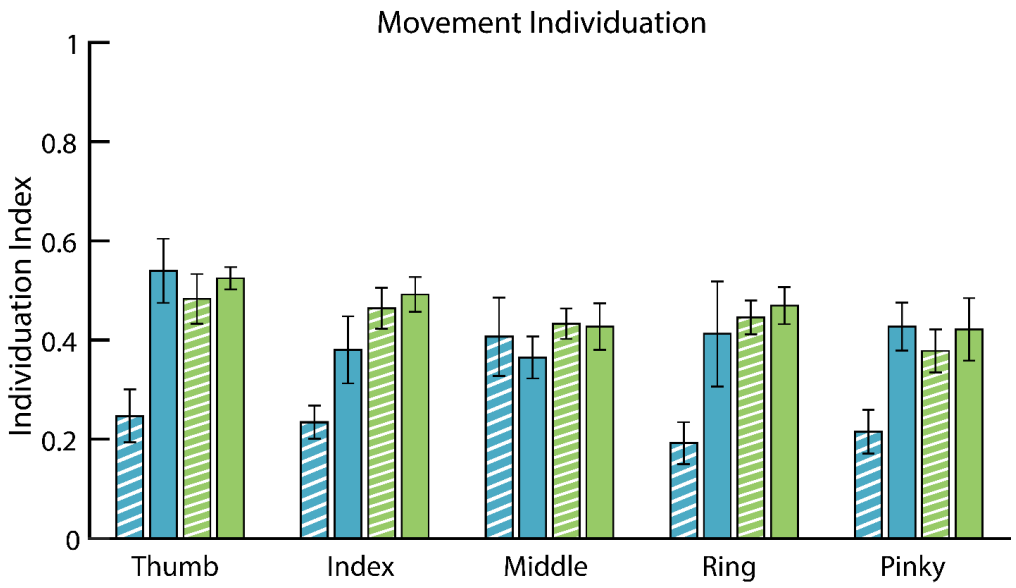

Figure 2.19: Movement Individuation for each type of single finger press for each hand. (Paretic: Dashed Blue, Non-paretic: Blue, Non-dominant: Dashed Green, and Dominant: Green). Error bars represent standard error.

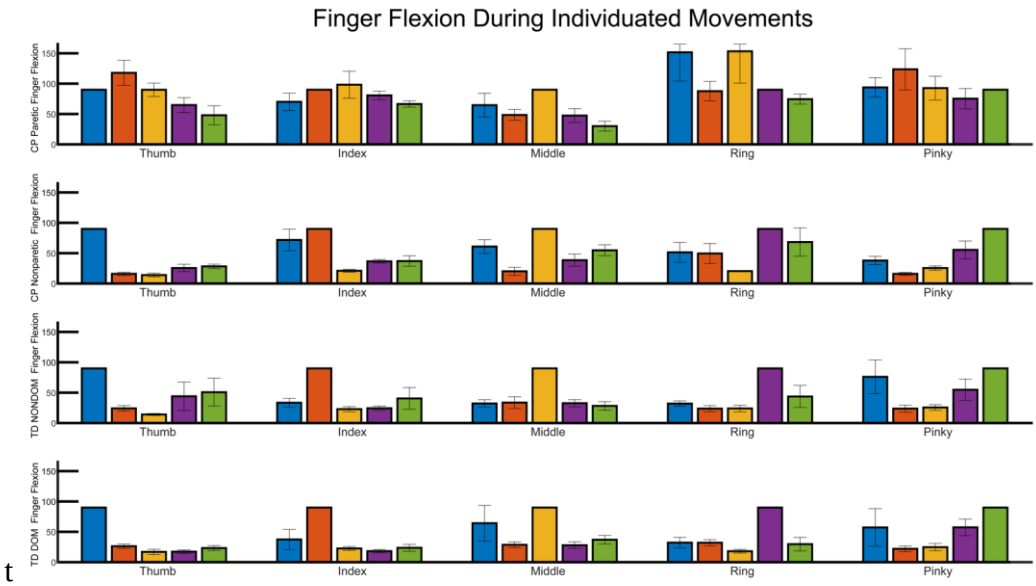

t

Figure 2.20: Finger flexions for each finger for each type of movement. A) Paretic CP, B) Non-paretic CP, C) Non-dominant TD, D) Dominant TD. (Thumb: Blue, Index: Orange, Middle: Yellow, Ring: Purple, Pinky: Green). Error bars represent standard error.

Movement individuation deviation, or the distribution of unintended movement relative to the location of the instructed finger, was slightly higher for the paretic hand compared to the and non-paretic hands and the hand of TD children (**Figure 2.21**). The pinky finger had notably higher deviation, thereby indicating that unintended movement was more widespread, while unintended flexion for other fingers was generally located more locally (**Figure 2.22**).

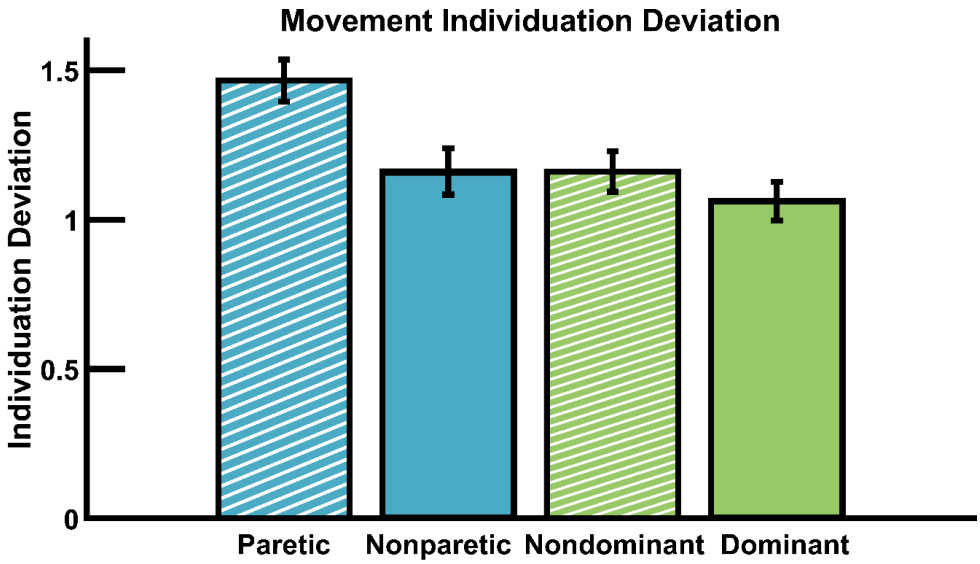

Figure 2.21: Movement individuation for each hand. Data is displayed for each hand (Paretic: Dashed Blue, Non-paretic: Blue, Non-dominant: Dashed Green, and Dominant: Green). Error bars represent standard error.

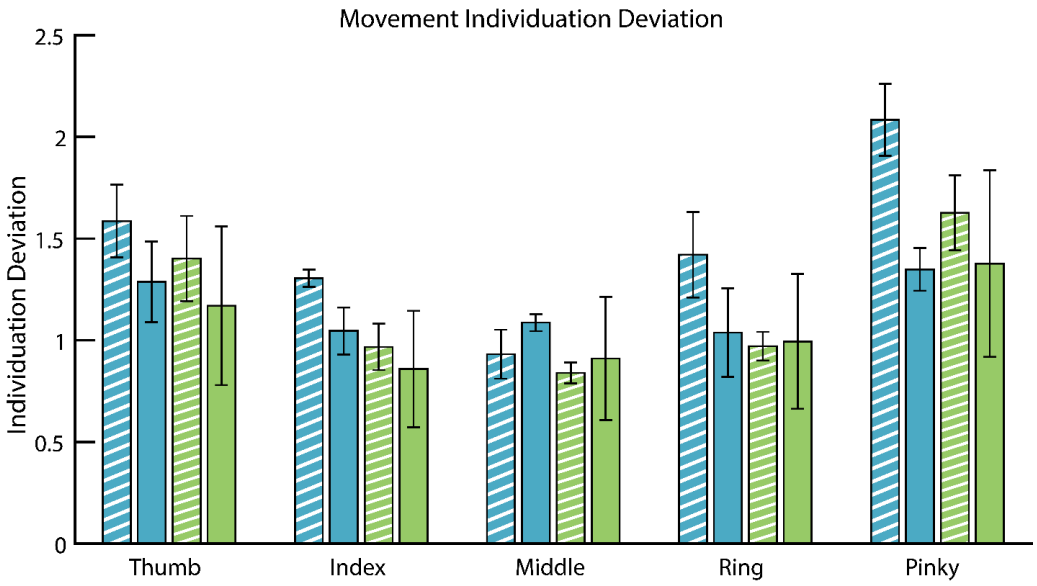

Figure 2.22: Movement individuation for each hand for each type of finger movement. Data is displayed for each type of single finger press for each hand (Paretic: Dashed Blue, Non-paretic: Blue, Non-dominant: Dashed Green, and Dominant: Green). Error bars represent standard error.

2.3.3 JTTHF

ANOVA results revealed that children with hCP had a significantly higher difference in JTTHF completion time between their hands than TD children did between their hands ($p < 0.001$, $\eta p^2 = 0.546$) (**Figure 2.23**). Examining each hand individually, the paretic hand JTTHF time was significantly longer than that of the non-paretic hand, non-dominant hand, or the dominant hand ($p \leq 0.001$). The paretic hand was more than 300 seconds slower than the non-paretic hand. All CP participants had difficulty writing with the paretic hand, three of four participants reached the maximum allowed time for that task. CP01 and CP03 reached the maximum allowed time for the majority of JTTHF tasks.

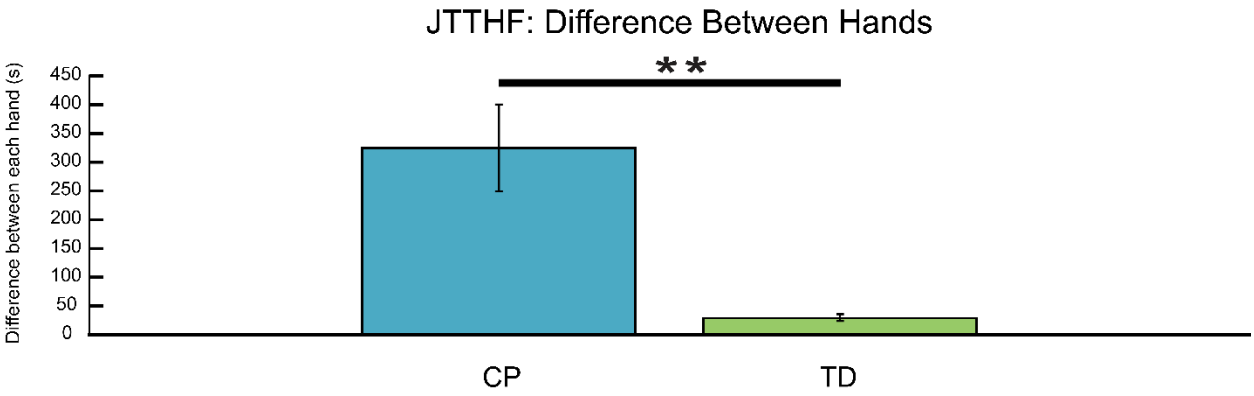

Figure 2.23: JTTHF times for each participant group. JTTHF times are the difference in total time each hand requires to complete all seven tasks. If a participant is unable to complete a subtask, then a maximum time of 120 seconds is assigned. The maximum possible score a participant can earn is 720 seconds. Error bars represent 95% Confidence Interval. * $p < 0.05$, * $p < 0.01$

2.3.4 Correlation Between Main Measures

Pearson correlations were calculated to determine the relationship between JTTHF scores, force individuation, and movement individuation across all hands (Table 2.2). Significant correlations were found between all three primary outcome measures. JTTHF time decreased as either force or movement individuation improved. Movement individuation and force individuation were positively correlated with each other.

Table 2.2: Main Outcome Correlations

TD & CP	**JTTHF**	**FI**	**MI**
JTTHF		-0.639, p = 0.000	-0.502, p=0.009
FI	-0.639, p = 0.000		0.573, p = 0.002
MI	-0.502, p=0.009	0.573, p = 0.002	

2.4 Discussion

Previous investigation into the individuation of TD children or children with hCP has been extremely limited. One previous study examined finger force individuation of adults with diplegic cerebral palsy and neurotypical adults [114] and found lower finger forces and less individuated force production in the CP group compared to the neurotypical group. Findings in neurotypical adults or post-stroke adults, however, may not be generalizable to populations of children who are still undergoing neural development. While individuation capability manifests within the first year after birth [125,126], this dexterity continues to develop throughout childhood. Primates experience postnatal development of cortico-motoneuronal connections that allow for highly skilled and dexterous hand movements. These connections take several years to fully mature [127,128]. Finger force individuation in TD children approaches the level found in adults around the time of ten years of age [122]. Since the brain insult producing hCP occurs before finger individuation capability is fully developed, fine manual dexterity is likely to be affected, although neural plasticity could potentially afford a means for children with hCP to adapt and gain individuated control.

Our results indicate that significant deficits in finger force and individuation may be present in children with hCP compared to TD children. This diminished individuation was most pronounced for the paretic hand but extended to the non-paretic hand as well, at least with respect to the dominant hand in TD children. Force individuation deficits were especially pronounced for the middle, ring, and pinky fingers. Interestingly, despite the heavy reliance of thumb sensorimotor control on the cortical neurons likely to be impacted by CP, our participants with hCP exhibited almost normal force individuation with the thumb, and the thumb function was relatively spared after compared to the other fingers.

Children with hCP exhibited a wider spread of force production across digits for both the paretic and non-paretic hands than TD children, as indicated by the FI_DEV values. This was especially apparent for the middle, ring, and pinky fingers. While for TD children uninstructed force production was largely limited to adjacent digits, in children with hCP significant force production was seen in all five digits for instructed force production with the middle, ring, or pinky finger. Thus, force individuation improved substantially for two-finger presses in TD children, but not nearly to the same extent for children with hCP.

As isometric force was being produced, it is unlikely that mechanical coupling played a significant role in the observed force individuation deficits. This premise is supported by the force data that shows limited force production in the fingers of the paretic hand when children with hCP were instructed to create force with the thumb, but substantial force produced by the thumb when instructed to create force with the middle or ring finger. Rather, these data suggest neurological coupling among muscles and muscle compartments controlling different digits. The HDEMG signals did reveal greater separation of the centroid of activation between presses of the index and middle fingers for TD children, thus suggesting better distinction of activation patterns, but overall the patterns were difficult to interpret. Across participants, EMG patterns often had more than one cluster of activation. Surprisingly, variance in activation pattern for repeated trials of the same type of finger press (e.g., index finger) was smallest for the paretic hand. A past study employing HD arrays found individuated EMG activation patterns in extensor muscles in neurotypical adults during creation of individuated finger extension forces [129]. It is possible that these activation patterns are not as well established in children. Alternatively, the fact that we were examining finger flexion rather than extension may have contributed to the difficulty we had in identifying distinct and consistent extrinsic muscle regions of activation.

Another study examining the spatial distribution of extrinsic flexor and extensor muscles during individuated finger movements of neurotypical adults also found high variation in the locations of activation clusters and multiple activation clusters [130]. Some researchers have suggested that a broader spatial activation during individuated finger force production is associated with wrist stabilization [131], but we supported participants' wrist and forearm were supported during testing.

Movement individuation was also impacted in the paretic hand in children with hCP, but unlike for FI, the MI of the non-paretic hand was not significantly impacted when compared to the non-dominant and dominant hands of the TD children. Similarly, the spread of unintended movement, as indicated by the MI_DEV metric, was greater for the paretic hand than for non-paretic hand or the hands of TD children. Movement individuation deficits were similar for all digits across the paretic hand (except for the middle finger which had less impairment of individuation), despite the greater mechanical coupling among the middle, ring, and pinky fingers. As for the force individuation, the movement individuation deficits appear to be neurologically driven. Interestingly, values for the MI index were much lower than for FI across all participants. While this may be attributable in part to biomechanical movement constraints and the task parameters, control of individuated movement may also prove more challenging. Even the dominant hand of TD children showed significant movement individuation deficits compared to adults, although it is difficult to compare study results as various studies may measure MI differently [112,132].. Participants in our study had an average age of 11; control of fine movements may continue to develop in adolescence [122], especially movement individuation.

Across hands, strong negative correlations were seen between force and movement individuation and time needed to complete the JTTHF. These results indicate an association between individuated control of fingertip force production and movement and the ability to perform skilled unimanual tasks. A past study with stroke survivors found that training individuation did lead to significant improvement in task performance, as measured with the JTTHF [112], but this remains to be shown in children with hCP. Movement and force individuation were also significantly, positively correlated, although the strength of correlation was moderate. The extent to which control of force individuation and movement individuation relies on common neural pathways remains to be determined.

There are several limitations to this study. The force individuation assessment was performed with all fingers extended and resting on load cells, and movement individuation was measured by examining task-independent finger flexion/extension. These tests are not necessarily indicative of how finger individuation is used during real world tasks. It may be useful to measure individuation of finger forces and finger movements for different types of grasps and tasks and determine how well the individuation metrics used in this study map to utilization of individuation in everyday tasks. Another limitation was the small sample size of the hCP group in this study, which may limit the generalizability of these results. The hCP sample population, while limited to individuals with hand function classified in the range MACS I-III, included a wide range of hand function capability. A larger sample size would allow participants to be grouped and analyzed according to their MACS classification.

2.5 Conclusion

In this study, we evaluated the finger individuation capability of TD children and children with hCP and correlated these capabilities with unimanual hand function using the JTTHF

measure. The paretic hand of children with hCP exhibited significant functional deficits in finger force individuation, finger movement individuation, and unimanual function compared to their paretic hand, and compared to the hands of TD children. Children with hCP had their unintended finger forces spread more evenly across the digits of the hand, while TD children's unintended finger forces were largely located in finger adjacent to the instructed finger(s). For finger movement individuation, children with hCP and TD children had similar distribution of unintended finger flexions across the fingers. Finger force individuation, finger movement individuation, and JTTHF times all had significant correlations with each other. These results indicate that children with hCP have significant deficits in finger individuation, and common clinical evaluations, such as the JTTHF, may somewhat accurately capture these deficits, and finger force and movement individuation may be jointly controlled to some degree, and it is uncertain if they each need separate targeted training or if individuation training of any kind would benefit both finger force and finger movement individuation.

In the future, interventional studies focused on improving finger force and finger movement individuation should be performed and these individuation evaluations can be used to determine the efficacy of the interventions. Finger movement individuation training has been shown to temporarily improve finger movement individuation in post-stroke adults and cause maintained improved finger posture changes [112]. It has also been shown that practice of individuated force production can improve individuation in neurotypical adults [133]. Interventional studies using force individuation training and movement individuation training should be performed to determine if these results apply to children with hCP.

CHAPTER 3: Contribution of the Ipsilesional and Contralesional Hemispheres to Finger Individuation

3.1 Introduction

Children with hemiplegic cerebral palsy (hCP) may retain ipsilateral corticospinal tract (CST) projections that typically developing (TD) children generally lose in the first few years of development [55,134,135]. These ipsilateral connections may influence individuated control of the fingers, potentially for better or worse. Ipsilateral CST projections to the paretic hand are a strong predictor for impaired hand function in children with hCP or epilepsy [134–136], yet in some cases the ipsilateral hemisphere may contribute positively to hand function [137] and higher ipsilateral stimulus recruitment curves (SRCs) are associated with improved performance in the Box and Block test [137].

Transcranial magnetic stimulation (TMS) affords a means of examining the ipsilateral and contralateral CST pathways, which are crucial to fine manual dexterity, including individuation. In neurotypical adults, TMS stimulation can evoke individuated finger forces when subjects are performing motor imagery (MI) [138]. The motor imagery can influence force direction, but not amplitude, resulting from a given TMS excitation [116]. In addition to evoking finger force, TMS can be used to evoke finger flexions with limited individuation of the movement, with specific fingers targeted by changing position and orientation of the TMS coil [139]. Similar studies for children, and especially children with neurological deficits. are lacking, thereby leading to gaps in our knowledge of the development and impairment of fine motor control.

The goal of this preliminary work was to explore the neurological basis of finger force individuation. We performed TMS stimulation of the motor cortex in both hemispheres in

children with hCP and TD children. TMS was used to either create MEPs in the targeted finger flexor muscle during MI or to perturb voluntary creation of fingertip force production. We hypothesized that motor imagery would facilitate individuated finger force production in TD children in response to TMS, and, to a lesser degree, in children with hCP. We also hypothesized that inhibitory use of TMS would decrease force individuation.

3.2 Methods

Children with hCP or typically developing (TD) children participated in the study. All participants were required to be 8-14 years old and to be free of any orthopedic issues affecting use of the hand or arm. Children with hCP needed to have a MACS score of I, II, or III to qualify. Additionally, participants could not have implanted devices incompatible with TMS (e.g., pacemaker, deep brain stimulation implant) or a history of epilepsy or seizures. Participants provided informed written assent, and their parents provide informed, written consent to participate in the protocol. The protocol was reviewed and approved by the Institutional Review Board of the University of North Carolina at Chapel Hill.

The location of the motor representation of the flexor digitorum superficialis (FDS) muscle within M1 was identified for each hemisphere for the paretic (hCP) or non-dominant hand (TD) [65]. If no hotspot could be located (e.g., ipsilateral stimulation for TD children), then the hotspot found for the non-paretic or dominant hand was used. The FDS hotspot was identified by exploration of M1 with TMS stimulation (Magpro TMS stimulator, MagVenture, Farum, Denmark). The region that generated the peak motor evoked potentials (MEP) within FDS was selected. Once the hotspot was identified, stimulation amplitude was gradually decreased to find the resting motor threshold (RMT), which is the minimum amplitude at which at least three of a set of 6 pulses produced an MEP of 50 microvolts or greater.

For all trials, the subject sat comfortably in a chair with their forearm supported in a pronated posture, their shoulder abducted (~45°), and the tip of each finger resting on a separate load cell (Nano-17 or Mini40, ATI Industrial Automation, Cary, NC) for force measurement. For the first set of trials, participants either rested or performed motor imagery of the index finger flexing and the other digits relaxing. During both conditions, either sham or real TMS stimulation was applied. For real stimulation trials, a pulse was delivered to the M1 FDS representation at 130% RMT [140]. The TMS-induced force from all fingers of the tested hand were recorded. During sham trials, the TMS coil was flipped such that no magnetic pulse was delivered, but the participant still heard the same sound from the coil and felt the coil against their head. Six stimulations were delivered for each set of conditions (e.g., contralateral, MI, real) for a total of 48 stimulations (Table 3.1). The six stimulations within a block were delivered five seconds apart. Sham and real stimulation to the contralateral and ipsilateral hemispheres were presented in blocks to help maintain coil position and angle relative to the head.

Table 3.1: Motor Imagery TMS Conditions

Hemisphere	Contralateral				Ipsilateral			
Motor Imagery	No MI		MI		No MI		MI	
TMS Status	Sham	Real	Sham	Real	Sham	Real	Sham	Real

In a second set of trials, participants performed voluntary flexion presses with the index finger to 25% of maximum voluntary contraction (MVC). Participants initiated the press after receiving a visual stimulus; at 120 ms [117] after the introduction of the visual stimulus, either sham stimulation or a single-pulse of 130% RMT TMS stimulus was delivered to either the ipsilateral or contralateral M1 to elicit FDS activation (Table 3.2). For each set of conditions (e.g., contralateral/ipsilateral, real/sham) there were six stimulations, for a total of 24

stimulations. Within each block, TMS pulses were delivered at least five seconds apart. Sham and real stimulation were again presented in blocks to maintain coil position relative to the head. The single TMS pulse was intended to disrupt brain activity in the targeted area, subsequently preventing, temporarily, that hemisphere from assisting in control of the force generation. TMS stimulation was applied prior to voluntary force production, so that the inhibitory effects of TMS on voluntary force individuation could be examined at several time points. TMS can have inhibitory effects [141] and the effects of TMS stimulation vary over time after the stimulation occurs, lasting for hundreds of milliseconds [142].

Table 3.2: Voluntary Finger Press TMS Conditions

Hemisphere	Contralateral		Ipsilateral	
TMS Status	Sham	Real	Sham	Real

3.2.1 Data Analysis

The individuation of TMS-induced forces was calculated using **Eqn. 3.1**:

$$FI_j = F_{instructed}/[\sum_{i=1}^{n}[\left[\left(\sum_{i=1}^{n}(F_{ij})\right)\right]/(n)] \quad (3.1)$$

Force angle, FA, was calculated in reference to the normal for the fingertip and surface of the load cell. Force angle and individuation were not examined in cases where no or negligible forces were evoked, as the low signal-to-noise ratio could lead to spurious results. TMS stimulation created artifacts in the EMG recordings that could obscure identification of MEPs. The artifacts had a consistent waveform shape but inconsistent amplitude. A normalized version of the TMS artifact was created from EMG recordings, and this normalized artifact was scaled to the amplitude of the artifact after each stimulation. Subtracting the two signals removed the artifact while leaving the MEP signal intact. After removing the artifact, the start of a MEP was then identified by the time at which the EMG amplitude exceeded the average baseline value by more than three standard deviations.

Motor Imagery Data Analysis: Data were collected with the factors: Motor Imagery (MI, no MI), the Hemisphere receiving stimulation (contralateral/ipsilateral), and Stim (real/sham). For TD participants, statistical testing focused on Motor Imagery during real, contralateral stimulation as ipsilateral and sham stimulation evoked only negligible forces. Repeated measures ANOVA was performed for the dependent measures: maximum index finger flexion force, FI, and FA. Data for the hCP subjects were examined in isolation as case studies due to the small sample size.

TMS-disrupted Force Individuation Data Analysis: Data were collected with the two factors: Stim (real/sham) and Hemisphere (contralateral/ipsilateral). For the TD subjects, repeated measures ANOVAs were performed to examine the impact of Hemisphere during real

stimulation trials (sham stimulation had negligible impact) on the following outcome measures: FI and FA at multiple time points after stimulation. Data for the hCP subjects were again examined as case studies.

3.3 Results

Five TD children and two children with hCP were recruited to participate in the TMS protocol (Table 3.3). All participants also completed the individuation assessment reported in Chapter 2. TD01 only completed the contralateral portions of the experiment before withdrawing from the remainder of the study due to fatigue. CP02 completed the contralateral portion of the MI experiment but withdrew from the remainder of the protocol due to a headache.

Table 3.3: Study Participant Data

TD Participants	**Sex**	**Age** (years)	**MACS** (I-V)
TD01	M	14	N/A
TD02	M	11	N/A
TD03	F	12	N/A
TD07	F	13	N/A
TD10	F	14	N/A
Mean ± SD	**2 M/3 F**	**12.8 ± 1.3**	N/A

hCP Participants	**Sex**	**Age** (years)	**MACS** (I-V)
CP02	M	10	1
CP04	M	12	1
Mean ± SD	**2 M**	**11.0 ± 1**	**1 ± 0**

3.3.1 Results: Motor Imagery

TD Motor Imagery: For the TD participants, MEPs were detected about 15 ms after contralateral TMS stimulation and evoked forces were detected about 35 ms after stimulation (**Figure 3.1**). For the TD participants, significant force production was observed only for real stimulation of the contralateral hemisphere (**Figure 3.2**). The ANOVA results revealed that MI

led to significant increases in FI ($p = 0.016$, $\eta p^2 = 0.238$), maximum force ($p < 0.001$, $\eta p^2 = 0.490$), and FA ($p < 0.008$, $\eta p^2 = 0.280$).

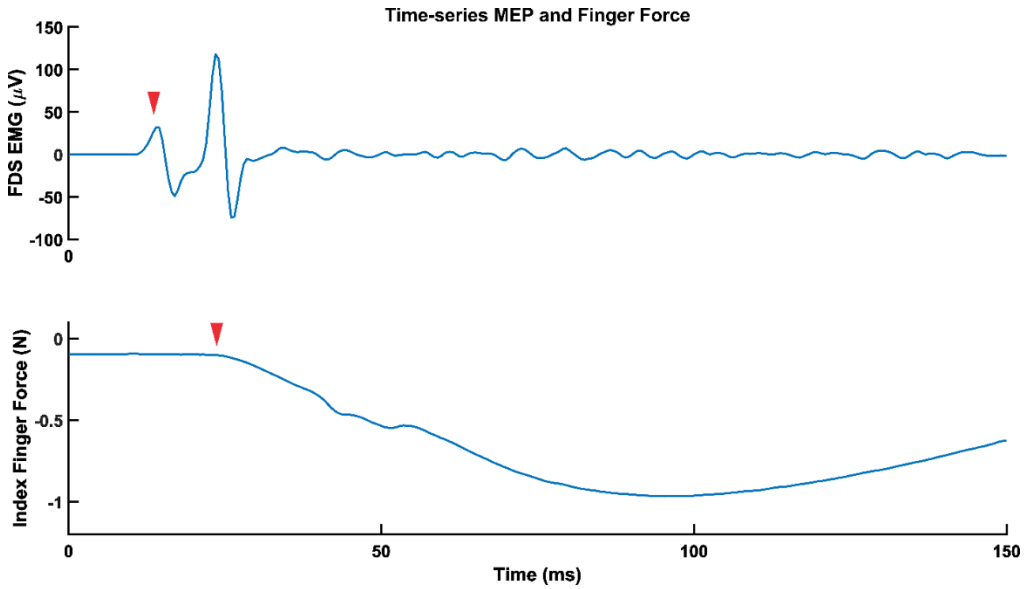

Figure 3.1: Time-series of representative MEP and Finger Force after TMS stimulation. TMS stimulation is delivered at 0 ms, the red triangles indicate initiation of the MEP and finger flexion force.

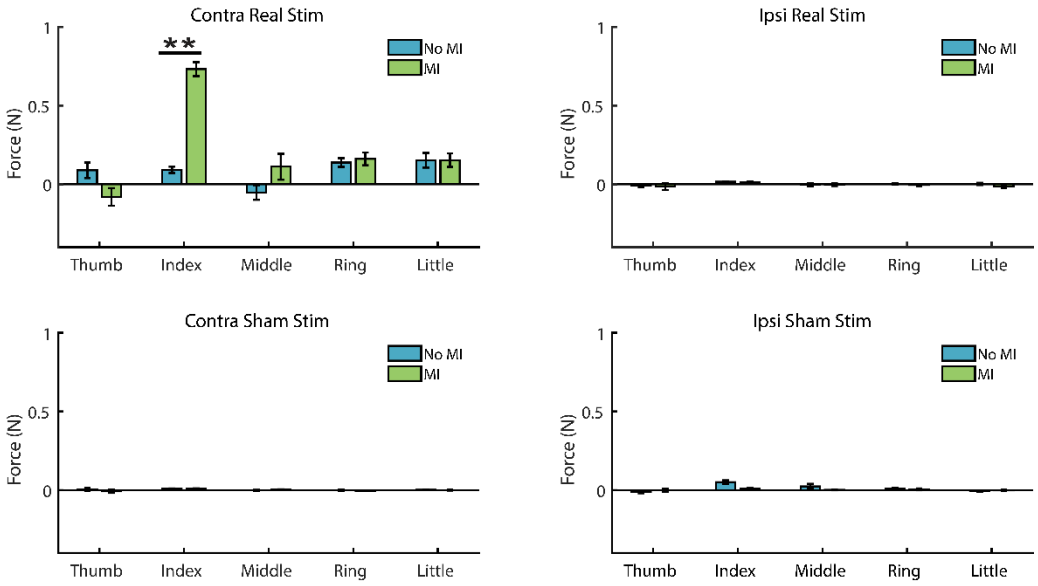

Figure 3.2: TD TMS evoked finger forces. Average forces for all fingers are shown for both real and sham stimulation, and stimulation applied to either hemisphere. Error bars represent standard error. Horizontal significance lines indicate that two groups are significantly different. * $p < 0.05$, ** $p < 0.01$.

This increase in force was localized to only the index finger, the finger the participant was instructed to imagine flexing in the MI scenario (**Figure 3.2**). Thus, the individuation index was significantly improved with MI compared to the No MI condition for the index finger only (**Figure 3.3**). FI for the index finger increased by 105%, more than doubling its value in the No MI condition. The fingers adjacent to the index finger (thumb and middle), saw little change in their portion of the overall flexion force, while fingers which were not adjacent to the index finger, ring and pinky, saw decreases in their share of the total flexion force.

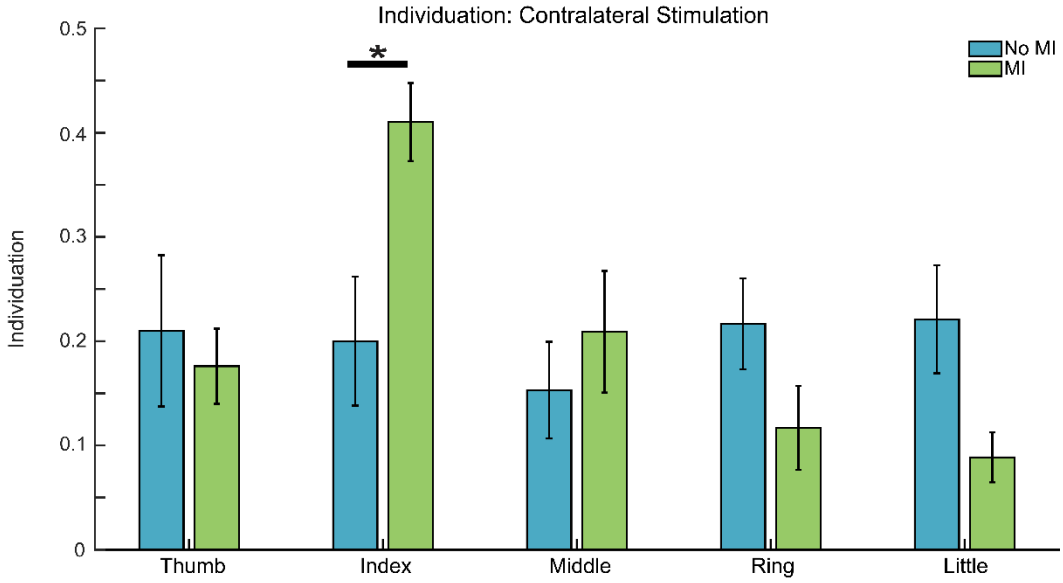

Figure 3.3: TD Finger force individuation calculated for each finger. In cases of Motor Imagery, the participant is actively imagining creating flexion force with the index finger. Error bars represent standard error. Horizontal significance lines indicate that two groups are significantly different. * $p < 0.05$, ** $p < 0.01$.

Index force angle decreased significantly during MI compared to the No MI condition from 59.9° to 31.7° (**Figure 3.4**). Here a smaller angle indicates that the force is directed more normally to the surface of the load cell. Other digits did not exhibit large changes in force direction, regardless of whether they were adjacent to the index finger or not.

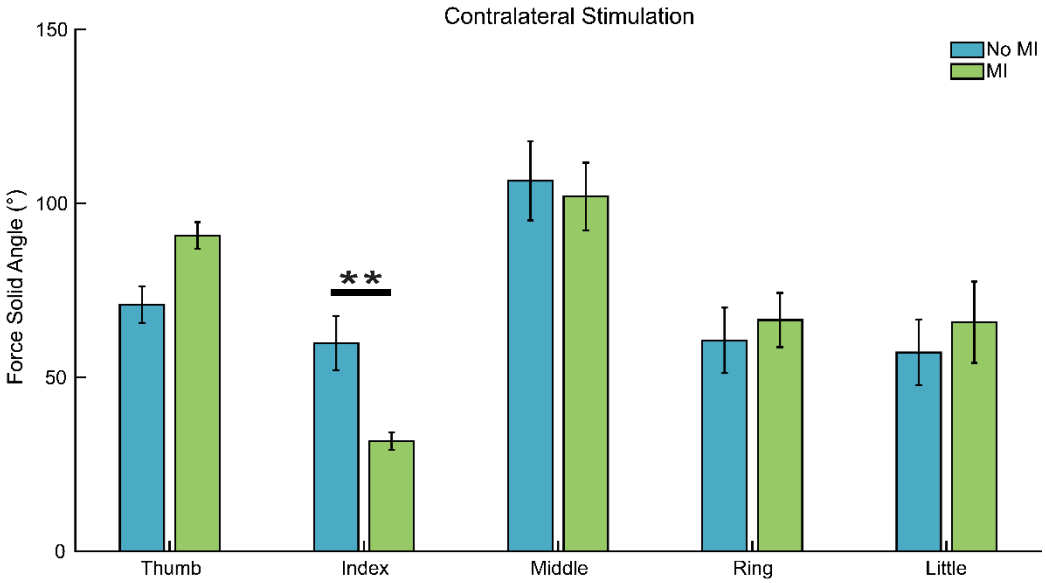

Figure 3.4: TD TMS evoked force angle. A force angle of "0" would represent force that was perfectly normal to the load cell (no force in the x or y direction). Error bars represent standard error. Horizontal significance lines indicate that two groups are significantly different. * $p < 0.05$, ** $p < 0.01$.

CP02 Motor Imagery: Real, contralateral stimulation evoked substantial finger forces from CP02, which were not seen during sham stimulation (**Figure 3.5**). Motor imagery increased both index finger and middle finger flexion force even though only flexion of the index finger was imagined. Average index flexion force increased by 54%, from 0.139 N to 2.14 N. Conversely, index flexion imagery led to a reversal of force direction in the thumb such that extension force was recorded. As CP02 only completed the contralateral portion of the MI experiment, no results for ipsilateral stimulation are available.

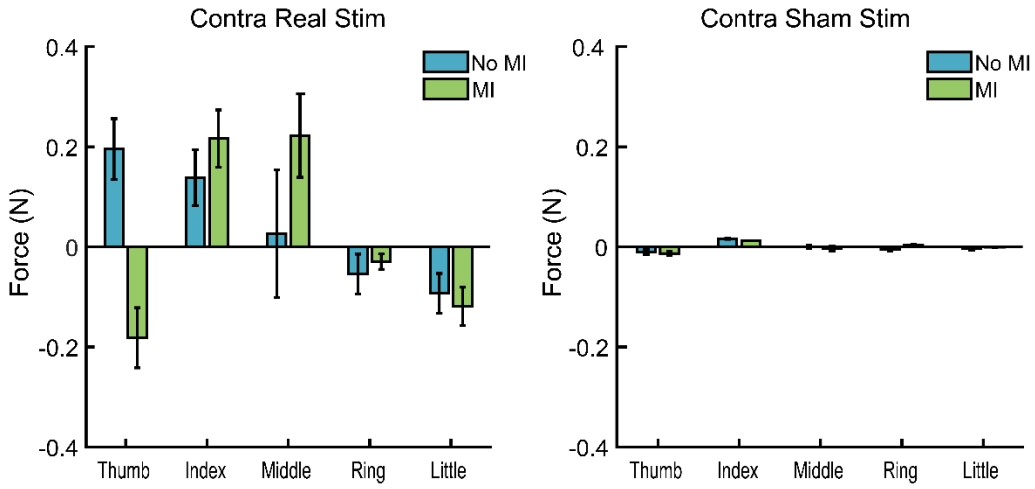

Figure 3.5: CP02 TMS evoked force for the contralateral hemisphere. Error bars represent standard error.

The effect of MI on finger force individuation was calculated according to each finger, for no MI trials and for MI trials (**Figure 3.6**). The portion of the force attributed to the index finger increased with MI from 0.188 to 0.291, an increase of 55%. The individuation index value for the index finger during MI, however, was still only slightly greater than that of the middle finger or thumb.

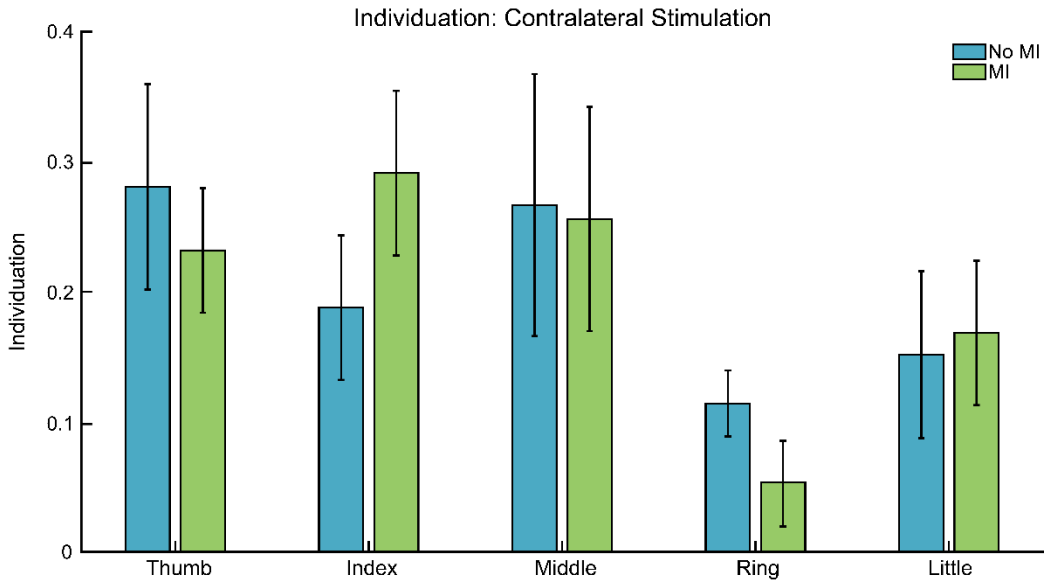

Figure 3.6: CP02 TMS evoked force individuation. Error bars represent standard error.

FA changed little for the index finger with MI (**Figure 3.7**) despite the increase in force magnitude, indicating that the force direction did not improve with MI. Other digits, however, appeared to be impacted by the MI. Thumb FA increased as more of a thumb extension force was created and middle finger FA decreased as the MI led to increased flexion force production in the middle finger.

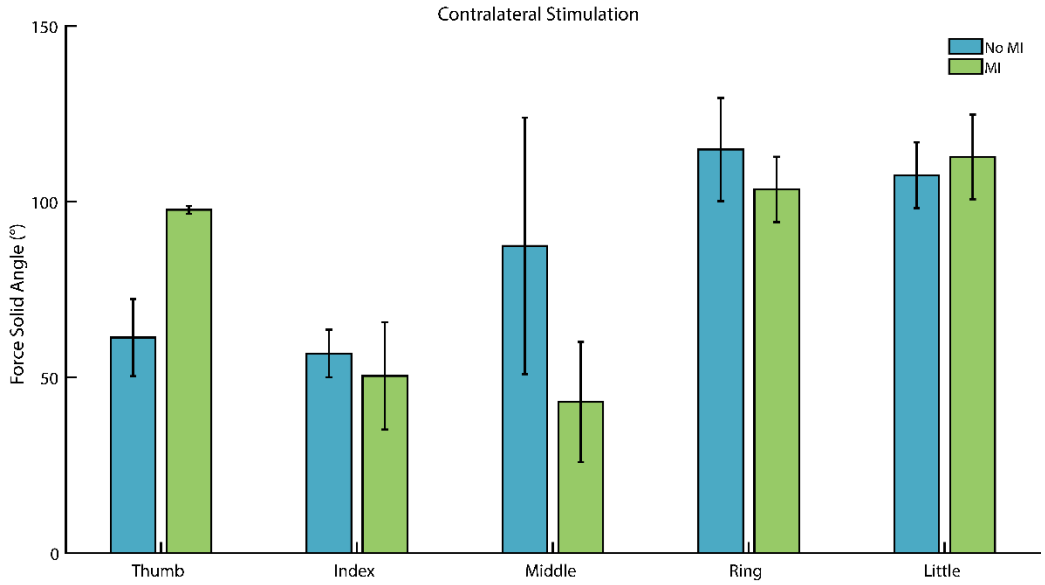

Figure 3.7: CP02 TMS evoked force angle. Error bars represent standard error.

CP04 Motor Imagery: CP04 successfully completed both the contralateral and ipsilateral portions of the experiment. Sham stimulation did not evoke forces, regardless of MI (**Figure 3.8**). Both contralateral and ipsilateral stimulation, however, evoked meaningful finger forces. MI appeared to increase thumb flexion forces regardless of which hemisphere was stimulated, but MI had little effect on the other fingers.

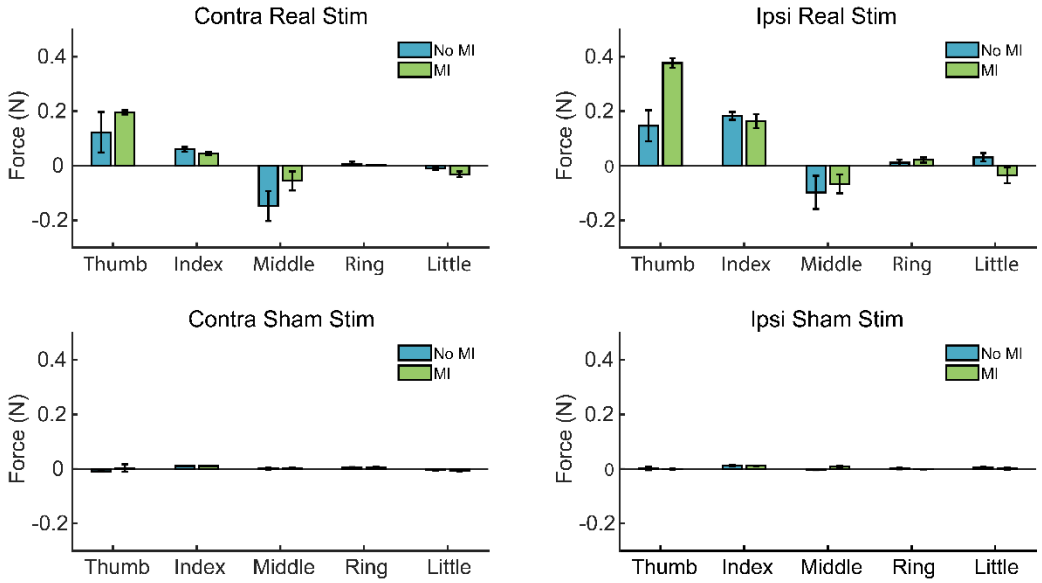

Figure 3.8: CP04 evoked finger forces. Error bars represent standard error.

MI failed to produce an improvement in the FI metric in the imagined index finger but did lead to substantially greater FI values in the thumb (**Figure 3.9**). This occurred for both contralateral and ipsilateral stimulation.

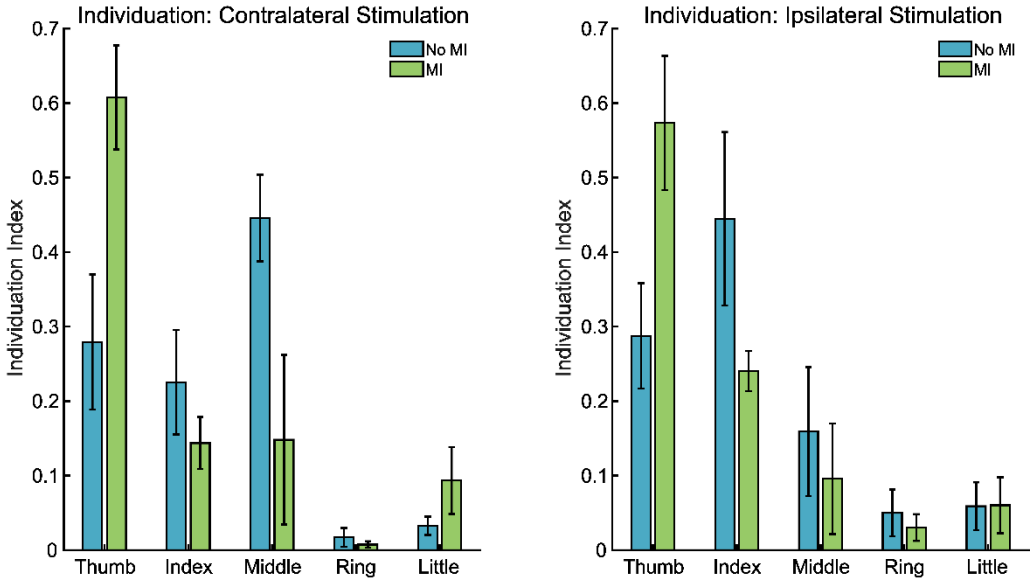

Figure 3.9: CP04 individuation of evoked finger forces. Error bars represent standard error.

The solid angle of force was calculated for each finger for trials with no MI and with MI (**Figure 3.10**). The thumb and the index finger saw the largest, and most consistent decreases in force angle due to MI when receiving ipsilateral stimulation.

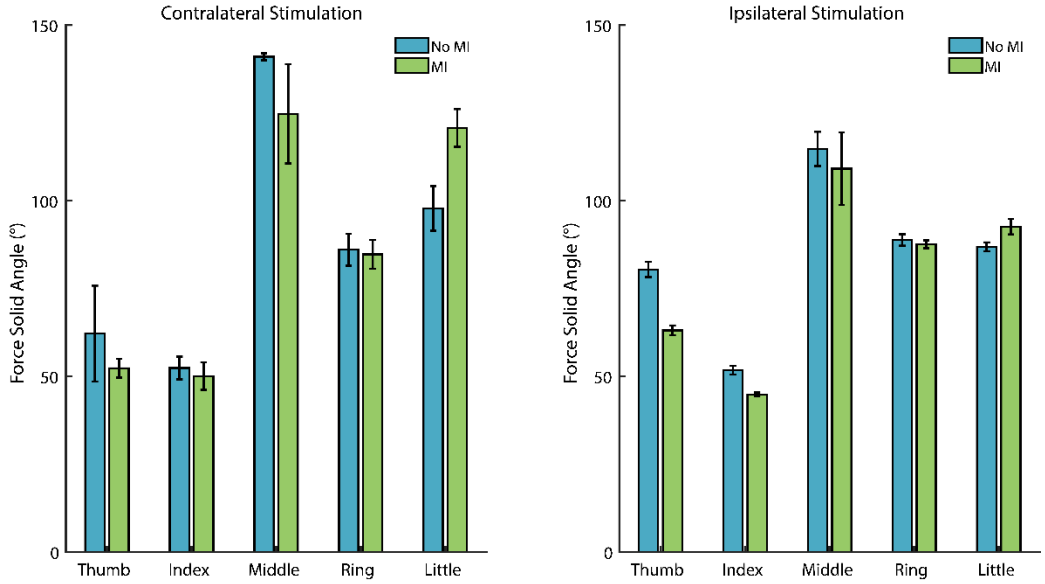

Figure 3.10: CP04 evoked force angle. Error bars represent standard error.

3.3.2 Perturbation of Voluntary Force Production

TD Perturbation of Voluntary Force: The participant received a Go-signal 120 ms before receiving a 130% RMT amplitude stimulation (**Figure 3.11**). MEPs and evoked forces occurred after stimulation and before the participants began a voluntary 25% MVC individuated index finger press. Outcome measures were evaluated after the MEP, during a post-MEP silent period, during the rise time of the voluntary force, and during the steady period for voluntary force.

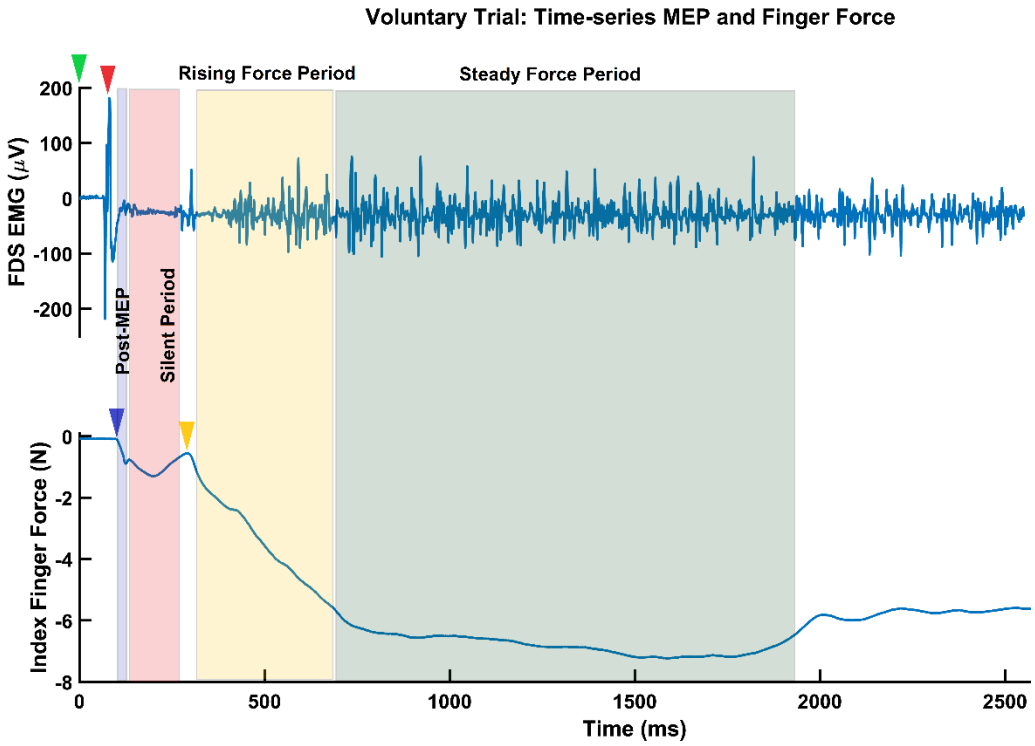

Figure 3.11: TD EMG and force for TMS-disrupted voluntary force production. The Go-signal is given at 0 ms (green arrow), the TMS stimulation is delivered at 120 ms (red arrow). TMS evoked forces begin after stimulation (blue arrow) and dissipate by 300 ms, at which point voluntary force production begins (yellow arrow). Voluntary force increases until about 800 ms, and then force reaches a steady state. The blue field indicates the MEP force period, the red field indicates the silent period, the yellow field indicates the rise time period, and the green field indicates the steady force period.

After verifying that sham stimulation had no impact on force generation, we focused out analysis on the real stimulation data. The ANOVA results revealed that contralateral stimulation decreased index FI during rise time ($p < 0.006$, $\eta p^2 = 0.300$) and the steady-state phase ($p < 0.010$, $\eta p^2 = 0.268$) compared to ipsilateral stimulation.,

Force individuation of the index finger at various points during the trial are presented in **Figure 3.12**. Stimulations were applied to either the contralateral or ipsilateral hemisphere. Contralateral stimulation increased post-MEP individuation but decreased individuation during rise time and steady time by 0.064 and 0.058, respectively. Ipsilateral stimulation had an opposite affect and decreased post-MEP individuation but increased individuation during rise time and steady time, by 0.024 and 0.035, respectively.

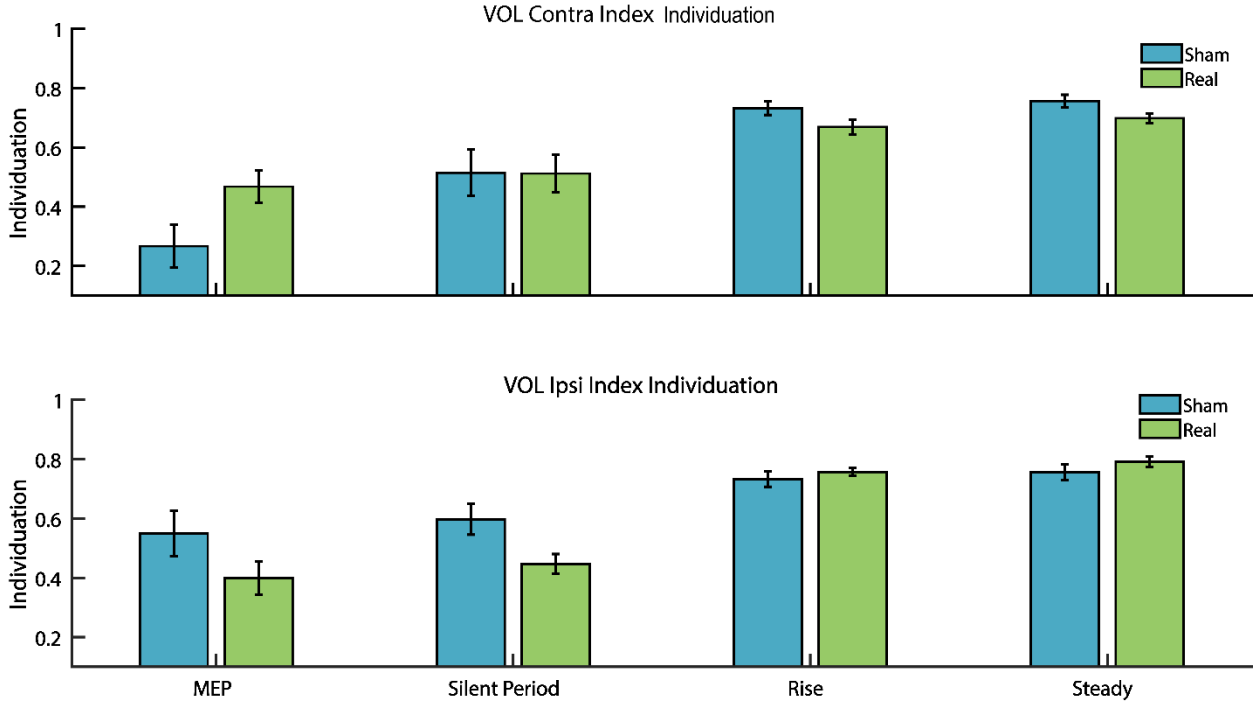

Figure 3.12: TD force individuation during TMS-disrupted, voluntary force production. Error bars represent standard error.

Contralateral stimulation significantly increased index FA during rise time compared to ipsilateral stimulation ($p < 0.005$, $\eta p^2 = 0.304$). The FA became less normal by by 4.1°. FA also increased during the steady-force time 4.6°, respectively (**Figure 3.13**). Ipsilateral stimulation decreased force angle during rise time and steady force time by 4.3° and 4.9°, respectively.

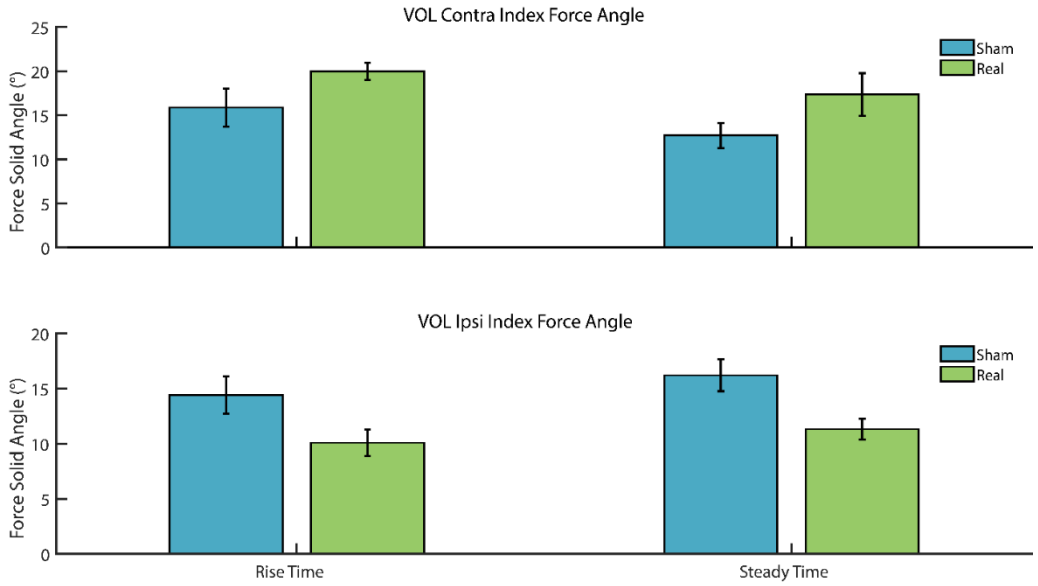

Figure 3.13: TD force angle during TMS-disrupted, voluntary force production. Error bars represent standard error.

CP Perturbation of Voluntary Force: Force individuation of the index finger and the thumb at various points during the trial for CP04 are presented in **Figure 3.14**. Stimulations were applied to either the contralateral or ipsilateral hemisphere. Contralateral stimulation evoked more force in the thumb (though a similar difference in comparison to sham), and ipsilateral stimulation evoked more force in the index finger.

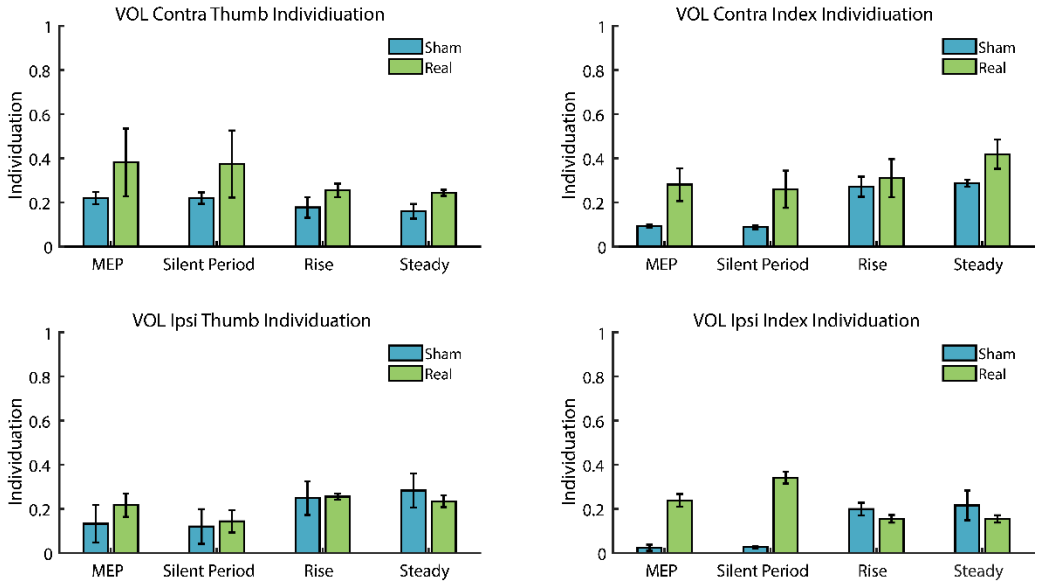

Figure 3.14: CP04 force individuation during TMS-disrupted, voluntary force production. Error bars represent standard error.

The angles of the index and thumb forces during the voluntary portion of force generation (rise time, and steady-force time) are presented in **Figure 3.15**. Stimulations were either sham or real and were applied to the index finger hotspot of either hemisphere. Contralateral and ipsilateral stimulation both increased force angle during rise and steady time, although contralateral stimulation produced a larger increase. During rise and steady-force times, contralateral and ipsilateral stimulation did not cause a consistent change in force angle compared to sham.

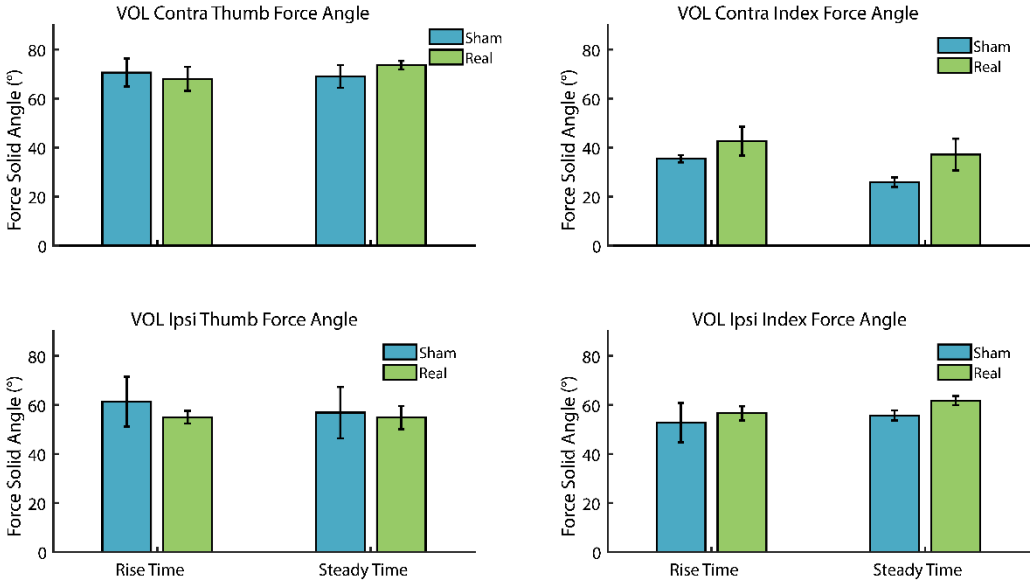

Figure 3.15: CP04 force angle during TMS-disrupted, voluntary force production. Error bars represent standard error.

3.4 Discussion

Motor Imagery: For TD children, motor imagery during TMS stimulation was able to successfully increase individuation of evoked finger forces during stimulation of the contralateral M1. To our knowledge this is the first examination of MI on finger force individuation of TMS-evoked forces in children. The effect of MI in children was similar to what has been reported for neurotypical adults [138] . The averaged evoked flexion force during MI was almost 1 N, or about 5% MVC, which is reasonable considering adults may have evoked forces around 3 N [116]. The individuation of evoked finger force and the magnitude of the force were less than those seen during volitional finger presses (**Figure 3.3, Figure 3.2**), in accordance with published results from neurotypical adults [115,138] . The lower evoked individuation indices may have resulted from a lower signal-to-noise ratio for the evoked data. Evoked forces were only ~5% of MVC while volitional force generation was 25% of MVC. Ipsilateral and sham contralateral stimulation did not evoke significant forces from any finger in the TD group.

In addition to increasing individuation of evoked forces, motor imagery decreased the angle of the evoked force of the index finger by about 40°. In the extended finger posture, FDS contributes to a significant extent to force generation normal to the fingertip and the surface of the load cell. Thus, excitation of FDS produces a more normally directed fingertip force. As with FI, this effect on FA was apparent only in the index finger, the one being flexed in the motor imagery.

TMS also evoked discernible forces in the participants with hCP. CP02 experienced only contralateral stimulation. For this participant, MI led to an increase in evoked index force, as well as an increase in FI for the index finger and a decrease in FA. CP04 produced sizeable, evoked forces when either the contralateral or ipsilateral hemisphere was stimulated, in contrast to TD children for whom ipsilateral stimulation had little effect. For CP04, ipsilateral stimulation

actually generated larger forces than contralateral stimulation. Thus, for this subject, strong ipsilateral corticospinal pathways projected to hand motoneurons. Stimulation of either hemisphere evoked a similar force distribution with large thumb flexion forces, smaller index flexion forces, and some middle finger extension force. It is possible that the similar force distribution evoked by each hemisphere was due to mirror movement characteristics of the subject [143], and overlapping motor representations of finger [144,145] making it difficult to isolate force production by a single finger. Interestingly, despite performing motor imagery of index finger flexion, FI increased for the thumb, but decreased for the index and middle fingers. This participant did have good, individuated force control of the thumb relative to the other digits. This may be indicative of relative sparing of neural pathways for the thumb; thus, excitation resulted in production of thumb flexion force despite MI targeting index finger flexion.

TMS has previously been used to evoke synergistic grip forces during active grip production; the investigators found the effect was primarily on force scaling and not direction [146]. Past studies, on neurotypical adults, found no difference in multi-finger control when the primary motor area is subjected to either faciliatory or inhibitory TMS [147], and therefore concluded that multi-finger coordination occurred outside of the M1 area. Our results, however, indicate that individuation of finger force is facilitated by the M1 area, at least in TD children.

TMS Perturbation of Voluntary Force: TMS-stimulation was applied to either the contralateral or ipsilateral M1 area 120 ms after the subject received a visual signal to begin force production. Force production was examined over time: immediately after the MEP, during the post-MEP EMG silent period, while voluntary force was increasing, and during steady state voluntary force production. The amount of resting or active finger force prior to TMS

stimulation can increase the effects of TMS stimulation [148]. We hoped that examining TMS effects on either hemisphere during voluntary force production would reveal effects which were not detectable during the post-stimulation faciliatory period during the MI experiment.

Despite ipsilateral stimulation not evoking meaningful finger forces during motor imagery, stimulation prior to voluntary force production seems to have affected force individuation and angle regardless of the hemisphere receiving the stimulation in TD children.

Contralateral stimulation increased finger force individuation following the MEP response, which is consistent with results during the MI experiment. However, as time passed and the voluntary force production began, contralateral stimulation caused a decrease in force individuation and caused the voluntary force to be less normally directed.

Ipsilateral stimulation, had the opposite effect of contralateral stimulation. It decreased individuation post-MEP but increased individuation and decreasing force angle during the voluntary phase of force production.

This shift from faciliatory to inhibitory effect of TMS is consistent with past results, where it was found that single-pulse TMS has a faciliatory effect immediately after stimulation but this effect quickly transitions to an inhibitory effect which lasts for hundreds of milliseconds [142]. However, the effects seem to last much longer than previously reported, well over a second after TMS stimulation, and at lower stimulation amplitudes.

Additionally, the converse response to ipsilateral stimulation is interesting and may indicate that the inhibitory interhemispheric interactions associated with the ipsilateral hemisphere may prevent higher levels of force individuation from being achieved to enhance grasp stability. The ipsilateral hemisphere normally has an inhibitory effect on the contralateral hemisphere [149], and this inhibitory effect is normally reduced during fine motor function of

the hand [150]. TMS-disruption of the ipsilateral hemisphere may have further reduced the inhibitory effect allowing for improved individuation.

CP04's response to TMS stimulation prior to voluntary force production differed from the response seen in TD children. Similar to the results seen during the MI experiment a larger response to stimulation was seen in the thumb than in the instructed index finger. The immediate response to both contralateral and ipsilateral stimulation increased individuation of the index finger but the later response (rise time, steady state) saw contralateral stimulation increase individuation and ipsilateral stimulation decrease individuation. This late-stage response to stimulation is similar to the response seen in TD children: disruption of the primary controlling hemisphere (contralateral for TD, ipsilateral for CP04) decreases force individuation, disruption of the other hemisphere increases force individuation. While the ipsilateral and contralateral hemispheres both contribute to finger force control, they influence control in different ways.

Limitations: This was a pilot study with very limited numbers of participants, especially for the hCP group. However, we were able to show that these techniques are feasible in the target population. In the future it would be desirable to use these assessments in combination with individuation training in an attempt to identify best responders to finger individuation training, or using TMS and MI to provide individuation training [151].

An additional factor that may have affected the force response of the CP participants to TMS is the effect resting force of a finger has on it evoked forces [148]. CP participants were instructed to relax their fingers while performing MI, but higher resting forces compared to TD participants would have influenced the evoked forces in a way not entirely controlled by the experiment.

TMS Safety Considerations: Prior to performing this study, one concern with performing TMS in children with hCP was that they might be at elevated risk for seizure during stimulation. To address these concerns, a review of the literature was performed to determine the safety of TMS in TD children and children with hCP.

On rare occasions, TMS can induce adverse events (headaches, seizures, etc.). TMS has a level of safety for TD children and children with CNS disorders (e.g. cerebral palsy) which is similar to the safety level in neurologically intact adults [152]. Four review articles found that single-pulse TMS was safe for typically developing children and children with various neurological conditions, including hCP [153–156]. These reviews found no instances of significant adverse reactions and suggest that TMS bears minimal risk to typically developing children or children with neurological conditions.

These reviews and original research articles support both the safety and usefulness of exploring motor connectivity in typically developing children and children with cerebral palsy using TMS. To further reduce risk, the TMS protocol we used was designed to conform to the recommendations of a perspective on TMS study design considerations, and uses similar study criteria for participant safety (such as inclusion/exclusion criteria) [157]. This risk assessment, and our attempts to further reduce risk, made us comfortable with performing the TMS protocol.

3.5 Overall Conclusions

In this study we evaluated the contribution of each hemisphere to individuated finger force control using TMS. We found that we could evoke individuated and well-directed finger force using motor imagery in TD children. TMS could evoked finger forces in children with hCP as well, but the impact of motor imagery was not as clear. In one participant with hCP motor imagery produced only small changes in force individuation, while in the other participant the

motor imagery of the index finger resulted in poorer individuation for the index finger but better individuation for the thumb. Importantly, ipsilateral stimulation in this participant showed a strong connection to the hand muscles. These ipsilateral connections in children with hCP warrant further exploration. In accordance with other studies, we found the single-pulse TMS to be well tolerated and safe. TMS has a level of safety for TD children and children with CNS disorders (e.g. cerebral palsy) which is similar to the safety level in neurologically intact adults [152]. Four review articles found that single-pulse TMS was safe for typically developing children and children with various neurological conditions, including hCP [153–156]. These reviews found no instances of significant adverse reactions and suggest that TMS bears minimal risk to typically developing children or children with neurological conditions. Consideration of study design, such as such as inclusion/exclusion criteria, can further reduce risk for participants [157].

CHAPTER 4: Development of a Finger Individuation Training Platform or Hemiplegic Cerebral Palsy

Adapted from: J. McCall et al., "Compliant Actuators for Hand Exoskeletons", in *2020 IROS Mech. And Des. Workshop*

Adapted from: J. McCall and D. Kamper, "High Compliance Pneumatic Actuators for Palmar Finger Extension", in *2021 43rd EMBC*

4.1 Introduction

With an incidence rate of three of every thousand lives births, cerebral palsy (CP) is the most common movement disorder in children. Currently 800,000 people in the U.S. alone have CP [3,118]. Children with CP are likely to have significant hand impairment [6,7], which can lead to decades of disability, as children with CP overwhelmingly live well into adulthood [8].

A common therapy for upper extremity rehabilitation involves repetitive practice of movement [133,158]. Techniques such as constraint-induced movement therapy [23,159,160] and HABIT [21,24,81,92,161,162] have been developed to encourage this targeted practice. Exoskeletons can also help to facilitate practice by providing assistance to enable completion of movement [163–165]. These devices tend to employ rigid actuators and structures that may introduce considerable mass with respect to the mass of the fingers and hand, especially in children. The added mass and inertia may disturb control and movement of the hand.

In an effort to reduce weight and improve comfort, soft actuators have been created [165–168]. These actuators typically consist of chambers that expand with fluid or air flow, thereby producing movement of attached body segments. Soft actuators are able to conform to irregular shapes, while offering potential improvements in fit, comfort and customization over devises with rigid actuators. Soft actuators may be invaluable when actuating the fingers and thumb in the

hand, where space is limited, adding mass is costly, and there are many degrees of freedom to control.

Current soft actuator design for the hand, however, is typically focused on pushing the digits into flexion from the dorsal side of the hand [166,169]. While flexion and grasp may be limited in children with CP, digit extension usually has even greater relative impairment in populations with motor impairment [170]. This extension can be assisted through soft actuators placed on the palmar side of the hand [112], but this arrangement adds to demands on the actuator in terms of compliance and tolerance for distortion during flexing. Palmar placement of the actuators, as opposed to dorsal placement, is desirable because the actuators can push rather than pull the fingers into extension. This leads to reduced compressive forces in the joint and eliminates rubbing on the joints. In past studies, we observed the potential for placing soft pneumatic actuators on the palmar side of the hand using a polyurethane-based actuator. However, this polyurethane-based actuator was difficult to fabricate and customize to different hand sizes and shapes [112,171,172]. PVC pneumatic actuators have been used by others in the past, but finger extension torque was limited [163]. We identified a need for new actuators which were easy to fabricate while achieving a low bending resistance and maintaining a high extension force. For this study, we designed and tested a variety of elastomer-based actuators and integrated them into a finger extension exoskeleton.

The goal of this work was to we design, fabricate, and test novel, elastomer-based pneumatic chambers that could be used on the palmar side of the hand to assist finger extension. To explore the potential solution space, we evaluated a set of chambers with varying characteristics: shape, size, and wall thickness. Each chamber was tested over a range of pressures (0-48.3 kPa) and bending angles (0-75°). Due to the palmar location of the actuator, it

is important to balance the trade-off between the ability to create large active extension forces and the need for low passive bending resistance. Finite element models of the pneumatic actuators were developed to enable further exploration of chamber properties. We hypothesized the that the rectangular cross-sectional shape would yield higher extension force and higher passive bending resistance than the semi-obround shape and that the extension force produced would increase with increased pressure and bending angle. Our target extension torque was 0.50 N-m (average extension force deficit of adult stroke survivor with severe hand impairment) [173] and our maximum target passive bending resistance torque was 0.05 N-m to achieve high compliance.

4.2 Methods

4.2.1 Methods: Actuator Design & Fabrication

Pneumatic chambers were designed in SolidWorks (Dassault Systèmes, France) and created with an elastomer using a molding process [174]. The 3D printed molds contained a two-part cavity. Placing an insert within the center of the cavity enabled creation of the chamber walls (**Figure 4.1**); a platinum-cured silicone rubber, Dragon Skin 20 (Smooth-On, Inc., US), was poured into the mold to fill the negative space left between the cavity and the insert, thereby forming the actuator. Dragon Skin 20 was selected based on its excellent ability to resist pressure compared to other silicone rubbers [165] while remaining sufficiently compliant to minimally impede desired chamber flexion.

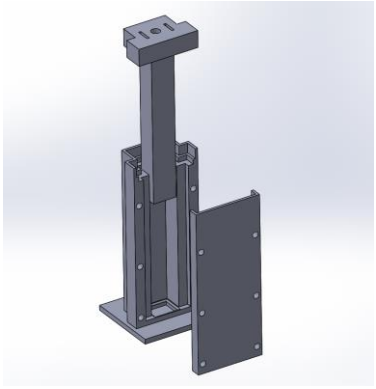

Figure 4.1: Actuator mold design. Open rectangular tube with insert retention at both ends.

Fourteen different types of actuator chambers were created, representing combinations of cross-sectional shape (semi-obround or rectangular) wall thickness (0.8-mm, 1.3-mm, or 1.8-mm), actuator width (7.2 mm, 9.6 mm, 12.1 mm) and depth (7.4 mm, 9.9 mm, 12.4 mm) (**Figure 4.2**). Changes in wall thickness and actuator width and depth were compared with baseline dimensions of 1.3-mm, 9.6 mm, and 9.9 mm (**Figure 4.2B**), respectively.

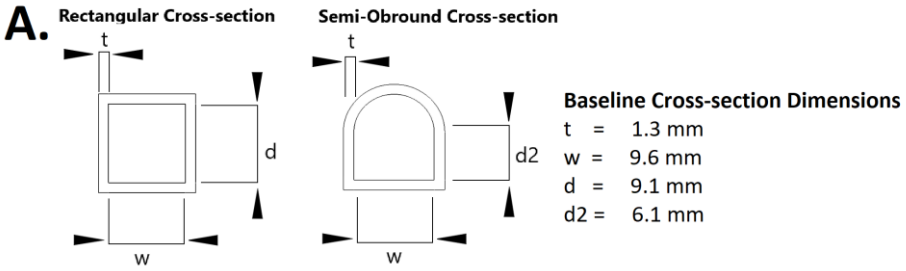

B.

	BASELINE		
Wall Thickness	0.8 mm	1.3 mm	1.8 mm
Actuator Depth	7.4 mm	9.9 mm	12.4 mm
Actuator Width	7.2 mm	9.6 mm	12.1 mm

Figure 4.2: Actuator Design and Dimensions. A. Cross-sectional dimensions of the baseline rectangular semi-obround actuators. B. The dimensional variations used to create different actuators.

Rectangular and semi-obround cross-sections were selected based on preliminary testing and past work [174] that identified the rectangular cross-section as generating the highest extension force and the semi-obround cross-section as having the lowest passive bending resistance out of a wider selection of cross-sectional shapes. Rectangular and semi-obround cross-sections have been successfully used in other pneumatic actuators [175,176]. The semi-obround chambers were fabricated with the same cross-sectional widths and areas as the rectangular chambers (**Figure 4.2A**) to facilitate direct comparison. Additionally, an existing polyurethane-based air chamber was tested [112] for comparison with the DragonSkin 20.

Actuator extension force and passive bending resistance were measured using a custom fixture which was intended to mimic articulation of a 7.6 cm long finger about the metacarpophalangeal joint (**Figure 4.3**). The tip of the fixture was in contact with a force/torque sensor (Mini40, ATI Industrial Automation, Inc., US) positioned perpendicular to the long axis of the fixture. Actuator inflation pressure was computer-controlled through a digital-to-analog converter (USB-3101, Measurement Computing, USA) and an electropneumatic servo valve (Proportion Air, USA). Actuators were tested at 5 pressures (0, 6.9, 20.7, 34.5, and 48.3 kPa) within the servo valve's range (0-69.0 kPa) and at 5 bending angles (15°, 30°, 45°, 60°, and 75°). Additionally, a vacuum was applied to each actuator to examine the impact on passive bending resistance.

Figure 4.3: Actuator and Test Fixture. A) Semi-obround actuator with overmolded air connector. B) Actuator test setup with loadcell and jointed fixture.

4.2.2 Methods: Actuator Simulation

One concern regarding previous polyurethane actuator designs was the propensity for kinks to form in the chamber at even moderate bending angles. The kink would greatly reduce the airflow and thus the extension force. To analyze airflow and chamber deformation of our actuators, a finite element model (FEM) of each of the fourteen actuator chambers was created in SolidWorks (**Figure 4.2**). Each chamber was represented as a mesh with approximately 10,000 tetrahedral elements. The total number of elements differed slightly for each model depending on shape and size. Elements had a size of approximately 2 mm on edge. Linear elastic isotropic characteristics and Dragon Skin 20 material properties were employed for the models.

Simulations were performed for each of the FEMs. Each actuator design was deformed to create a 35° bend and the passive bending resistance was measured during the deformation (**Figure 4.4**). The minimum channel diameter and 5 PSI airflow rate of each actuator was sampled at several bending angles. The deformed actuator model was sampled at the point at which is had a 15° angle and was then pressurized to 1, 3, and 5 PSI and the extension forces generated were measured.

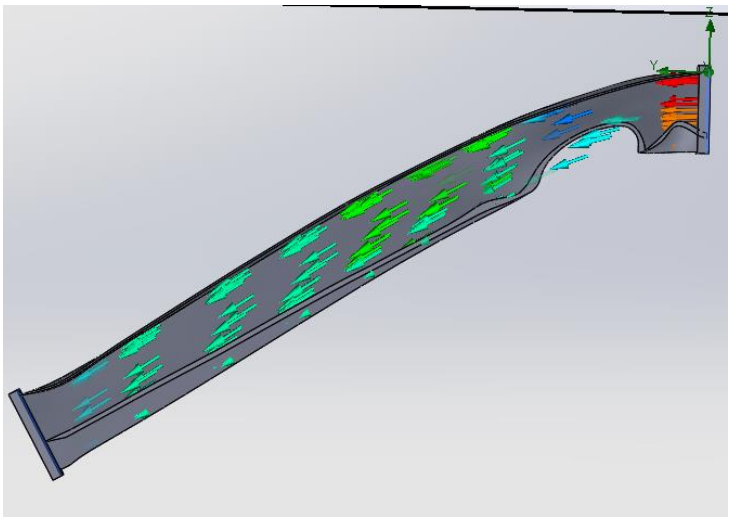

Figure 4.4: Cross-section of a chamber after deflection. Post-deformation flow trajectories are visible.

4.2.3 Data Analysis

Empirically Tested and Simulated Actuators:

Repeated measures ANOVAs were performed, for the empirically obtained data and simulation data, using SPSS to determine the effect of the between-sample actuator characteristics (shape, width, depth, and wall thickness) on extension force at the "fingertip". Joint angle and actuator pressure comprised the within-sample factors. Evidence of a significant effect led to post-hoc Tukey tests to examine differences among levels of the significant independent factor. This procedure was repeated for the dependent variable of the fingertip force resulting from passive resistance to bending the actuator. To validate the simulation results, Pearson correlation coefficients were computed between the passive bending resistances and extension forces of the empirical and simulated data. P-values of 0.05 or less were considered significant.

4.3 Results

4.3.1 Results: Actuator Fabrication and Testing

The fourteen actuators, one for each set of parameters, were successfully fabricated out of DragonSkin 20. After fabrication, uniformity of wall thickness was measured in three chambers with different nominal wall thicknesses. The measured wall thickness for each chamber was (mean ± standard deviation): 0.78±0.05 mm, 1.22±0.06 mm, and 1.82±0.04 mm, respectively. On average the mean thickness was within 0.04 mm of the desired value and the standard deviation did not exceed 0.06 mm.

4.3.1.1 Active Extension Force

Actuator characteristics: The actuators with a 0.8-mm wall thickness were unable to withstand pressures greater than 20.7 kPa, so data was analyzed in two sets. One set (All-Pressures) included all pressures but excluded data from the 0.8-mm actuators, while the other set (All-Thicknesses) included all actuators but excluded pressures greater than 20.7 kPa. For the All-Thicknesses dataset, the between-sample factors of shape ($p = 0.01$) and wall thickness ($p = 0.02$) were found to be significant, and each explained a significant portion of the variance in active extension force generated ($\eta p^2 = 0.71$ and $\eta p^2 = 0.73$, respectively) (Table 4.1**)**. Extension forces for the rectangular actuators were greater than those for the obround actuators. Post-hoc Tukey test revealed that extension force was greater for the 1.3-mm wall thickness than for the 0.8-mm thickness ($p=0.02$). The extension force did not significantly increase as wall depth and width increased ($p = 0.15$). For the All-Pressures dataset, shape also significantly affected extension force ($p = 0.04$), with greater extension forces for the rectangular shape. Depth approached having a significant impact on extension force ($p = 0.07$); the greatest depth generated 0.50 N more force than the smallest depth (**Figure 4.5**).

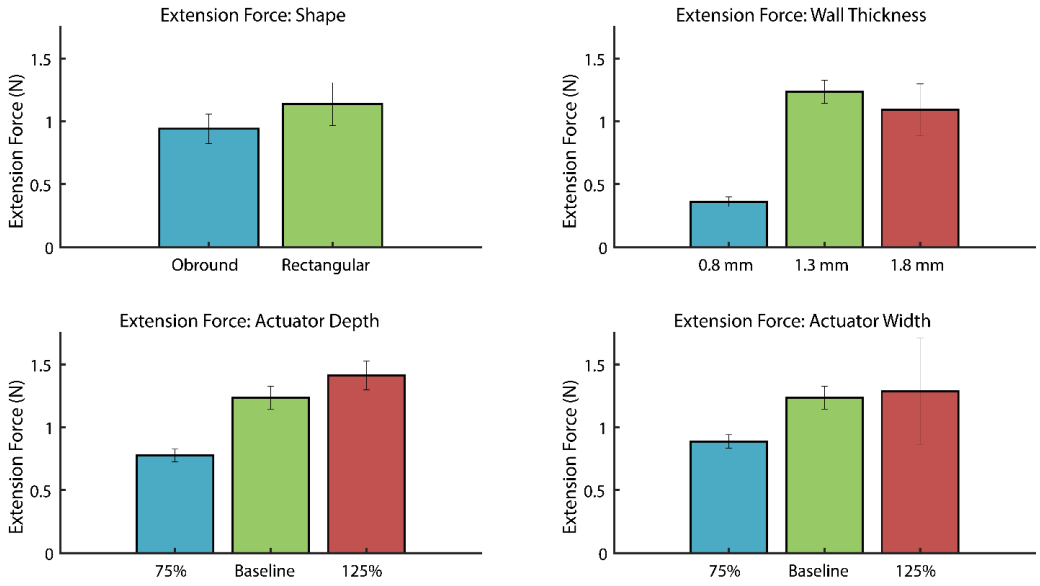

Figure 4.5: Average actuator extension force according to actuator characteristics. Values are averaged across range of pressures and bending angles. Error bars represent standard error.

Actuator pressure: Across actuators, extension force consistently increased as pressure increased up to 48.3 kPa. (**Figure 4.6**). The within-sample factor of pressure explained a significant amount of the variance for the All-Thicknesses and All-Pressures datasets ($p = 0.02$, $\eta p^2 = 0.66$; $p = 0.04$, $\eta p^2 = 0.57$, respectively) (Table 4.1). Maximum fingertip extension forces surpassed 3.0 N for some of the actuators at the 48.3 kPa pressurization. A maximum "fingertip" extension force of 3.6 N was obtained for the rectangular shape with the 1.8-mm wall thickness. This translates into 0.33 N-m of torque at the joint of the test fixture. The increase in extension force with increasing pressure was typical across all test angles.

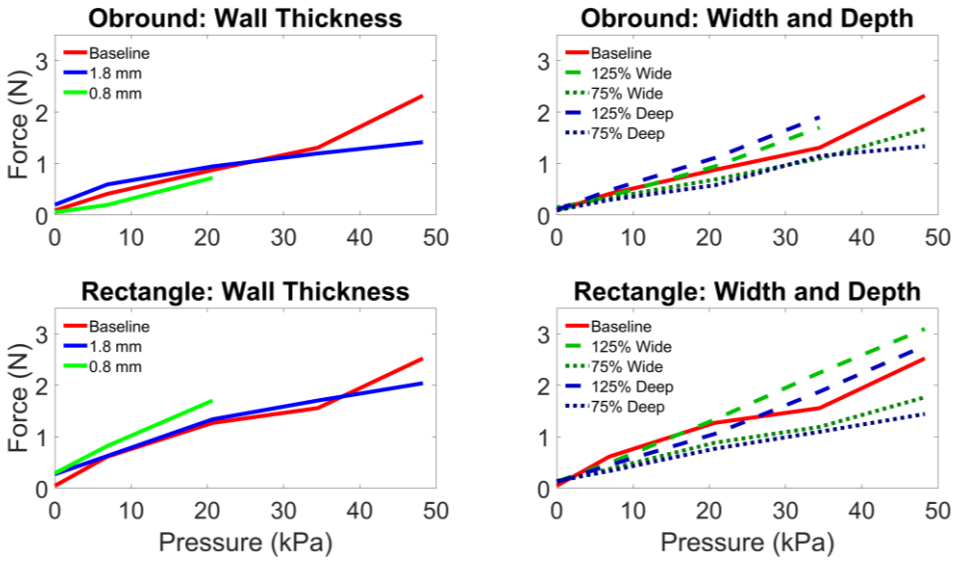

Figure 4.6:. Extension Force over Range of Pressures. The extension force created by different actuators for a joint rotation of 45° of flexion across a range of pressures. **Top row**: obround shape. **Bottom row**: rectangular shape. **Left column**: different wall thicknesses. **Right column**: different widths and depths - dotted lines indicate smallest values and dashed lines indicate largest values.

Joint angle: Extension force creation tended to be greater at more flexed joint postures across other conditions up to roughly 45° of flexion. Beyond this level of bending, extension force remained fairly constant (**Figure 4.7**). The relationship at 20.7 kPa depicted in **Figure 4.7** was typical across pressures. The within-sample effect for bending angle was significant and explained a large portion of the variance for the All-Thicknesses and All-Pressures datasets ($p = 0.05$, $\eta p^2 = 0.43$; $p < 0.01$, $\eta p^2 = 0.84$) (Table 4.1). The two highest extension forces were produced at 75° of flexion and a pressure of 48.3 kPa (5.4 N for the rectangular shape with the greatest width and 4.8 N for the rectangular cross-sectional shape with the greatest depth). Both actuators underwent plastic deformation at this joint angle and pressure and expanded excessively. The greatest extension force (3.6 N), without excessive expansion, occurred at 60° of flexion, and a pressure of 48.3 kPa.

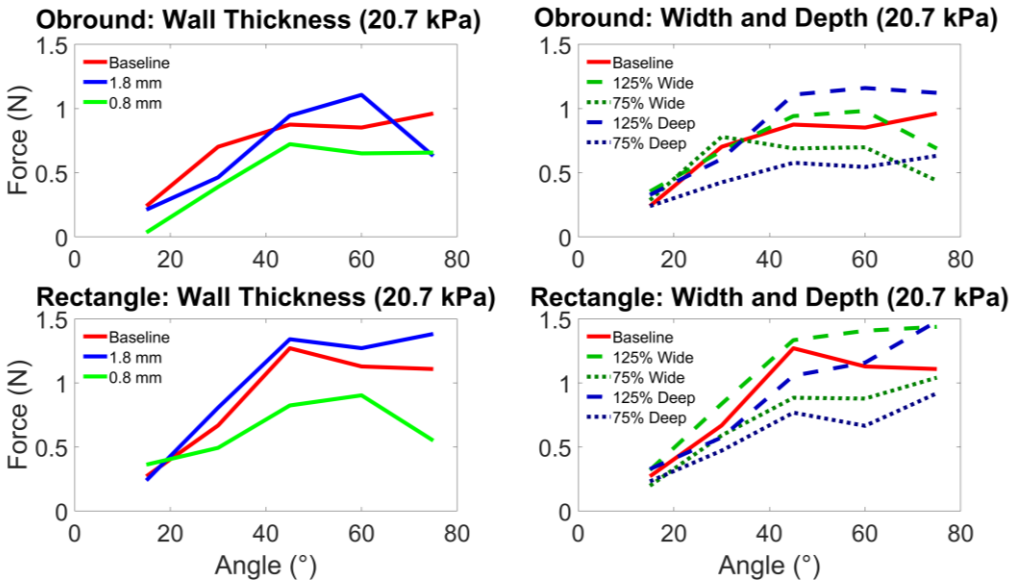

Figure 4.7: Extension Force over Range of Flexion Angles. The extension force created by different actuators pressurized to 20.7 kPa across a range of angles. Top row: obround shape. Bottom row: rectangular shape. Left column: different wall thicknesses. Right column: different widths and depths - dotted lines indicate smallest parameter values and dashed lines indicate largest values.

Table 4.1: Repeated Measures Analysis of Extension Force

Between-Sample Effects – All Thicknesses			**Average Extension Force - All Thicknesses**		
	p	**np^2**	**Level 1**	**Level 2**	**Level 3**
Shape	0.01	0.71	0.49 *	0.36*	N/A
Thickness	0.02	0.73	0.28*	0.46	0.53*
Depth	0.15	0.47	0.34	0.43	0.49
Width	0.47	0.22	0.39	0.42	0.47
Between-Sample Effects - All Pressures			**Average Extension Force - All Pressures**		
	p	**np^2**	**Level 1**	**Level 2**	**Level 3**
Shape	0.04	0.60	0.98*	0.72*	N/A
Thickness	0.69	0.03	0.88	0.81	N/A
Depth	0.07	0.65	0.57	0.91	1.07
Width	0.23	0.44	0 .66	0.91	0.98

Effect Levels 1-3: Shape: Rectangular, semi-obround; Thickness: 0.76mm, 1.27mm, 1.78mm; Depth: 7.4mm, 9.9mm, 12.4 mm; Width: 7.2mm, 9.6mm, 12.1 mm. * Indicates groups are significantly different: $p < 0.05$. Significance is indicated within each row across levels.

4.3.1.2 Passive Bending Resistance

Passive bending resistance of the actuators was examined at atmospheric pressure and under a vacuum. At atmospheric pressure, the between-sample effects of actuator shape, thickness, depth, and width were not significant (Table 4.2). Passive bending resistance was 0.07 N higher for the rectangular actuators on average, but the difference was not significant. There was no significant change in force due actuator depth, width, or wall thickness (**Figure 4.8**).

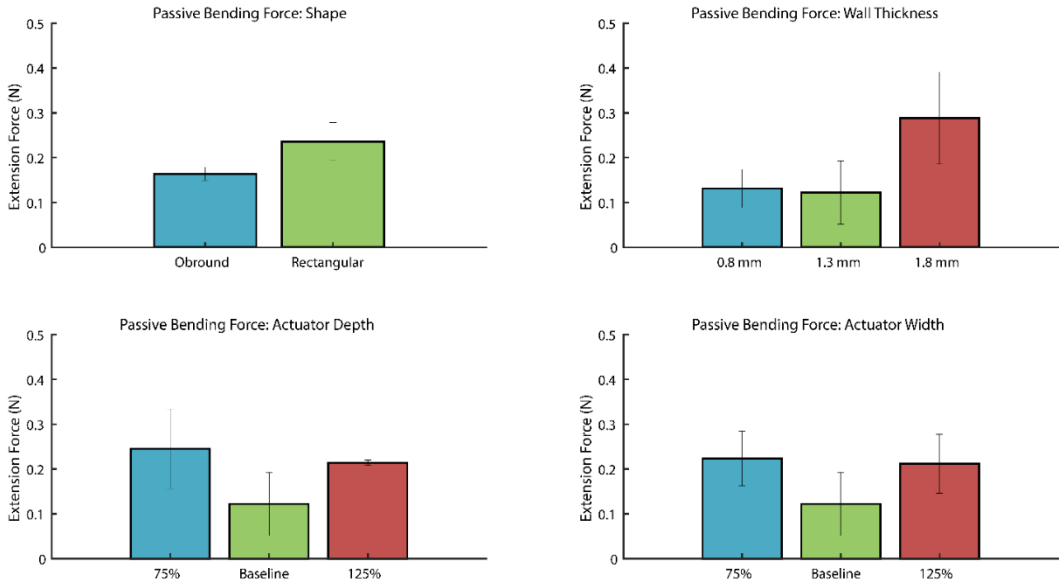

Figure 4.8: Average passive bending force according to different actuator characteristics. Values are averaged across range of pressures and bending angles.

Passive bending resistance in some cases begins to increase substantially as extreme bending angles are approached (**Figure 4.9**). Application of the vacuum flattened the shape of the actuators and decreased passive bending resistance by an average of 0.15±0.08 N (Table 4.2). For actuators under vacuum, the thickness, depth, and width had significant between-sample effects (Table 4.2***Error! Reference source not found.***). Passive bending resistance was smaller for the actuators with 1.3-mm thick walls than for those with other wall thicknesses ($p < 0.01$),

and for actuators with depths of 9.9 mm in comparison to 7.4 mm in depth (p = 0.02). At angles of 15°, and 30°, the vacuum almost eliminated the passive bending resistance. At greater bending angles, it served to limit passive bending resistance to 0.02 N at 45°, 0.13 N at 60°, and 0.38 N at 75°.

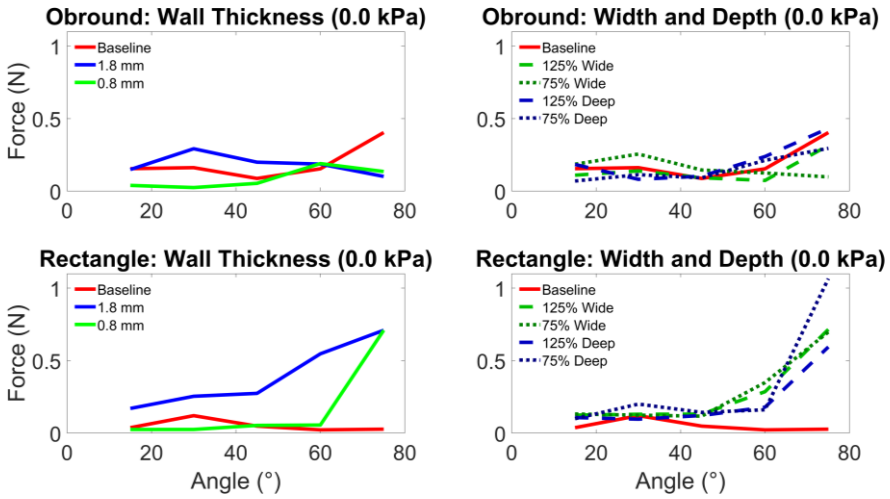

Figure 4.9: Passive Bending Resistance over Range of Flexion Angles. Top row: obround shape. Bottom row: rectangular shape. Left column: different wall thicknesses. Right column: different widths and depths - dotted lines indicate smallest parameter values and dashed lines indicate largest values.

Table 4.2 Repeated Measures Analysis of Passive Bending

	Between-Sample Effects - Passive Bending		**Average Passive Bending Force – Atmospheric pressure (N)**		
	p	***np²***	***Level 1***	***Level 2***	***Level 3***
Shape	0.27	0.20	0.40	0.33	N/A
Thickness	0.19	0.42	0.36	0.28	0.49
Depth	0.30	0.33	0.44	0.26	0.41
Width	0.35	0.29	0.42	0.27	0.41
	Between-Sample Effects - Vacuum		**Decrease Passive Bending Force – Vacuum (Δ N)**		
	p	***np²***	***Level 1***	***Level 2***	***Level 3***
Shape	0.44	0.10	0.07	0.06	N/A
Thickness	0.01	0.86	- 0.02*,†	0.12*	0.10†
Depth	0.02	0.72	0.02*	0.11*	0.07
Width	0.04	0.64	0.03	0.11	0.05

Effect Levels 1-3: Shape: Rectangular, semi-obround; Thickness: 0.76mm, 1.27mm, 1.78mm; Depth: 7.4mm, 9.9mm, 12.4 mm; Width: 7.2mm, 9.6mm, 12.1 mm. Symbols indicate significantly different groups: *,† $p < 0.05$. Significance is indicated within each row across levels.

4.3.2 Results: Actuator Simulation

Validation of Simulations by Empirical Data: Simulations of passive bending were performed at 15° and 30° of flexion for all 14 actuator iterations. Across cross-sectional shape, wall thickness, chamber depth, and chamber width, the Pearson correlation analyses revealed significant agreement between the empirical and simulation data (15°: $R = 0.659$, $p = 0.001$; 30°: $R = 0.606$, $p = 0.022$). Simulations of inflation were performed at 15° for 20.7 kPa of pressure. At 15° of flexion, the Pearson correlation between simulated and empirical extension forces was positive ($R = 0.452$) and approached significance ($p = 0.105$).

SolidWorks Actuator Cross-section: The ANOVA performed on simulation data indicated that shape and depth had a significant effect ($p=0.043$, $p = 0.001$) on minimum cross-sectional distance, the minimum separation of the top and bottom walls of the actuator along central cross-section, during bending of the chamber and each explained a significant portion of the variance ($\eta p^2 = 0.523$, $\eta p^2 = 0.896$). Minimum cross-sectional distance was increased by a non-significant amount as wall thickness increased from 0.8 mm to 1.8 mm ($p = 0.233$). On average, increasing wall thickness from 0.8 mm to 1.8 mm increased the minimum cross-sectional distance by 1.1 mm. Minimum cross-sectional distance was increased by a significant amount as actuator depth increased from 75% to 125% ($p<.001$). On average, increasing actuator depth from 75% to 125% increased the minimum cross-sectional distance by 3.8 mm. Minimum cross-sectional distance was decreased by a non-significant amount as actuator width increased from 75% to 125% ($p=0.176$). On average, increasing actuator width from 75% to 125% decreased minimum cross-sectional distance by 1.2 mm. Minimum cross-sectional distance was decreased by a non-significant amount as actuator bending increased from 0 to 30°. On average,

increasing actuator bending angle from 0° to 30° decreased minimum cross-sectional distance by 4.4 mm. Large changes in minimum cross-sectional distance only occurred after the angle increased to 23° or more, and actuators with thick walls or reduced widths were largely unaffected even at the higher bending angles. The actuators with the largest decreases in minimum cross-sectional distance were the 0.8-mm wall actuator for the obround cross section (decreased by 5.3 mm) and the 125% width actuators for the obround and rectangular cross sections (decreased by 9.1 mm, and 3.4 mm).

SolidWorks Actuator Flowrate: The ANOVA examining the effect of chamber parameters on flowrate through the chamber revealed that depth and width significantly affected flowrate ($p < 0.001$, $\eta p^2 \geq 0.990$). In general, deeper and wider actuators led to greater flowrates. The 125% depth actuators had a flowrate 0.018 kg/s greater than the 75% depth actuators, an increase of more than 50%. The 125% width actuators had a flowrate 0.008 kg/s greater than 75% depth actuators. In contrast, shape and wall thickness did not have a significant effect on flowrate ($p > 0.05$).

4.3.3 Results: Hand Exoskeleton Prototype Fabrication and Testing

After completing empirical and simulation testing of actuator designs, we identified the baseline rectangular actuator (1.3-mm wall thickness, width of 9.6 mm, and depth of 9.9 mm) as having the best set of characteristics, it had high extension force and low passive bending resistance. Thinner walled actuators could not handle high enough pressures, thicker walled actuators had higher passive bending resistance. Wider or deeper actuators may have difficulty fitting on the hand. Using these actuators, we created a prototype hand exoskeleton (**Figure 4.10**). The chambers were 150 mm in length to span an entire adult finger. Lycra tubes were then sewn to the palmar side of a glove and the actuators were inserted into the Lycra tubes. These

tubes helped to guide expansion of the pneumatic chambers and limit interference between chambers on adjacent digits. Lycra was selected as the fabric to minimize any additional passive bending resistance.

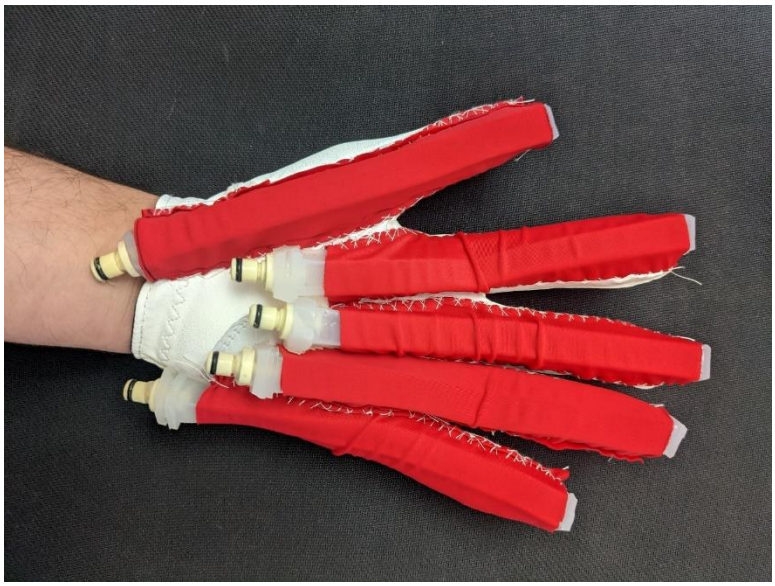

Figure 4.10: Hand Exoskeleton Prototype. Athletic glove with Lyrca tubes and elastomeric actuators (Dragon Skin 20). Worn on the left hand.

The operating bandwidth of these actuators was determined by examining the force production rate at of the actuator when at a 45° bending angle. The actuator was pressurized to each of the following levels: 6.9, 20.7, 34.5, and 48.3 kPa. The time it took each actuator to reach 95% of the stable maximum extension force was determined to be, in order of increasing pressure, 1.0, 0.7, 0.38, and 2.1 seconds. The time to pressurize decreases as pressure increases, until pressure reaches 48.3 kPa, at which point the actuator begins undergoing prolonged expansion and possible plastic deformation. This actuator deformation slows the rate of pressurization. It could be eliminated by using a stretch-limiting material in addition to the Dragon Skin 20. The time for pressurization was lowest for 34.5 kPa, taking only 0.38 seconds

(**Figure 4.11**). This means that the glove could facilitate multiple finger movements, extensions, or restrictions per second.

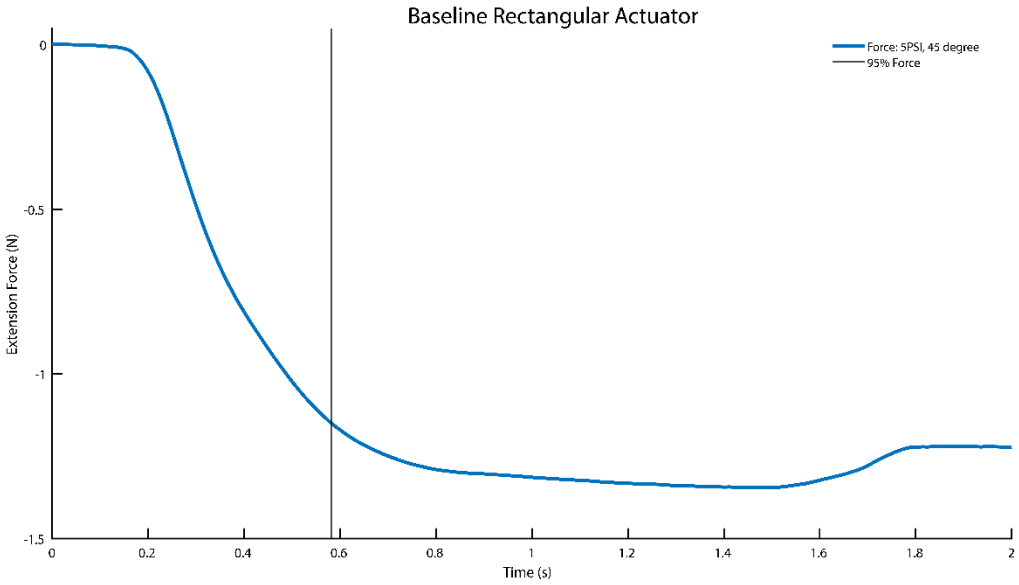

Figure 4.11: Representative example of a baseline rectangular actuator extension force. Pressurized to 34.5 kPa. The vertical black line indicates the point at which 95% of steady state force has been reached, 0.3750 seconds after the start of pressurization.

The polyurethane actuator design, which the Dragon Skin 20 actuator was created to replace, was previously tested to determine the obtainable flexion/extension rate (voluntary flexion, pressurized extension) which a user wearing the glove could achieve [177]. It was found that the polyurethane actuator could perform a flexion/extension cycle every 1.66 seconds. This test was repeated using the Dragon Skin 20 actuator in the glove, the pressurized extension was performed at a pressure of 34.5 kPa. The Dragon Skin actuator was able to perform a flexion/extension cycle in an average of only 1.1 seconds (**Figure 4.12**). This enables a maximum rate of 3340 cycles per hour, which is a substantial improvement over the maximum 2169 cycles per hour measured for the polyurethane actuator design.

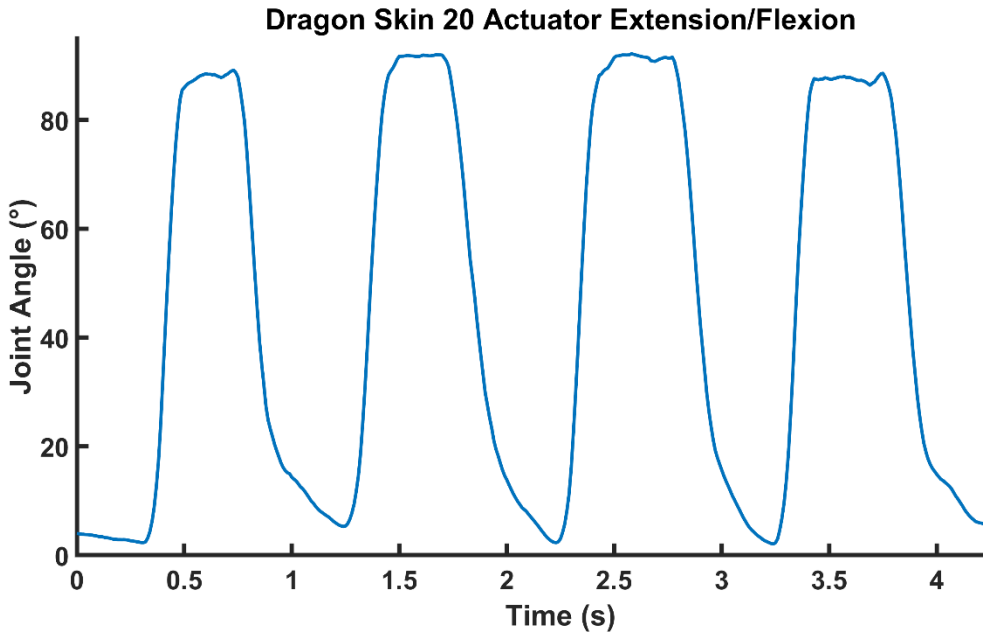

Figure 4.12: Flexion/Extension cycle of exoskeleton prototype. During extension, glove was pressurized to 34. kPa. Joint angle measurement was capped at a maximum value of 80°.

The functionality of the glove during an actual grasp was then tested (**Figure 4.13**). The glove was instructed to 1) provide finger extension torque, 2) allow hand positioning for object grasp, 3) deflate to allow object grasp, and 4) and then pressurize to cause release of the bottle. The glove was able to successfully facilitate finger extension and did not interfere with the ability to grasp and release a water bottle.

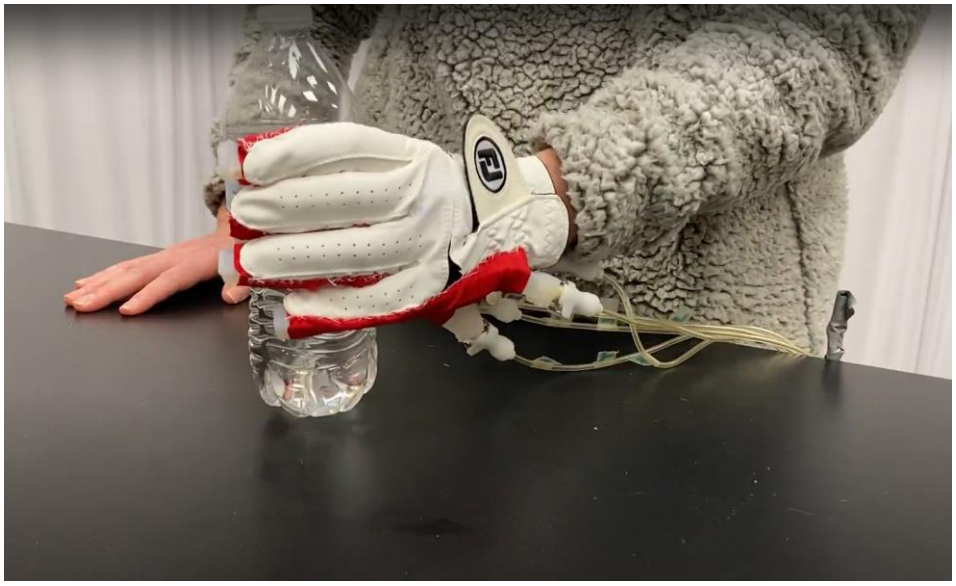

Figure 4.13: Grasp and transport of water bottle while wearing exoskeleton prototype. Actuators were pressurized to facilitate finger extension prior to grasp and release of the water bottle after transport.

These newly developed actuators and exoskeleton prototype were then incorporated into a previously developed platform for training individuated movement of the digits. The glove includes 10 resistive bend sensors (Flexpoint Bend Sensor, 2", unlaminated) positioned over the metacarpophalangeal, proximal interphalangeal, and thumb interphalangeal joints. These data are recorded by a microprocessor (Rabbitcore 3400, Digi Inc.) which wirelessly (XBEE Pro, Digi Inc.) transmits the data to a computer running a custom virtual reality environment (Unity, Unity Technologies, USA) consisting of a virtual keyboard and avatar hand. In this manner, user movement of the actual finger can produce corresponding movement of the finger on an avatar hand. Sufficient finger flexion causes the key under the avatar finger to be played. The soft exoskeleton supports practice of individuated movements by resisting inadvertent finger flexion and assisting finger extension. **Figure 4.14** provides an overview of the information flow among the different system components.

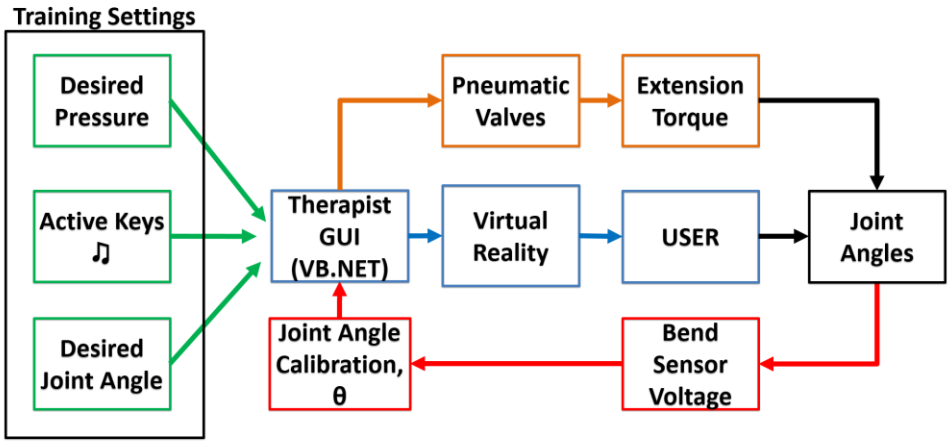

Figure 4.14: Block Diagram of Training Platform.

Two new therapy modes were introduced to expand the capabilities of the system. The bimanual therapy mode (**Figure 4.15)** allows two instrumented gloves to be used to control two separate hand avatars in the virtual environment. The music therapy mode incorporates simple pre-set songs to train movement of specified digits. Musical notes (e.g., ♫) scroll across the staff to guide users as to which keys to press and their timing.

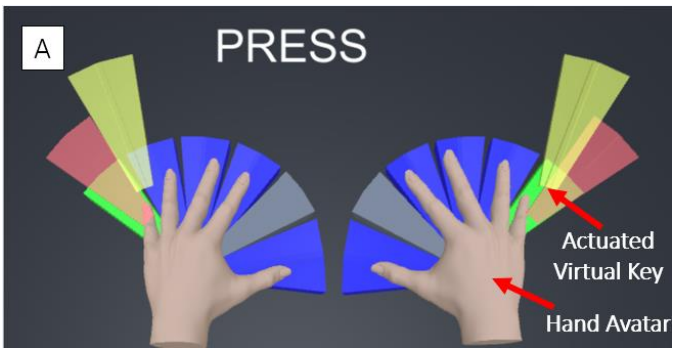

Figure 4.15: Bimanual training mode for VR keyboard.

The updated individuation training system was evaluated for functionality. After the training system was modified, but before the polyurethane actuators were replaced by the elastomeric actuators, the system was tested by five neurotypical adults for three sessions each

(15 sessions total). The system successfully performed over the fifteen hours of operation. Based on feedback from the users, we decided to develop actuators which were more customizable and more easily fabricated, with higher extension torque and less tendency to kink at high bending angles. This led to the development of the Dragon Skin 20 based actuators.

4.4 Discussion

Wearable, actuated devices for hand rehabilitation are currently being studied for use in a variety of patient populations, including individuals with CP [163,165]. Many of these individuals need active assistance for digit extension due to limited voluntary activation of digit extensor muscles and involuntary, detrimental activation of digit flexor muscles [173]. Previously developed exoskeletons typically employed rigid actuators such as electric motors to provide extension assistance [164]. These rigid actuators are relatively heavy and bulky. Soft actuators possess potential advantages in terms of weight, bulk, and flexibility, but have typically been used to create active finger flexion. Active assistance of finger extension could be achieved by placing soft actuators on the palmar side of the digit and inflating the actuator to extend the digit. This actuator arrangement is easier on the joints as they are pushed rather than pulled into extension, thereby reducing joint contact forces. Additionally, the actuators do not need to stretch to accommodate joint flexion, as would be needed with a dorsal location. The palmar location does not preclude interaction with real objects. When deflated, the thin chambers permit dexterous manipulation of objects. For the palmar placement, however, a trade-off exists between the potential to provide active extension and the passive resistance to finger flexion created by the presence of the actuators. As clinical populations may exhibit deficits in finger flexion as well as extension, it is important to minimize external flexion resistance.

We designed soft actuators, intended for palmar placement. The actuators were easy to fabricate from the Dragon Skin 20 and required minimal equipment. The actuators provided substantial extension force at the "fingertip" of the fixture (up to 3.6 N) and extension torque (0.33 N-m) at low pressures. While this is less than the 0.50 N-m target torque, the actuators performed favorably in comparison with other pneumatic actuators, when accounting for differences in actuator size and pressure. Extension torque might be further increased by increasing pressure beyond 48.3 kPa (force increased roughly linearly with pressure). The DragonSkin actuators provided extension forces four times greater than the previous polyurethane actuator [112], and greater torque than PVC actuators at half of the input pressure (0.09 Nm of torque for 96 kPa of pressure)[163]. Actuator extension force increased with bending angle until 45° of bending and remained relatively constant at greater angles. Beyond 45°, kinking in the chamber may have restricted air flow, thereby preventing further force increases. Considerable extension force was still seen, however, even at 75° of flexion.

Experimental testing revealed that actuator shape and wall thickness were found to have the greatest effect on finger extension force of the parameters tested. A rectangular cross-section produced higher extension forces than the obround cross-section, and thicker actuator walls increased extension force at low pressures. The thicker walls also enabled the use of higher pressures. Rectangular actuators may have produced higher extension due to their greater surface area resulting in a greater cross-sectional area under pressure, which is associated with greater extension force [178]. To minimize passive bending resistance, we did not incorporate features such as torque-compensating layers or complex geometries, such as sinusoidal channels [165] or multiple segments [179]. This also simplified fabrication, although these features could be incorporated if greater extension force is required.

The designed pneumatic chambers remained very compliant. Passive resistance to bending was low. On average, the actuators successfully met the target of less than 0.05 N-m passive bending resistance. The average passive bending torque was 0.02 N-m, and only 0.01 N-m under vacuum. Thus, the actuators are acceptable for placement on the palmar surface of the digits. Passive resistance of the chambers to imposed bending was most affected by cross-sectional shape, with rectangular actuators having higher passive bending resistance than semi-obround actuators. Passive bending resistance did not consistently increase as actuator depth, width or wall thickness increased, but did tend to increase as the bending angle increased. Applying a vacuum pressure to the actuators significantly decreased the passive bending resistance of the actuators. The vacuum also helped to flatten the pneumatic chambers, thereby providing a low profile.

The actuator with the best balance of extension force and passive bending resistance was the rectangular actuator with 1.3-mm wall thickness and baseline width and depth of 9.6 mm and 9.9 mm. Actuators with these baseline depth and width values had the lowest passive bending resistance and had similar extension force compared actuators with increased depth or width. However, if a vacuum can used to sufficiently decrease the passive bending force, then it may be appropriate to focus solely on maximizing extension force through the use of thicker-walled actuators, which can withstand higher pressures.

The SolidWorks simulations found that thin-walled actuators and wider actuators saw greater narrowing of the chamber during bending, although airflow simulations found that this narrowing did not cause large decreases in flow. In fact, regardless of actuator characteristics, none of the actuators saw significant changes in flowrate up to the 30° of flexion simulated. This is likely due to the relatively large cross-sectional areas used for these actuators, especially

compared to past PVC actuators [163]. At greater flexion angles, however, flow restrictions may become apparent.

While we performed an expansive exploration of the parameter space for the actuators, the search was not exhaustive. Other shapes or geometries may further improve performance. We were able to identify a set of parameters for easily fabricated actuators that performed well in terms of producing active extension assistance while minimally impacting flexion, but we did not examine robustness. Future cyclic loading should be performed to examine the impact of repetitive use on actuator properties, including material fatigue. The impact of temperature should also be explored.

Use of a cotton-based fabric rather than Lycra material may improve incorporation of the actuators into a soft exoskeleton. While the Lycra is attractive for its small resistance to passive bending, less stretch might better control chamber expansion to produce stronger active extension assistance. This fabric may also support the use of higher air pressures. Preliminary experiments were performed with combining the elastomer-based actuator and fabric tubes into a single composite material (**Figure 4.16**). DragonSkin 20 was thinned with mineral spirits until it achieved a very low viscosity. The thinned elastomer was then wetted onto a fabric tube. The fabric absorbed the material and the elastomer was given time to cure. Multiple layers of elastomer were applied, and an airtight elastomer/fabric actuator was fabricated. Composite material actuators of this type might achieve very low bending resistance, and weight while still being very robust and able to withstand high pressures.

Figure 4.16: Composite Material Actuator. Lycra fabric embedded with DragonSkin 20.

We conclude that the actuators presented here would be appropriate for use in a finger extension hand exoskeleton, and that they compare favorably to past, similar exoskeletons. Actuator performance varied as predicted with changes in actuator dimensions, and these elastomeric actuators do not have the same issue with pressurization at high bending angles that PVC actuators have. The Dragon Skin 20 actuators successfully provided high extension torque and low passive bending resistance, especially low bending resistance under the application of vacuum.

CHAPTER 5: Conclusions, and Future Work

5.1 Conclusions

In Chapter 1, it was found that most upper limb evaluations of motor function for children with hemiplegic cerebral palsy (hCP) were focused on more proximal joints, such as the shoulder or elbow, or gross movements of the hands. Few evaluations of fine motor control of the hand were identified, despite the importance of such sensorimotor control to overall function. We identified finger individuation as a critical aspect of hand function that has been insufficiently explored in the hCP population.

In Chapter 2, deficits in the ability of children with hCP to independently control their fingers were demonstrated. Children with hCP displayed greatly reduced finger movement individuation and force individuation in their paretic hand compared to their typically developing (TD) peers. Significant deficits in force individuation were also seen in the non-paretic hand. These deficits appeared to have a neurological origin as analysis of HD-EMG data showed less differentiation in activation patterns with task for children with hCP. Movement and force individuation correlated significantly with each other and with clinical hand function assessment scores when examined across populations and dominant/non-dominant hands. Children with hCP appeared to have greater movement individuation deficits than force individuation deficits for the paretic hand, while the nonparetic hand had negligible movement individuation deficits compared to the dominant and non-dominant hands of the TD children.

In Chapter 3, we examined the contributions of contralateral and ipsilateral corticospinal pathways to control of individuated finger forces. In TD children, motor imagery significantly increased the finger forces elicited by transcranial magnetic stimulation (TMS) of the contralateral M1 hemisphere. The increase was specific for the index finger being imagined and

thus led to increased force individuation only for the targeted digit. During voluntary individuated force production, TMS disruption of the contralateral hemisphere caused an increase in the solid angle of the finger force with respect to the normal direction and decreased individuation. During voluntary individuated force production, TMS disruption of the ipsilateral hemisphere caused a decrease in the solid angle of the finger force and increased individuation. However, for the hCP participant motor increased evoked forces and individuation of force for the thumb rather than the imagined index finger. The thumb had a much higher level of function than the index finger. Ipsilateral and Contralateral hemispheres evoked similar individuation patterns, but the ipsilateral side evoked higher magnitude finger forces. Motor imagery during ipsilateral stimulation appeared to decrease the solid angle of the force. During voluntary force, real stimulation of either hemisphere caused a decrease in force amplitude. During voluntary individuated force production, TMS disruption of the contralateral hemisphere caused increased individuation. During voluntary individuated force production, TMS disruption of the ipsilateral hemisphere caused decreased individuation.

In Chapter 4, We described the simulation, fabrication, and performance of elastomeric actuators. Finite element model simulations were performed which were able to help guide and identify suitable actuators for fabrication and testing. We successfully fabricated the soft, pneumatic actuators and were able to identify actuator characteristics which gave adequately high extension torque and low passive bending resistance. The best performing actuator design was incorporated into a glove to create a hand exoskeleton. User testing of the exoskeleton found that the glove was able to provide reasonable finger extension torque while still allowing the user to interact with everyday objects. This exoskeleton was useable with an improved version of a finger individuation training platform.

5.2 Future Work

Further testing of more children, especially children with hCP, would expand our knowledge of the development of fine motor control in the hand and how this progression is impacted by CP. Designing low-cost versions of the instruments used to evaluate force and movement individuation would allow for clinical uptake. This could also encourage multi-site data collection efforts.

Additional TMS data for TD and hCP populations should be collected. This pilot study showed the feasibility of conducting such experiments with these populations. Ideally, magnetic resonance imaging of each subject's brain would be performed to enable use of guided neuronavigation for more precise application of TMS stimulation. It would also be beneficial to examine the use of repetitive TMS and motor imagery as tools for training hand function in children.

The actuators for the hand exoskeleton need additional testing to determine their robustness. Cyclical testing of actuators would determine how quickly actuators become damaged and if their performance changes with use over time. Once validated, these actuators could be incorporated into clinical studies examining the efficacy of finger individuation training for children with hCP. The efficacy of different training modalities (e.g., unimanual training, bimanual training, combined use of the hand exoskeleton and functional electrical stimulation) should be examined. Training of individuated finger force, in addition to individuated motion, should be explored. The finger force individuation assessment platform can be adapted for use as a force individuation training platform.

REFERENCES

[1] Cans C. Surveillance of cerebral palsy in Europe: a collaboration of cerebral palsy surveys and registers. Dev Med Child Neurol. 2000;42:816–24. doi: 10.1111/j.1469-8749.2000.tb00695.x

[2] Oskoui M, Coutinho F, Dykeman J, Jetté N, Pringsheim T. An update on the prevalence of cerebral palsy: A systematic review and meta-analysis. Dev Med Child Neurol. 2013;55(6):509–19. doi: 10.1111/dmcn.12080

[3] Hurley DS, Sukal-Moulton T, Msall ME, Gaebler-Spira D, Krosschell KJ, Dewald JP. The Cerebral Palsy Research Registry: Development and Progress Toward National collaboration in the United States. J Child Neurol. 2011;26(12):1534–41. doi: 10.1177/0883073811408903

[4] Tonmukayakul U, Shih STF, Bourke-Taylor H, Imms C, Reddihough D, Cox L, et al. Systematic review of the economic impact of cerebral palsy. Res Dev Disabil. 2018;80(March):93–101.

[5] Cans C, De-la-Cruz J, Mermet MA. Epidemiology of cerebral palsy. Paediatr Child Health (Oxford). 2008;18(9):393–8. doi: 10.1016/j.paed.2008.05.015

[6] Paul Uvebrant. Hemiplegic Cerebral Palsy Aetiology and Outcome. Acta Paediatr. 1988;77(345):1–100.

[7] Fedrizzi E, Pagliano E, Andreucci E, Oleari G. Hand function in children with hemiplegic cerebral palsy: prospective follow-up and functional outcome in adolescence. Dev Med Child Neurol. 2003;45:85–91.

[8] Westbom L, Bergstrand L, Wagner P, Nordmark E. Survival at 19 years of age in a total population of children and young people with cerebral palsy. Dev Med Child Neurol. 2011;53(9):808–14. doi: 10.1111/j.1469-8749.2011.04027.x

[9] Jaspers E, Desloovere K, Bruyninckx H, Molenaers G, Klingels K, Feys H. Review of quantitative measurements of upper limb movements in hemiplegic cerebral palsy. Gait Posture. 2009;30(4):395–404. doi: 10.1016/j.gaitpost.2009.07.110

[10] Klingels K, Jaspers E, Van de Winckel A, De Cock P, Molenaers G, Feys H. A systematic review of arm activity measures for children with hemiplegic cerebral palsy. Clin Rehabil. 2010;24(10):887–900. doi: 10.1177/0269215510367994

[11] Lemmens RJ, Timmermans AA, Janssen-Potten YJ, Smeets RJ, Seelen HA. Valid and reliable instruments for arm-hand assessment at ICF activity level in persons with hemiplegia: a systematic review. BMC Neurol. 2012;12:21.

[12] Gilmore R, Sakzewski L, Boyd R. Upper limb activity measures for 5- to 16-year-old children with congenital hemiplegia: A systematic review. Dev Med Child Neurol.

2010;52(1):14–21. doi: 10.1111/j.1469-8749.2009.03369.x

[13] Greaves S, Imms C, Dodd K. Assessing bimanual performance in young children with hemiplegic cerebral palsy : a systematic review. Dev Med Child Neurol. 2010;52:413–21. doi: 10.1111/j.1469-8749.2009.03561.x

[14] Jebsen RH, Taylor N, Trieschmann RB, Trotter MJ, Howard LA. An objective and Standardized test of hand function. Arch Phys Med Rehabil. 1969;50:311–9.

[15] Randall M, Imms C, Carey LM, Pallant JF. Rasch analysis of the Melbourne assessment of unilateral upper limb function. Dev Med Child Neurol. 2014;56(7):665–72. doi: 10.1111/dmcn.12391

[16] Krumlinde-Sundholm L, Eliasson AC. Development of the assisting hand assessment: A Rasch-built measure intended for children with unilateral upper limb impairments. Scand J Occup Ther. 2003;10(1):16–26. doi: 10.1080/11038120310004529

[17] Davids JR, Peace LC, Wagner L V., Gidewall MA, Blackhurst DW, Roberson WM. Validation of the Shriners Hospital for Children Upper Extremity Evaluation (SHUEE) for children with hemiplegic cerebral palsy. J Bone Jt Surg - Ser A. 2006;88(2):326–33. doi: 10.2106/JBJS.E.00298

[18] Tomhave WA, Van Heest AE, Bagley A, James MA. Affected and contralateral hand strength and dexterity measures in children with hemiplegic cerebral palsy. J Hand Surg Am. 2015;40(5):900–7. doi: 10.1016/j.jhsa.2014.12.039

[19] Hung YC, Charles J, Gordon AM. Influence of accuracy constraints on bimanual coordination during a goal-directed task in children with hemiplegic cerebral palsy. Exp Brain Res. 2010;201(3):421–8. doi: 10.1007/s00221-009-2049-1

[20] Burtner PA, Poole JL, Torres T, Medora AM, Abeyta R, Keene J, et al. Effect of Wrist Hand Splints on Grip, Pinch, Manual Dexterity, and Muscle Activation in Children with Spastic Hemiplegia: A Preliminary Study. J Hand Ther. 2008;21(1):36–43. doi: 10.1197/j.jht.2007.08.018

[21] Bleyenheuft Y, Arnould C, Brandao MB, Bleyenheuft C, Gordon AM. Hand and Arm Bimanual Intensive Therapy Including Lower Extremity (HABIT-ILE) in Children With Unilateral Spastic Cerebral Palsy: A Randomized Trial. Neurorehabil Neural Repair. 2015;29(7):645–57. doi: 10.1177/1545968314562109

[22] Fong KNK, Jim ESW, Dong VAQ, Cheung HKY. “Remind to move”: A pilot study on the effects of sensory cueing treatment on hemiplegic upper limb functions in children with unilateral cerebral palsy. Clin Rehabil. 2013;27(1):82–9. doi: 10.1177/0269215512448199

[23] Stearns GE, Burtner P, Keenan KM, Qualls C, Phillips J. Effects of constraint-induced movement therapy on hand skills and muscle recruitment of children with spastic hemiplegic cerebral palsy. NeuroRehabilitation. 2009;24(2):95–108. doi: 10.3233/NRE-

2009-0459

[24] Abo Nour AA, Saleh MG, Elnagmy EH. Impact of Combining Mirror Therapy and Habit On Hand Grip Strength in Children with Hemiparesis. Int J Physiother. 2016;3(4):460–8. doi: 10.15621/ijphy/2016/v3i4/111055

[25] Sanal-Top C, Karadag-Saygi E, Saçaklıdır R, Duruöz MT. Duruöz Hand Index: Is it valid and reliable in children with unilateral cerebral palsy? Dev Neurorehabil. 2019;22(2):75–9. doi: 10.1080/17518423.2017.1326536

[26] Rameckers EAA, Smits-Engelsman BCM, Duysens J. Children with spastic hemiplegia are equally able as controls in maintaining a precise percentage of maximum force without visually monitoring their performance. Neuropsychologia. 2005;43(13):1938–45. doi: 10.1016/j.neuropsychologia.2005.03.003

[27] Smits-Engelsman BCM, Rameckers EAA, Duysens J. Late developmental deficits in force control in children with hemiplegia. Neuroreport. 2004;15(12):1931–5. doi: 10.1097/00001756-200408260-00020

[28] Gillick BT, Krach LE, Feyma T, Rich TL, Moberg K, Thomas W, et al. Primed low-frequency repetitive transcranial magnetic stimulation and constraint-induced movement therapy in pediatric hemiparesis: A randomized controlled trial. Dev Med Child Neurol. 2014;56(1):44–52. doi: 10.1111/dmcn.12243

[29] Smits-Engelsman BCM, Rameckers EAA, Duysens J. Muscle force generation and force control of finger movements in children with spastic hemiplegia during isometric tasks. Dev Med Child Neurol. 2005;47(5):337–42. doi: 10.1017/S0012162205000630

[30] Gaillard F, Cacioppo M, Bouvier B, Bouzille G, Newman CJ, Pasquet T, et al. Assessment of bimanual performance in 3-D movement analysis: Validation of a new clinical protocol in children with unilateral cerebral palsy. Ann Phys Rehabil Med. 2019;63:408–15. doi: 10.1016/j.rehab.2019.06.008

[31] Yildizgören MT, Nakipoğlu Yüzer GF, Ekiz T, Özgirgin N. Effects of neuromuscular electrical stimulation on the wrist and finger flexor spasticity and hand functions in cerebral palsy. Pediatr Neurol. 2014;51(3):360–4. doi: 10.1016/j.pediatrneurol.2014.05.009

[32] Xu K, Wang L, Mai J, He L. Efficacy of constraint-induced movement therapy and electrical stimulation on hand function of children with hemiplegic cerebral palsy: A controlled clinical trial. Disabil Rehabil. 2012;34(4):337–46. doi: 10.3109/09638288.2011.607213

[33] Aarts PB, Jongerius PH, Geerdink YA, van Limbeek J, Geurts AC. Modified Constraint-Induced Movement Therapy combined with Bimanual Training (mCIMT-BiT) in children with unilateral spastic cerebral palsy: How are improvements in arm-hand use established? Res Dev Disabil. 2011;32(1):271–9. doi: 10.1016/j.ridd.2010.10.008

[34] Sugden D, Utley A. Interlimb Coupling in Children with Hemiplegic Cerebreal Palsy. Dev Med Child Neurol. 1991;37:293–309.

[35] Moura RCF, Santos C, Collange Grecco L, Albertini G, Cimolin V, Galli M, et al. Effects of a single session of transcranial direct current stimulation on upper limb movements in children with cerebral palsy: A randomized, sham-controlled study. Dev Neurorehabil. 2017;20(6):368–75. doi: 10.1080/17518423.2017.1282050

[36] Rönnqvist L, Rösblad B. Kinematic analysis of unimanual reaching and grasping movements in children with hemiplegic cerebral palsy. Clin Biomech. 2007;22(2):165–75. doi: 10.1016/j.clinbiomech.2006.09.004

[37] Chen HC, Chen CL, Kang LJ, Wu CY, Chen FC, Hong WH. Improvement of upper extremity motor control and function after home-based constraint induced therapy in children with unilateral cerebral palsy: Immediate and long-term effects. Arch Phys Med Rehabil. 2014;95(8):1423–32. doi: 10.1016/j.apmr.2014.03.025

[38] Utley A, Sugden D. Interlimb coupling in children with hemiplegic cerebral palsy during reaching and grasping at speed. Dev Med Child Neurol. 1998;40(6):396–404. doi: 10.1111/j.1469-8749.1998.tb08215.x

[39] Hyde C, Fuelscher I, Enticott PG, Reid SM, Williams J. Rapid on-line control to reaching is preserved in children with congenital spastic hemiplegia: Evidence from double-step reaching performance. J Child Neurol. 2015;30(9):1186–91. doi: 10.1177/0883073814556310

[40] Butler EE, Ladd AL, LaMont LE, Rose J. Temporal-spatial parameters of the upper limb during a Reach & Grasp Cycle for children. Gait Posture. 2010;32(3):301–6. doi: 10.1016/j.gaitpost.2010.05.013

[41] Rudisch J, Butler J, Izadi H, Zielinski IM, Aarts P, Birtles D, et al. Kinematic parameters of hand movement during a disparate bimanual movement task in children with unilateral Cerebral Palsy. Hum Mov Sci. 2016;46:239–50. doi: 10.1016/j.humov.2016.01.010

[42] Utley A, Steenbergen B, Sugden DA. The influence of object size on discrete bimanual co-ordination in children with hemiplegic cerebral palsy T. Disabil Rehabil. 2009;26(10):603–13. doi: 10.1080/09638280410001696674

[43] Mailleux L, Jaspers E, Ortibus E, Simon-Martinez C, Desloovere K, Molenaers G, et al. Clinical assessment and three-dimensional movement analysis: An integrated approach for upper limb evaluation in children with unilateral cerebral palsy. PLoS One. 2017;12(7):e0180196. doi: 10.1371/journal.pone.0180196

[44] Mutsaarts M, Steenbergen B, Meulenbroek R. A detailed analysis of the planning and execution of prehension movements by three adolescents with spastic hemiparesis due to cerebral palsy. Exp Brain Res. 2004;156(3):293–304. doi: 10.1007/s00221-003-1789-6

[45] Smits-Engelsman BCM, Klingels K, Feys H. Bimanual force coordination in children with

spastic unilateral cerebral palsy. Res Dev Disabil. 2011;32(5):2011–9. doi: 10.1016/j.ridd.2011.04.007

[46] Xu K, He L, Mai J, Yan X, Chen Y. Muscle recruitment and coordination following constraint-induced movement therapy with electrical stimulation on children with hemiplegic cerebral palsy: A randomized controlled trial. PLoS One. 2015;10(10):e0138608. doi: 10.1371/journal.pone.0138608

[47] Xu K, Mai J, He L, Yan X, Chen Y. Surface Electromyography of Wrist Flexors and Extensors in Children With Hemiplegic Cerebral Palsy. PM R. 2015;7(3):270–5. doi: 10.1016/j.pmrj.2014.09.009

[48] Eyre JA, Taylor JP, Villagra F, Smith M, Miller S. Evidence of activity-dependent withdrawal of corticospinal projections during human development. Neurology. 2001;57(9):1543–54. doi: 10.1212/WNL.57.9.1543

[49] Holmefur M, Kits A, Bergström J, Krumlinde-Sundholm L, Flodmark O, Forssberg H, et al. Neuroradiology can predict the development of hand function in children with unilateral cerebral palsy. Neurorehabil Neural Repair. 2013;27(1):72–8. doi: 10.1177/1545968312446950

[50] Kuo H-C, Ferre CL, Carmel JB, Gowatsky JL, Stanford AD, Rowny SB, et al. Using diffusion tensor imaging to identify corticospinal tract projection patterns in children with unilateral spastic cerebral palsy. Dev Med Child Neurol. 2017;59(1):65–71. doi: 10.1111/dmcn.13192

[51] Shiran SI, Weinstein M, Sirota-Cohen C, Myers V, Ben Bashat D, Fattal-Valevski A, et al. MRI-based radiologic scoring system for extent of brain injury in children with hemiplegia. Am J Neuroradiol. 2014;35(12):2388–96. doi: 10.3174/ajnr.A3950

[52] Simon-Martinez C, Mailleux L, Ortibus E, Fehrenbach A, Sgandurra G, Cioni G, et al. Combining constraint-induced movement therapy and action-observation training in children with unilateral cerebral palsy: A randomized controlled trial. BMC Pediatr. 2018;18(1):250. doi: 10.1186/s12887-018-1228-2

[53] Yu S, Carlson HL, Mineyko A, Brooks BL, Kuczynski A, Hodge J, et al. Bihemispheric alterations in myelination in children following unilateral perinatal stroke. NeuroImage Clin. 2018;20(June):7–15. doi: 10.1016/j.nicl.2018.06.028

[54] Woodward KE, Carlson HL, Kuczynski A, Saunders J, Hodge J, Kirton A. Sensory-motor network functional connectivity in children with unilateral cerebral palsy secondary to perinatal stroke. NeuroImage Clin. 2019;21(July 2018):101670. doi: 10.1016/j.nicl.2019.101670

[55] Van der Aa NE, Verhage CH, Groenendaal F, Vermeulen RJ, De Bode S, Van Nieuwenhuizen O, et al. Neonatal neuroimaging predicts recruitment of contralesional corticospinal tracts following perinatal brain injury. Dev Med Child Neurol. 2013;55(8):707–12. doi: 10.1111/dmcn.12160

[56] Bleyenheuft Y, Thonnard JL. Predictive and reactive control of precision grip in children with congenital hemiplegia. Neurorehabil Neural Repair. 2010;24(4):318–27. doi: 10.1177/1545968309353327

[57] Weinstein M, Green D, Rudisch J, Zielinski IM, Benthem-Muñiz M, Jongsma MLA, et al. Understanding the relationship between brain and upper limb function in children with unilateral motor impairments: A multimodal approach. Eur J Paediatr Neurol. 2018;22(1):143–54. doi: 10.1016/j.ejpn.2017.09.012

[58] Weinstein M, Green D, Geva R, Schertz M, Fattal-Valevski A, Artzi M, et al. Interhemispheric and intrahemispheric connectivity and manual skills in children with unilateral cerebral palsy. Brain Struct Funct. 2014;219(3):1025–40. doi: 10.1007/s00429-013-0551-5

[59] Schertz M, Shiran SI, Myers V, Weinstein M, Fattal-Valevski A, Artzi M, et al. Imaging Predictors of Improvement from a Motor Learning-Based Intervention for Children with Unilateral Cerebral Palsy. Neurorehabil Neural Repair. 2016;30(7):647–60. doi: 10.1177/1545968315613446

[60] Weinstein M, Myers V, Green D, Schertz M, Shiran SI, Geva R, et al. Brain Plasticity following Intensive Bimanual Therapy in Children with Hemiparesis: Preliminary Evidence. Neural Plast. 2015;2015:798481–13. doi: 10.1155/2015/798481

[61] Bleyenheuft Y, Grandin CB, Cosnard G, Olivier E, Thonnard J-L. Corticospinal Dysgenesis and Upper-Limb Deficits in Congenital Hemiplegia: A Diffusion Tensor Imaging Study. Pediatrics. 2007;120(6):e1502–11. doi: 10.1542/peds.2007-0394

[62] Hodge J, Goodyear B, Carlson H, Wei XC, Kirton A. Segmental Diffusion Properties of the Corticospinal Tract and Motor Outcome in Hemiparetic Children with Perinatal Stroke. J Child Neurol. 2017;32(6):550–9. doi: 10.1177/0883073817696815

[63] Sgandurra G, Biagi L, Fogassi L, Sicola E, Ferrari A, Guzzetta A, et al. Reorganization of the Action Observation Network and Sensory-Motor System in Children with Unilateral Cerebral Palsy: An fMRI Study. Neural Plast. 2018;2018:6950547–15. doi: 10.1155/2018/6950547

[64] Lemée JM, Chinier E, Ali P, Labriffe M, Ter Minassian A, Dinomais M. (Re)organisation of the somatosensory system after early brain lesion: A lateralization index fMRI study. Ann Phys Rehabil Med. 2019;63(5):416–21. doi: 10.1016/j.rehab.2019.02.001

[65] Vandermeeren Y, Davare M, Duque J, Olivier E. Reorganization of cortical hand representation in congenital hemiplegia. Eur J Neurosci. 2009;29(4):845–54. doi: 10.1111/j.1460-9568.2009.06619.x

[66] Vandermeeren Y, Bastings E, Fadiga L, Olivier E. Long-latency motor evoked potentials in congenital hemiplegia. Clin Neurophysiol. 2003;114(10):1808–18. doi: 10.1016/S1388-2457(03)00161-5

[67] Vandermeeren Y, Sébire G, Grandin CB, Thonnard JL, Schlögel X, De Volder AG. Functional reorganization of brain in children affected with congenital hemiplegia: fMRI study. Neuroimage. 2003;20(1):289–301. doi: 10.1016/S1053-8119(03)00262-3

[68] Crajé C, van Elk M, Beeren M, van Schie HT, Bekkering H, Steenbergen B. Compromised motor planning and Motor Imagery in right Hemiparetic Cerebral Palsy. Res Dev Disabil. 2010;31(6):1313–22. doi: 10.1016/j.ridd.2010.07.010

[69] Steenbergen B, Meulenbroek RGJ. Deviations in upper-limb function of the less-affected side in congenital hemiparesis. Neuropsychologia. 2006;44(12):2296–307. doi: 10.1016/j.neuropsychologia.2006.05.016

[70] Verrel J, Bekkering H, Steenbergen B. Eye-hand coordination during manual object transport with the affected and less affected hand in adolescents with hemiparetic cerebral palsy. Exp Brain Res. 2008;187(1):107–16. doi: 10.1007/s00221-008-1287-y

[71] Kuczynski AM, Kirton A, Semrau JA, Dukelow SP. Bilateral reaching deficits after unilateral perinatal ischemic stroke: A population-based case-control study. J Neuroeng Rehabil. 2018;15(1):77. doi: 10.1186/s12984-018-0420-9

[72] Kuczynski AM, Dukelow SP, Semrau JA, Kirton A. Robotic quantification of position sense in children with perinatal stroke. Neurorehabil Neural Repair. 2016;30(8):762–72. doi: 10.1177/1545968315624781

[73] Auld ML, Boyd RN, Moseley GL, Ware RS, Johnston LM. Impact of tactile dysfunction on upper-limb motor performance in children with unilateral cerebral palsy. Arch Phys Med Rehabil. 2012;93(4):696–702. doi: 10.1016/j.apmr.2011.10.025

[74] Gordon AM, Hung Y-C, Brandao M, Ferre CL, Kuo H-C, Friel K, et al. Bimanual Training and Constraint-Induced Movement Therapy in Children With Hemiplegic Cerebral Palsy. Neurorehabil Neural Repair. 2011;25(8):692–702. doi: 10.1177/1545968311402508

[75] Hung YC, Casertano L, Hillman A, Gordon AM. The effect of intensive bimanual training on coordination of the hands in children with congenital hemiplegia. Res Dev Disabil. 2011;32(6):2724–31. doi: 10.1016/j.ridd.2011.05.038

[76] Cohen-Holzer M, Katz-Leurer M, Reinstein R, Rotem H, Meyer S. The effect of combining daily restraint with bimanual intensive therapy in children with hemiparetic cerebral palsy: A self-control study. NeuroRehabilitation. 2011;29(1):29–36. doi: 10.3233/NRE-2011-0674

[77] Brandão MB, Ferre C, Kuo HC, Rameckers EAA, Bleyenheuft Y, Hung YC, et al. Comparison of structured skill and unstructured practice during intensive bimanual training in children with unilateral spastic cerebral palsy. Neurorehabil Neural Repair. 2014;28(5):452–61. doi: 10.1177/1545968313516871

[78] Sakzewski L, Provan K, Ziviani J, Boyd RN. Comparison of dosage of intensive upper

limb therapy for children with unilateral cerebral palsy: How big should the therapy pill be? Res Dev Disabil. 2015;37:9–16. doi: 10.1016/j.ridd.2014.10.050

[79] Cohen-Holzer M, Sorek G, Schless S, Kerem J, Katz-Leurer M. The influence of a constraint and bimanual training program using a variety of modalities, on upper extremity functions and gait parameters among children with hemiparetic cerebral palsy: A case series. Phys Occup Ther Pediatr. 2016;36(1):17–27. doi: 10.3109/01942638.2014.990549

[80] Cohen-Holzer M, Sorek G, Kerem J, Katz-Leurer M. The impact of combined constraint-induced and bimanual arm training program on the perceived hand-use experience of children with unilateral cerebral palsy. Dev Neurorehabil. 2017;20(6):355–60. doi: 10.1080/17518423.2016.1238017

[81] Saussez G, Brandão MB, Gordon AM, Bleyenheuft Y. Including a lower-extremity component during Hand-Arm Bimanual Intensive Training does not attenuate improvements of the upper extremities: A retrospective study of randomized trials. Front Neurol. 2017;8(SEP):495. doi: 10.3389/fneur.2017.00495

[82] Hung YC, Henderson ER, Akbasheva F, Valte L, Ke WS, Gordon AM. Planning and coordination of a reach-grasp-eat task in children with hemiplegia. Res Dev Disabil. 2012;33(5):1649–57. doi: 10.1016/j.ridd.2012.04.003

[83] Dong VA, Fong KNK, Chen Y-F, Tseng SSW, Wong LMS. 'Remind-to-move' treatment versus constraint-induced movement therapy for children with hemiplegic cerebral palsy: a randomized controlled trial. Dev Med Child Neurol. 2017;59(2):160–7. doi: 10.1111/dmcn.13216

[84] Bishop L, Gordon AM, Kim H. Hand Robotic Therapy in Children with Hemiparesis: A Pilot Study. Am J Phys Med Rehabil. 2017;96(1):1–7. doi: 10.1097/PHM.0000000000000537

[85] Picelli A, La Marchina E, Vangelista A, Chemello E, Modenese A, Gandolfi M, et al. Effects of Robot-Assisted Training for the Unaffected Arm in Patients with Hemiparetic Cerebral Palsy: A Proof-of-Concept Pilot Study. Behav Neurol. 2017;2017:8349242–8. doi: 10.1155/2017/8349242

[86] Cohen-Holzer M, Sorek G, Schweizer M, Katz-Leurer M. The influence of a constraint and bimanual training program using a variety of modalities on endurance and on the cardiac autonomic regulation system of children with unilateral cerebral palsy: A self-control clinical trial. NeuroRehabilitation. 2017;41(1):119–26. doi: 10.3233/NRE-171463

[87] Klingels K, Meyer S, Mailleux L, Simon-martinez C, Hoskens J, Monbaliu E, et al. Time Course of Upper Limb Function in Children with Unilateral Cerebral Palsy: A Five-Year Follow-Up Study. Neural Plast. 2018;2018:2831342–9. doi: 10.1155/2018/2831342

[88] Sakzewski L, Ziviani J, Boyd RN. Best responders after intensive upper-limb training for children with unilateral cerebral palsy. Arch Phys Med Rehabil. 2011;92(4):578–84. doi:

10.1016/j.apmr.2010.12.003

[89] Klingels K, Feys H, De Wit L, Jaspers E, Van De Winckel A, Verbeke G, et al. Arm and hand function in children with unilateral cerebral palsy: A one-year follow-up study. Eur J Paediatr Neurol. 2012;16(3):257–65. doi: 10.1016/j.ejpn.2011.08.001

[90] Rich TL, Menk JS, Rudser KD, Feyma T, Gillick BT. Less-Affected Hand Function in Children With Hemiparetic Unilateral Cerebral Palsy: A Comparison Study With Typically Developing Peers. Neurorehabil Neural Repair. 2017;31(10–11):965–76. doi: 10.1177/1545968317739997

[91] Sakzewski L, Ziviani J, Boyd R. The relationship between unimanual capacity and bimanual performance in children with congenital hemiplegia. Dev Med Child Neurol. 2010;52(9):811–6. doi: 10.1111/j.1469-8749.2009.03588.x

[92] Gordon AM, Schneider JA, Chinnan A, Charles JR. Efficacy of a hand-arm bimanual intensive therapy (HABIT) in children with hemiplegic cerebral palsy: A randomized control trial. Dev Med Child Neurol. 2007;49(11):830–8. doi: 10.1111/j.1469-8749.2007.00830.x

[93] Van de Winckel A, Klingels K, Bruyninckx F, Wenderoth N, Peeters R, Sunaert S, et al. How does brain activation differ in children with unilateral cerebral palsy compared to typically developing children, during active and passive movements, and tactile stimulation? An fMRI study. Res Dev Disabil. 2013;34(1):183–97. doi: 10.1016/j.ridd.2012.07.030

[94] James S, Ziviani J, Ware RS, Boyd RN. Randomized controlled trial of web-based multimodal therapy for unilateral cerebral palsy to improve occupational performance. Dev Med Child Neurol. 2015;57(6):530–8. doi: 10.1111/dmcn.12705

[95] Friel KM, Kuo HC, Carmel JB, Rowny SB, Gordon AM. Improvements in hand function after intensive bimanual training are not associated with corticospinal tract dysgenesis in children with unilateral cerebral palsy. Exp Brain Res. 2014;232(6):2001–9. doi: 10.1007/s00221-014-3889-x

[96] Cohen-Holzer M, Katz-Leurer M, Meyer S, Green D, Parush S. The Effect of Bimanual Training with or Without Constraint on Hand Functions in Children with Unilateral Cerebral Palsy: A Non-Randomized Clinical Trial. Phys Occup Ther Pediatr. 2017;37(5):516–27. doi: 10.1080/01942638.2017.1280871

[97] Klingels K, Feys H, Molenaers G, Verbeke G, Van Daele S, Hoskens J, et al. Randomized trial of modified constraint-induced movement therapy with and without an intensive therapy program in children with unilateral cerebral palsy. Neurorehabil Neural Repair. 2013;27(9):799–807. doi: 10.1177/1545968313496322

[98] Brandão MB, Mancini MC, Ferre CL, Figueiredo PRP, Oliveira RHS, Gonçalves SC, et al. Does Dosage Matter? A Pilot Study of Hand-Arm Bimanual Intensive Training (HABIT) Dose and Dosing Schedule in Children with Unilateral Cerebral Palsy. Phys

Occup Ther Pediatr. 2018;38(3):227–42. doi: 10.1080/01942638.2017.1407014

[99] Friel KM, Kuo HC, Fuller J, Ferre CL, Brandão M, Carmel JB, et al. Skilled Bimanual Training Drives Motor Cortex Plasticity in Children with Unilateral Cerebral Palsy. Neurorehabil Neural Repair. 2016;30(9):834–44. doi: 10.1177/1545968315625838

[100] Fiori S, Guzzetta A, Pannek K, Ware RS, Rossi G, Klingels K, et al. Validity of semi-quantitative scale for brain MRI in unilateral cerebral palsy due to periventricular white matter lesions: Relationship with hand sensorimotor function and structural connectivity. NeuroImage Clin. 2015;8:104–9. doi: 10.1016/j.nicl.2015.04.005

[101] Islam M, Nordstrand L, Holmström L, Kits A, Forssberg H, Eliasson AC. Is outcome of constraint-induced movement therapy in unilateral cerebral palsy dependent on corticomotor projection pattern and brain lesion characteristics? Dev Med Child Neurol. 2014;56(3):252–8. doi: 10.1111/dmcn.12353

[102] Charles JR, Wolf S, Schneider JA, Gordon A. Efficacy of a child-friendly form of constraint-induced therapy in hemiplegic cerebral palsy: a randomized control trial. Dev Med Child Neurol. 2006;48(8):635–42.

[103] Gordon AM, Charles J, Wolf S. Efficacy of Constraint-Induced Movement Therapy on Involved Upper-Extremity Use in Children With Hemiplegic Cerebral Palsy Is Not Age-Dependent. Pediatrics. 2006;117(3):e363–73. doi: 10.1542/peds.2005-1009

[104] Kuhtz-Buschbeck JP, Sundholm LK, Eliasson A-C, Forssberg H. Quantitative assessment of mirror movements in children and adolescents with hemiplegic cerebral palsy. Dev Med Child Neurol. 2007;42(11):728–36. doi: 10.1111/j.1469-8749.2000.tb00034.x

[105] Ebner-karestinos D, Flament B, Arnould C, Thonnard J-LL, Bleyenheuft Y, Ebner-karestinos D. Precision grip control while walking down a step in children with unilateral cerebral palsy. PLoS One. 2018;13(2):e0191684. doi: 10.1371/journal.pone.0191684

[106] Sakzewski L, Ziviani J, Abbott DF, Macdonell RAL, Jackson GD, Boyd RN. Randomized trial of constraint-induced movement therapy and bimanual training on activity outcomes for children with congenital hemiplegia. Dev Med Child Neurol. 2011;53(4):313–20. doi: 10.1111/j.1469-8749.2010.03859.x

[107] Culicchia G, Nobilia M, Asturi M, Santilli V, Paoloni M, De Santis R, et al. Cross-Cultural Adaptation and Validation of the Jebsen-Taylor Hand Function Test in an Italian Population. Rehabil Res Pract. 2016;2016:8970917–12. doi: 10.1155/2016/8970917

[108] Beagley SB, Reedman SE, Sakzewski L, Boyd RN. Establishing Australian norms for the jebsen taylor test of hand function in typically developing children aged five to 10 years: A pilot study. Phys Occup Ther Pediatr. 2016;36(1):88–109. doi: 10.3109/01942638.2015.1040571

[109] Lang CE, Beebe JA. Relating movement control at 9 upper extremity segments to loss of hand function in people with chronic hemiparesis. Neurorehabil Neural Repair.

2007;21(3):279–91. doi: 10.1177/1545968306296964

[110] Wolbrecht ET, Rowe JB, Chan V, Ingemanson ML, Cramer SC, Reinkensmeyer DJ. Finger strength, individuation, and their interaction: Relationship to hand function and corticospinal tract injury after stroke. Clin Neurophysiol [Internet]. 2018;129(4):797–808. doi: 10.1016/j.clinph.2018.01.057

[111] Xu J, Ejaz N, Hertler B, Branscheidt M, Widmer M, Faria A V., et al. Separable systems for recovery of finger strength and control after stroke. J Neurophysiol [Internet]. 2017;118(2):1151–63. doi: 10.1152/jn.00123.2017

[112] Thielbar KO, Lord TJ, Fischer HC, Lazzaro EC, Barth KC, Stoykov ME, et al. Training finger individuation with a mechatronic-virtual reality system leads to improved fine motor control post-stroke. J Neuroeng Rehabil. 2014;11(1):1–11. doi: 10.1186/1743-0003-11-171

[113] HJ C, SR C, Jeong E, SJ K. Finger exercise with keyboard playing in adults with cerebral palsy: A preliminary study. J Exerc Rehabil. 2013;9(4):420–5. doi: 10.12965/jer.130050

[114] Kong J, Kim K, Joung HJ, Chung CY, Park J. Effects of spastic cerebral palsy on multi-finger coordination during isometric force production tasks. Exp Brain Res [Internet]. 2019;237(12):3281–95. doi: 10.1007/s00221-019-05671-3

[115] Wilhelm LA, Martin JR, Latash ML, Zatsiorsky VM. Finger enslaving in the dominant and non-dominant hand. Hum Mov Sci [Internet]. 2014;33(1):185–93. doi: 10.1016/j.humov.2013.10.001

[116] Park W, Li S. Neuroscience Letters No graded responses of finger muscles to TMS during motor imagery of isometric finger forces. Neurosci Lett [Internet]. 2011;494(3):255–9. doi: 10.1016/j.neulet.2011.03.027

[117] Li S, Stevens JA, Rymer WZ. Clinical Neurophysiology Interactions between imagined movement and the initiation of voluntary movement : A TMS study. Clin Neurophysiol [Internet]. 2009;120(6):1154–60. doi: 10.1016/j.clinph.2008.12.045

[118] Kirby RS, Wingate MS, Van Naarden Braun K, Doernberg NS, Arneson CL, Benedict RE, et al. Prevalence and functioning of children with cerebral palsy in four areas of the United States in 2006: A report from the Autism and Developmental Disabilities Monitoring Network. Res Dev Disabil. 2011;32(2):462–9. doi: 10.1016/j.ridd.2010.12.042

[119] Kim SW, Shim JK, Zatsiorsky VM, Latash ML. Finger inter-dependence: Linking the kinetic and kinematic variables. Hum Mov Sci. 2008;27(3):408–22. doi: 10.1016/j.humov.2007.08.005

[120] Raghavan P, Petra E, Krakauer JW, Gordon AM. Patterns of Impairment in Digit Independence After Subcortical Stroke. J Neurophysiol [Internet]. 2005;95(1):369–78. doi: 10.1152/jn.00873.2005

[121] Xu J, Ejaz N, Hertler B, Branscheidt M, Widmer M, Faria A V., et al. Separable systems for recovery of finger strength and control after stroke. J Neurophysiol. 2017;118(2):1151–63. doi: 10.1152/jn.00123.2017

[122] Shim JK, Oliveira MA, Hsu J, Huang J, Park J, Clark JE. Hand digit control in children: Age-related changes in hand digit force interactions during maximum flexion and extension force production tasks. Exp Brain Res. 2007;176(2):374–86. doi: 10.1007/s00221-006-0629-x

[123] Eliasson A-C, Krumlinde-Sundholm L, Rösblad B, Beckung E, Arner M, Ohrvall A-M, et al. The Manual Ability Classification System (MACS) for children with cerebral palsy: scale development and evidence of validity and reliability. Dev Med Child Neurol [Internet]. 2006;48(7):549–54.

[124] Lang CE, Schieber MH. Reduced Muscle Selectivity During Individuated Finger Movements in Humans After Damage to the Motor Cortex or Corticospinal Tract. J Neurophysiol [Internet]. 2004;91(4):1722–33. doi: 10.1152/jn.00805.2003

[125] Kimmerle M, Ferre CL, Kotwica KA, Michel GF. Development of role-differentiated bimanual manipulation during the infant's first year. Dev Psychobiol. 2010;52(2):168–80. doi: 10.1002/dev.20428

[126] Wallace PS, Whishaw IQ. Independent digit movements and precision grip patterns in 1-5-month-old human infants: Hand-babbling, including vacuous then self-directed hand and digit movements, precedes targeted reaching. Neuropsychologia. 2003;41(14):1912–8. doi: 10.1016/S0028-3932(03)00128-3

[127] Armand J, Olivier E, Edgley SA, Lemon RN. Postnatal development of corticospinal projections from motor cortex to the cervical enlargement in the macaque monkey. J Neurosci. 1997;17(1):251–66. doi: 10.1523/jneurosci.17-01-00251.1997

[128] Rathelot JA, Strick PL. Subdivisions of primary motor cortex based on cortico-motoneuronal cells. Proc Natl Acad Sci U S A. 2009;106(3):918–23. doi: 10.1073/pnas.0808362106

[129] Hu X, Suresh NL, Xue C, Rymer WZ. Extracting extensor digitorum communis activation patterns using high-density surface electromyography. Front Physiol. 2015;6(OCT):1–9. doi: 10.3389/fphys.2015.00279

[130] van Beek N, Stegeman DF, van den Noort J, Veeger DHEJ, Maas H. Activity patterns of extrinsic finger flexors and extensors during movements of instructed and non-instructed fingers. J Electromyogr Kinesiol. 2018;38:187–96.

[131] Dupan SSG, Stegeman DF, Maas H. Distinct neural control of intrinsic and extrinsic muscles of the hand during single finger pressing. Hum Mov Sci [Internet]. 2018;59(April):223–33. doi: 10.1016/j.humov.2018.04.012

[132] Lang CE, Schieber MH. Differential Impairment of Individuated Finger Movements in

Humans After Damage to the Motor Cortex or the Corticospinal Tract. J Neurophysiol. 2004;91(4):1722–33. doi: 10.1152/jn.00805.2003

[133] Chiang H, Slobounov SM, Ray W. Practice-related modulations of force enslaving and cortical activity as revealed by EEG. Clin Neurophysiol. 2004;115(5):1033–43. doi: 10.1016/j.clinph.2003.12.019

[134] Baranello G, Sebastiano DR, Pagliano E, Visani E, Ciano C, Fumarola A, et al. Hand function assessment in the first years of life in unilateral cerebral palsy: Correlation with neuroimaging and cortico-spinal reorganization. Eur J Paediatr Neurol. 2016;20(1):114–24. doi: 10.1016/j.ejpn.2015.09.005

[135] Ke J, Holmström L, Vollmer B, Tedroff K, Islam M, Persson JKE, et al. Hand function in relation to brain lesions and corticomotor-projection pattern in children with unilateral cerebral palsy. Dev Med Child Neurol. 2010;52(2):145–52.

[136] Koudijs SM, Leijten FSS, Ramsey NF, van Nieuwenhuizen O, Braun KPJ. Lateralization of motor innervation in children with intractable focal epilepsy-A TMS and fMRI study. Epilepsy Res [Internet]. 2010;90(1–2):140–50. doi: 10.1016/j.eplepsyres.2010.04.004

[137] Zewdie E, Damji O, Ciechanski P, Seeger T, Kirton A. Contralesional Corticomotor Neurophysiology in Hemiparetic Children with Perinatal Stroke: Developmental Plasticity and Clinical Function. Neurorehabil Neural Repair. 2017;31(3):261–71. doi: 10.1177/1545968316680485

[138] Li S, Latash ML, Zatsiorsky VM. Effects of motor imagery on finger force responses to transcranial magnetic stimulation. 2004;20:273–80. doi: 10.1016/j.cogbrainres.2004.03.003

[139] Fricke C, Gentner R, Rumpf JJ, Weise D, Saur D, Classen J. Differential spatial representation of precision and power grasps in the human motor system. Neuroimage [Internet]. 2017;158(June):58–69. doi: 10.1016/j.neuroimage.2017.06.080

[140] Fridman EA, Hanakawa T, Chung M, Hummel F, Leiguarda RC, Cohen LG. Reorganization of the human ipsilesional premotor cortex after stroke. Brain. 2004;127(4):747–58. doi: 10.1093/brain/awh082

[141] Peurala SH, M. Müller-Dahlhaus JF, Arai N, Ziemann U. Interference of short-interval intracortical inhibition (SICI) and short-interval intracortical facilitation (SICF). Clin Neurophysiol. 2008;119(10):2291–7. doi: 10.1016/j.clinph.2008.05.031

[142] Nakamura H, Kitagawa H, Kawaguchi Y, Tsuji H. Intracortical facilitation and inhibition after transcranial magnetic stimulation in conscious humans. J Physiol. 1997;498(3):817–23. doi: 10.1113/jphysiol.1997.sp021905

[143] Rich TL, Nemanich S, Chen CY, Sutter EN, Feyma T, Krach LE, et al. Ipsilateral Corticospinal Tract Excitability Contributes to the Severity of Mirror Movements in Unilateral Cerebral Palsy: A Case Series. Clin EEG Neurosci. 2020;51(3):185–90. doi:

10.1177/1550059419899323

[144] Sanes JN, Donoghue JP, Thangaraj V, Edelman RR, Warach S. Shared Neural Substrates Controlling Hand Movements in Human Motor Cortex. Science (80-). 1995;268(5218):1775–7.

[145] Marneweck M, Kuo H, Smorenburg ARP, Ferre CL, Flamand VH, Gupta D, et al. The Relationship Between Hand Function and Overlapping Motor Representations of the Hands in the Contralesional Hemisphere in Unilateral Spastic Cerebral Palsy. 2018; doi: 10.1177/1545968317745991

[146] Baud-bovy G, Prattichizzo D, Rossi S. Contact forces evoked by transcranial magnetic stimulation of the motor cortex in a multi-finger grasp. 2008;75:723–36. doi: 10.1016/j.brainresbull.2008.01.005

[147] Li S. Analysis of Increasing and Decreasing Isometric Finger Force Generation and the Possible Role of the Corticospinal System in This Process. Motor Control. 2013;17:221–37.

[148] Latash ML, Li S. Finger interactions studied with transcranial magnetic stimulation during multi-finger force production tasks. 2003;114:1445–55. doi: 10.1016/S1388-2457(03)00105-6

[149] Gerloff C, Cohen LG, Floeter MK, Chen R, Corwell B, Hallett M. Inhibitory influence of the ipsilateral motor cortex on responses to stimulation of the human cortex and pyramidal tract. J Physiol. 1998;510(1):249–59. doi: 10.1111/j.1469-7793.1998.249bz.x

[150] Morishita T, Uehara K, Funase K. Changes in interhemispheric inhibition from active to resting primary motor cortex during a fine-motor manipulation task. J Neurophysiol. 2012;107(11):3086–94. doi: 10.1152/jn.00888.2011

[151] Mihelj E, Bächinger M, Kikkert S, Ruddy K, Wenderoth N. Mental individuation of imagined finger movements can be achieved using TMS-based neurofeedback. Neuroimage [Internet]. 2021;242(August):118463. doi: 10.1016/j.neuroimage.2021.118463

[152] Allen CH, Kluger BM, Buard I. Safety of Transcranial Magnetic Stimulation in Children: A Systematic Review of the Literature. Pediatr Neurol. 2017;68:3–17. doi: 10.1016/j.pediatrneurol.2016.12.009

[153] Krishnan C, Santos L, Peterson MD, Ehinger M. Safety of noninvasive brain stimulation in children and adolescents. Brain Stimul [Internet]. 2015;8(1):76–87. doi: 10.1016/j.brs.2014.10.012

[154] Gilbert DL, Garvey MA, Bansal AS, Lipps T, Zhang J, Wassermann EM. Should transcranial magnetic stimulation research in children be considered minimal risk? Clin Neurophysiol. 2004;115(8):1730–9. doi: 10.1016/j.clinph.2003.10.037

[155] Zewdie E, Ciechanski P, Kuo HC, Giuffre A, Kahl C, King R, et al. Safety and tolerability of transcranial magnetic and direct current stimulation in children: Prospective single center evidence from 3.5 million stimulations. Brain Stimul [Internet]. 2020;13(3):565–75. doi: 10.1016/j.brs.2019.12.025

[156] Frye RE, Rotenberg A, Ousley M, Pascual-Leone A. Transcranial magnetic stimulation in child neurology: Current and future directions. J Child Neurol. 2008;23(1):79–96. doi: 10.1177/0883073807307972

[157] Gillick BT, Gordon AM, Feyma T, Krach LE, Carmel J, Rich TL, et al. Non-Invasive Brain Stimulation in Children With Unilateral Cerebral Palsy: A Protocol and Risk Mitigation Guide. Front Pediatr [Internet]. 2018;6(March):1–9. doi: 10.3389/fped.2018.00056

[158] Slobounov S, Ray W, Cao C, Chiang H. Modulation of cortical activity as a result of task-specific practice. Neurosci Lett. 2007;421(2):126–31. doi: 10.1016/j.neulet.2007.04.077

[159] Wallen M, Ziviani J, Herbert R, Evans R, Novak I. Modified constraint-induced therapy for children with hemiplegic cerebral palsy: A feasibility study. Dev Neurorehabil. 2008;11(2):124–33. doi: 10.1080/17518420701640897

[160] Deluca SC, Case-Smith J, Stevenson R, Ramey SL. Constraint-induced movement therapy (CIMT) for young children with cerebral palsy: Effects of therapeutic dosage. J Pediatr Rehabil Med. 2012;5(2):133–42. doi: 10.3233/PRM-2012-0206

[161] Charles JR, Gordon AM. Development of hand-arm bimanual intensive training (HABIT) for improving bimanual coordination in children with hemiplegic cerebral palsy. Dev Med Child Neurol [Internet]. 2006;48(11):931–6.

[162] Green D, Schertz M, Farquharson MY, Fattal-valevski A, Gordon AM, Moore A, et al. A multi-site study of functional outcomes following a themed approach to hand-arm bimanual intensive therapy for children with hemiplegia. Dev Med Child Neurol. 2013;55(6):527–33. doi: 10.1111/dmcn.12113

[163] Nam C, Rong W, Li W, Cheung C, Ngai W, Cheung T, et al. An Exoneuromusculoskeleton for Self-Help Upper Limb Rehabilitation After Stroke. Soft Robot. 2020;00(00):1–22. doi: 10.1089/soro.2020.0090

[164] Taheri H, Rowe JB, Gardner D, Chan V, Gray K, Bower C, et al. Design and preliminary evaluation of the FINGER rehabilitation robot: Controlling challenge and quantifying finger individuation during musical computer game play. J Neuroeng Rehabil. 2014;11(1):1–17. doi: 10.1186/1743-0003-11-10

[165] Yap HK, Lim JH, Nasrallah F, Cho Hong Goh J, Yeow CH. Characterisation and evaluation of soft elastomeric actuators for hand assistive and rehabilitation applications. J Med Eng Technol. 2016;40(4):199–209. doi: 10.3109/03091902.2016.1161853

[166] Yap HK, Ng HY, Yeow CH. High-Force Soft Printable Pneumatics for Soft Robotic

Applications. Soft Robot. 2016;3(3):144–58. doi: 10.1089/soro.2016.0030

[167] Sun Y, Yap HK, Liang X, Guo J, Qi P, Ang MH, et al. Stiffness Customization and Patterning for Property Modulation of Silicone-Based Soft Pneumatic Actuators. Soft Robot. 2017;4(3):251–60. doi: 10.1089/soro.2016.0047

[168] Jun Zhang, Jun Sheng, Ciar´an T. O'Neill, Conor J. Walsh, Robert J. Wood, Jee-Hwan Ryu, Jaydev P. Desai and MCY. Robotic Artificial Muscles : Current Progress and Future Perspectives for Biomimetic Actuators. Rob Auton Syst [Internet]. 2016;75:203–20.

[169] Tang ZQ, Heung HL, Tong KY, Li Z. A Probabilistic Model-Based Online Learning Optimal Control Algorithm for Soft Pneumatic Actuators. IEEE Robot Autom Lett. 2020;5(2):1437–44. doi: 10.1109/LRA.2020.2967293

[170] Conrad MO, Kamper DG. Isokinetic strength and power deficits in the hand following stroke. Clin Neurophysiol [Internet]. 2012;123(6):1200–6. doi: 10.1016/j.clinph.2011.10.004

[171] Lord TJ, Keefe DM. Development of a Haptic Keypad for Training Finger Individuation after Stroke. 2011;1–2. doi: 10.1109/ICVR.2011.5971844

[172] Simone LK, Sundarrajan N, Luo X, Jia Y, Kamper DG. A low cost instrumented glove for extended monitoring and functional hand assessment. J Neurosci Methods. 2007;160(2):335–48. doi: 10.1016/j.jneumeth.2006.09.021

[173] Barry AJ, Kamper DG, Stoykov ME, Triandafilou K, Roth E. Characteristics of the severely impaired hand in survivors of stroke with chronic impairments. Top Stroke Rehabil. 2021;00(00):1–11. doi: 10.1080/10749357.2021.1894660

[174] McCall J V, Readling C, Kamper DG, Ieee M. Compliant Actuators for Hand Exoskeletons. In: IROS Mechanisms and Design. 2020.

[175] Heung HL, Tang ZQ, Shi XQ, Tong KY, Li Z. Soft Rehabilitation Actuator With Integrated Post-stroke Finger Spasticity Evaluation. Front Bioeng Biotechnol. 2020;8(February):1–10. doi: 10.3389/fbioe.2020.00111

[176] Zhang J, Wang T, Wang J, Wang MY, Li B, Zhang JXJ, et al. Geometric Confined Pneumatic Soft–Rigid Hybrid Actuators. Soft Robot. 2020;00(00):1–9. doi: 10.1089/soro.2018.0157

[177] McCall J V., Ludovice MC, Blaylock JA, Kamper DG. A Platform for Rehabilitation of Finger Individuation in Children with Hemiplegic Cerebral Palsy. IEEE Int Conf Rehabil Robot. 2019; doi: 10.1109/ICORR.2017.8009213

[178] Shapiro Y, Wolf A, Gabor K. Bi-bellows: Pneumatic bending actuator. Sensors Actuators, A Phys. 2011;167(2):484–94. doi: 10.1016/j.sna.2011.03.008

[179] Heung KHL, Tong RKY, Lau ATH, Li Z. Robotic Glove with Soft-Elastic Composite

Actuators for Assisting Activities of Daily Living. Soft Robot. 2019;6(2):289–304. doi: 10.1089/soro.2017.0125